UNIVERSITA' DEGLI STUDI
DI MODENA E REGGIO EMILIA

PhD Program in Molecular and Regenerative Medicine

XXXIV Cycle

Melanosomal two-pore channel 2 as a new therapeutic target for the treatment of malignant melanoma

Candidate: Letizia Campanini

Tutor: Prof. Alessandra Marconi

Coordinator of the PhD Program: Prof. Michele De Luca

2020-2021

ABSTRACT

Melanoma originates from melanocytes and is the most aggressive form of skin cancer, since it has a high metastatic potential and does not respond to current therapies. It is a complex and heterogeneous multifactorial disease, presenting genetic, clinical, histopathological and biological variants. Although early melanomas can be cured by surgical excision, metastases are very difficult to treat due to their high aggressiveness and resistance to common therapies, for this reason it is essential to identify new targets for the development of therapeutic treatments.

A factor that may be a mediator of melanoma progression is TPC2, an ionic channel that regulates a number of cellular functions by releasing Ca^{2+} in response to the second messenger NAADP. This channel localizes on the membrane of intracellular acidic compartments, including melanosomes and appears to be involved in several aspects related to tumorigenesis and metastatization. The inhibition of NAADP signaling strongly reduced the growth and invasiveness of mouse melanoma cells, whereas human melanoma cells with different phenotype and microenvironment showed contrasting results. Therefore, in this project we studied the role of TPC2 in melanoma with different aggressiveness and microenvironments, assuming that melanosomal TPC2 activation was crucial for melanoma progression.

We observed an increase of TPC2 expression in primary human melanomas with higher Breslow Index and in VGP compared to RGP melanoma cell lines in 2D and 3D models. Of note, although nodular melanoma presents different clinical and histopathological features than malignant melanomas, also this subtype expressed high TPC2 level, suggesting an important role of this channel in tumor growth and invasion through the dermis. Althought, the analysis in the TCGA showed a decrease TPCN2 mRNA expression in melanoma metastasis, on the contrary TPC2 protein expression increased in melanoma metastasis compared to primary tumor of the same patient. Similarly, high TPC2 expression were noted in skin metastasis compared to RGP human primary melanoma cell lines of the same patients, and pleural metastasis, while lymph node metastasis showed low level of TPC2. Investigating the role of the channel in cancer progression, we observed an inhibition of cell proliferation rate in a dose and time-dependent manner after Nar treatment in 2D and 3D models. In addition, we noted a reduction of migration capacity and a decreased invasion in type I collagen of RGP primary melanoma spheroids after Nar treatment. Finally, TPC2 blocking decreased the expression of tumor invasion markers, suggesting a role of the channel in epithelium-mesenchymal transition and in melanoma progression.

Since melanoma cells have previously been hypothesized to increase their invasive capacity by releasing melanosomes into the dermis, we have supposed that TPC2 channel may contribute to the regulation of melanosomes traffic and in this way also to tumor aggressiveness. As expected, melanoma cells showed an increase expression of melanosomal markers and intracellular melanin

amount after TPC2 blocking, while the release of melanin did not occur, indicating that TPC2 blocking could also inhibit the process of maturation of melanosomes and/or the release of melanin. Moreover, it has recently observed that melanosomes released by melanoma cells, are incorporated by fibroblasts favoring their transformation into CAFs, thus promoting the formation of a pro-tumor niche. In this study, we observed that fibroblasts treated with melanoma-conditioned medium, showed the expression of melanosomal markers and increased their migratory capacity, while we did not notice differences in proliferative capacity. Of note, both fibroblasts treated with melanoma-conditioned medium and fibroblasts in co-culture with melanoma cells, generally increased the expression of α-SMA and FAP, specific markers of CAFs. Therefore, since Nar affects melanosomes release by melanoma cells, Nar treatment may prevent fibroblasts transformation. Indeed, fibroblasts cultivated with conditioned medium of melanoma cells pre-treated with Nar showed reduce migratory capacity. Finally, assessing if TPC2 modulation may influence melanoma drug responses, we observed a synergistically reduction of spheroid area after TPC2 silencing and DTIC treatment.
In conclusion, TPC2 seems to act both on melanoma cells and microenvironment, proving to be an interesting new therapeutic target and Nar may represent a new potential treatment for melanoma towards a personalized medicine.

TABLE OF CONTENTS

1. INTRODUCTION

1.1 THE ION CHANNEL TPC2

1.1.1 Two-Pore Channels (TPCs)

TPCs (*Two-pore channels*) are cation-permeable channels that belong to the superfamily of the voltage-gated ion channels [1]. The TPC gene is widespread across the animal kingdom, although of the three existing isoforms only two are present in human and other primates: TPC1 and TPC2 [2]. TPCs localize to the endo-lysosomal system, with TPC1 located on endosomes membranes, while TPC2 is mainly expressed on the membranes of lysosomes, late endosomes and melanosomes [3]. They are so-called because they contain 2 homologous Shaker-like domains with six-transmembrane (6-TM) regions (Figure 1.1). In particular, they function as a homodimer, with each subunit containing two 6-TM domain helices, in which the C-terminal of the first 6-TM domain is connected with the N-terminal of the other 6-TM by an helix-loop-helix motif [4]. The dimerization of TPCs is necessary to form the 4-domain structure that enables the channel functionality. Although homodimerization is prevalent due to the different localization of TPC1 and TPC2, their weakly overlapping subcellular distribution may well allow some heterodimerization in selected subcompartments [3,5]. The first four helices of each subunits are voltage sensing domains (VSDs), however several conserved features of a canonical voltage sensing domain are absent in the VSD1 of TPC2, thus rendering it voltage insensitive [6]. The ion conduction pore consists of the fifth and six helices, and the pore selectivity is achieved by not only a 'filter', which is an asparagine-gated size sieve, but also a gate, which opens and closes while also restricting the size and charge of ions [4,6].

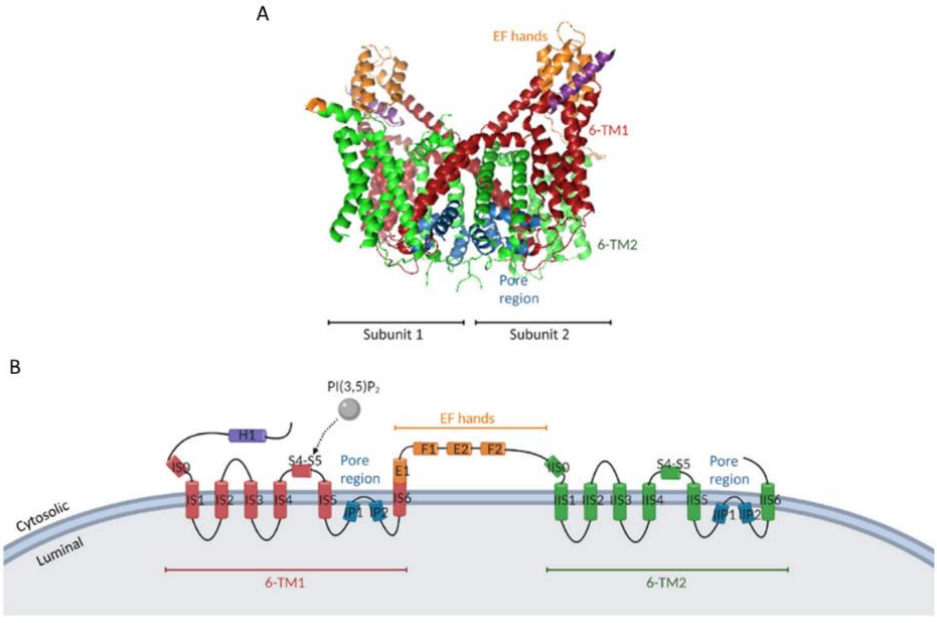

Figure 1.1 Structure of human TPC2. (A) Side view of the 3D structure of TPC2. (B) Topology and domain arrangement of a single subunit in TPC2 [4].

The mechanism of action of these channels and their regulation are not still entirely understood: different studies have shown that the channel could be activated by endolysosomal 3,5-biphosphate phosphatidylinositol [$PI(3,5)P_2$] or adenine nicotinic acid dinucleotide phosphate (NAADP) [2]. These two molecules seem to bind the channel with different mechanisms: the binding site of $PI(3,5)P_2$ is located in the first subunit of the homodimer of the channels [6], while it is assumed that NAADP does not interact directly with TPCs, but with an accessory protein not still identified [7,8].

NAADP evokes endolysosomal cations release via TPC1 or TPC2 with distinctive isoform-specific ion selectivity: TPC1 seems to be more permeable to monovalent cations as H^+ and K^+ [1,9,10]; while TPC2 mediated Ca^{2+} release from endolysosomal organelles, triggering numerous calcium-dependent signalling involved in different cellular functions. Otherwise, TPC1 and TPC2 are Na^+-selective channels, when are activated by endolysosomal $PI(3,5)P_2$ but not by NAADP [11,12], although in a study of Pitt et al. $PI(3,5)P_2$ have no effect on TPC1 open probability, but this lipid appears to alter the conducting properties of TPC1 by increasing the permeability of H^+ and Na^+ relative to Ca^{2+} [9]. TPC1 channels can also be activated by cytosolic calcium [9] and by a voltage-mediated regulation [4,6,13].

In addition to NAADP and $PI(3,5)P_2$, TPC2 channels can be regulated by Mg^{2+}, with cytosolic Mg^{2+} inhibiting the TPC2 outward current while lysosomal Mg^{2+} inhibits both the outward and inward currents [14]; protein kinases P38 and c-Jun N-terminal kinase (JNK) that inhibit TPC2 NAADP-mediated Ca^{2+} release [14] and endolysosomal Ca^{2+} concentration and luminal pH, which regulate the sensitivity and reversibility of NAADP binding via TPC2 [15]. Both TPC1 and TPC2 are N-glycosilated, probably luminally, so as to have protection in a highly acidic environment. Such glycosylation seems to regulates TPCs sensitivity to activation by NAADP as observed by mutations in the glycosylation sites near the putative pore [16].

TPCs mainly regulates Ca^{2+} release from acidic intracellular store, thus participating in a wide range of physiological processes. In the last years TPCs have been related to the regulation of many biological functions including fertilization and embryogenesis [17], roles in both insulin and glucagon secretion by the endocrine pancreas [18,19], osteoclastogenesis [20], neuronal and skeletal muscle differentiation [21,22], smooth muscle contraction [23], autophagic process of cardiomyocytes both basal and induced conditions [24] and exocytosis of cytolytic granules by cytotoxic T cells [25]. Furthermore, TPCs are involved in different pathological conditions, such as Parkinson's disease [26], Alzheimer's disease [27], fatty liver disease [28], infection with Ebola virus [29] and in cancer processes such as neoangiogenesis [30,31], autophagy [32] and metastatic progression [33].

1.1.2 TPC2 and pigmentation

Melanocytes are up to 8% of the epidermal population and are the main responsible for skin pigmentation. Although melanocytes are located in the basal layer of epidermis they lack desmosomes and tonofilaments, but they produce specific organelles, termed melanosomes, in which

melanin pigment is synthesized and deposited [34]. Melanocytes present numerous dendrites with which they contact keratinocytes for the transfer of mature melanosomes, which provides protection from the sun's ultraviolet (UV) rays. Defects in melanin synthesis cause defects in pigmentation, visual defects and increase susceptibility to melanoma [35,36].

In 2008, in a genome-wide association study on Europeans it has been noted that TPC2 has two single nucleotide polymorphisms (SNPs), M484L and G734E, responsible for the change from dark to blond hair color [37]. Both polymorphisms activate the channel: the M484L variant shows an increase in the sensitivity of the channel to PI(3,5)P2, while the G734E variant is responsible for inhibiting channel inactivation by ATP [38]. Additionally, recent studies shown that TPC2 serves as a negative regulator of pigmentation when activated by $PI(3,5)P_2$, since the Na^+ current increases melanosomal membrane potential and acidity, interfering with tyrosinase activity and melanin biosynthesis [39,40] (Figure 1.2).

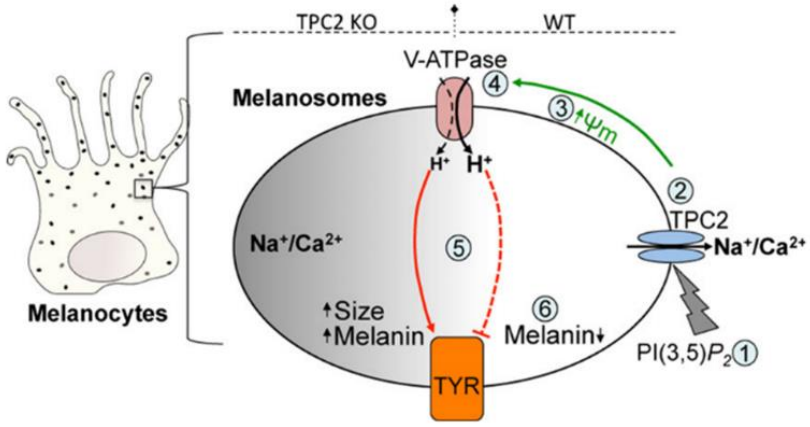

Figure 1.2 Model of regulation of pigmentation mediated by TPC2 activation in melanosomes [40].

TPC2 not only regulates pigmentation by acting on melanosome pH but also regulates melanosome size, indeed melanosomes that do not express TPC2 are less acidic and larger than the others [41]. According to previous data, people with fair skin have melanocytes with smaller and more acidic melanosomes, which present a reduced tyrosinase activity; on the contrary people with dark skin have larger and less acidic melanosomes, in which there is a higher tyrosinase activity [42,43].

Finally, it has been identified a role of TPC2 in cell pigmentation by the analysis of its interactome. Indeed, in mammalian cells TPC2 interacts with Rab GTPase, which are regulators of endolysosomal trafficking dynamics and cell pigmentation [44].

1.1.3 TPC2 in tumors

Recently the involvement of TPC2 in cancer has gained increasing attention, since it has been shown that this endolysosomal channel regulates numerous cellular functions [4]. Among the pathophysiological processes related to tumorigenesis, it has been observed a role of TPC2 in neo-angiogenesis (Figure 1.3). During this process tumor cells release vascular endothelial growth factor

(VEGF) that triggers signal transduction to facilitate Ca^{2+} signaling, leading to endothelial cell proliferation [45]. Recently it has been demonstrated that the VEGFR2/NAADP/TPC2 Ca^{2+} signaling pathway is critical for VEGF-induced angiogenesis *in vitro* and *in vivo*. In fact, both the use of Ned-19 (a NAADP antagonist) and TPC2 silencing *in vitro*, and also TPC2 KO *in vivo* mouse studies, show an inhibition of angiogenesis induced by VEGFR2 activation [30]. Similarly Naringenin, a TPCs inhibitor about we will discuss in the next paragraph, inhibits VEGF-induced angiogenesis [31], suggesting an important role of TPC2 in the neo-angiogenetic process.

TPC2 is also involved in tumor progression, since after TPC2 silencing by short interfering RNA (siRNA) tumor cells proliferate more slowly [32]. In addition, after siRNA or pharmacological inhibition with Ned-19 cancer cells show reduced adhesion, formation of leading edges and migration in *in vitro* models, and reduced formation of lung metastases in *in vivo* mouse model of mammary cancer cells [32,46].

In particular, in a mammary cancer cell line the blockage of the channel inhibits the normal recycling of β_1-integrin, a protein involved in cancer cells migration, leading to an accumulation of the protein in early endosomes [46]. According to literature, disturbances in Ca^{2+} homeostasis alter trafficking and lead to the fusion of endocytic vesicles, thus after TPCs silencing or pharmacological inhibition of the channel it has been observed an accumulation of enlarged acidic vesicles in HUH7 human liver cancer and T24 human urinary bladder cancer cell lines [46]. Moreover, in a breast cancer cell line TPC2 silencing reduces epidermal growth factor (EGF)-induced vimentin expression, but has no effect on EGF-induced E-Cadherin expression, suggesting that in this context the effect is not due to general inhibition of the epithelial-mesenchymal transition [47].

Another mechanism that seems to play a dual role in cancer is autophagy, which initially limits the growth of tumor cells in normal tissue while subsequently promotes tumorigenesis in cancer tissue by overcoming microenvironmental stresses and conferring resistance to chemotherapy [48]. The role of TPC2 in autophagy is debated, a recent study reported that TPC2 overexpression inhibited the fusion between autophagosome and lysosome, blocking the autophagic process, in 4T1 mouse breast cancer and in HeLa human cervical cancer cell lines [32].

Moreover, recently it has been seen that TPC2 is involved in the regulation of the HIPPO pathway. The channel regulates the expression of one of the main components of this pathway, TAZ, increasing in cancer cells the expression of PD-L1, that is one of the most important factors promoting the process of tumor escape [49].

Several recent studies also suggest a role of TPC2 in melanoma, in particular TPC2 blocking by Ned-19 inhibits the proliferation rate, migration and adhesivity of B16 mouse melanoma cells *in vitro* as well as growth, vascularization and metastatic potential of B16 tumors in *in viv*o mouse model [33]. Similarly in MNT-1 human melanoma cells loss of TPC2 decreases cell proliferation, migration and invasion, while increases melanin content [50]. This is possible due to independent mechanisms: via regulation of MIFT protein levels, a major regulator of melanoma progression, and on the other hand

via MIFT-independent regulation of tyrosinase activity by TPC2 [50]. On the other hand, unexpectedly, in CHL1 human metastatic melanoma cell line TPC2 is found to increase the metastatic traits. TPC2 silencing impairs cell adhesion to type I collagen matrix, increases invasion capability and induces the expression of bona fide YAP/TAZ target genes. Thus indicate an activation of YAP/TAZ, which are target genes of the HIPPO signaling pathway, that is involved in different mechanisms of tumor progression [51,52]. The opposite role played by TPC2 in different melanoma cell lines may be indicative that the function of this ion channel can be pro-tumoral or anti-tumoral according to the cell phenotype and microenvironment.

Future studies will allow to identify the mechanisms underlying the involvement of this channel in the process of tumorigenesis and metastatic progression. Therefore, TPC2 could be a new pharmacological target for the treatment of several cancers, including melanoma.

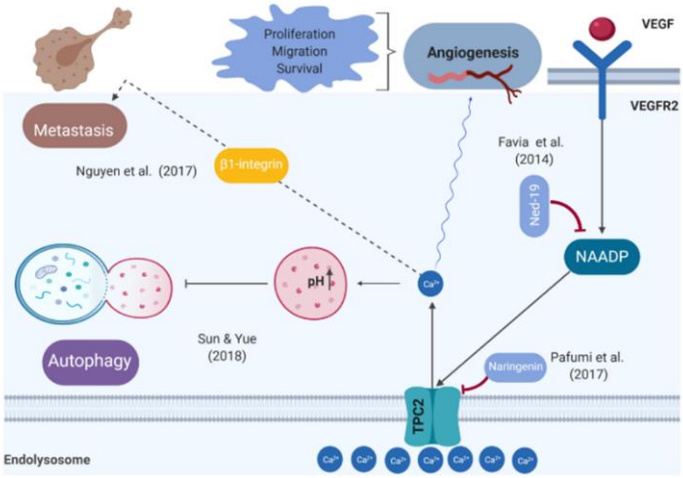

Figure 1.3 Schematic representation of the role of TPC2 in pathophysiological processes related to cancer [45].

1.1.4 Naringenin

Naringenin (Nar) [5,7-dihydroxy-2-(4-hydroxyphenyl)chroman-4-one] is a natural flavanone (a type of flavonoid) found in citrus fruits such as oranges, lemons and grapefruit and in some vegetables such as tomatoes [53,54] (Figure 1.4). Most of the reported data obtained from *in vitro* and *in vivo* studies show that Nar has broad biological effects on human health, which includes antioxidant, anti-inflammatory, anticancer and anti-diabetic activities [55,56]. At the same time, some pre-clinical studies have also suggested an efficacy in the treatment of different disorders including hyperglycemia, diabetes, liver steatosis and cardiovascular disorders [57].

Nar, thanks to the ability to cross the biological membranes by passive diffusion [58], regulates the activities of different ion channels by inhibiting or activating them. Several studies have shown that this molecule inhibits the ionic channels TRPM3 [59], TRPP2 [60], TPC1 and TPC2 [31,50], while activates BK_{Ca} channels (large conductance Ca^{2+}-activated K^+ channels) in cardiomyocytes [61]. Although the mechanism of action has not yet been fully clarified, in the most recent studies via electrophysiological analysis it has been observed that Nar reversibly blocks the conduction of TPCs

[31]. In particular, Nar antagonizes the ability of VEGF to mediate neo-angiogenesis, inhibiting the VEGF- and NAADP-evoked Ca^{2+} response in endothelial cells [31,62]. Interestingly, a study of molecular docking predicts selective binding sites for Nar in the TPC2 structure, suggesting that Nar is in contact with the hydrophobic residues that constitute the pore region of the channel, creating a physical barrier that impedes the passage of cations [63].

Recently, it has been observed that Nar regulates cellular melanogenesis, indeed treated mouse melanoma cells show an increase of intracellular melanin concentration and melanogenic proteins in a dose-dependent manner [64,65].

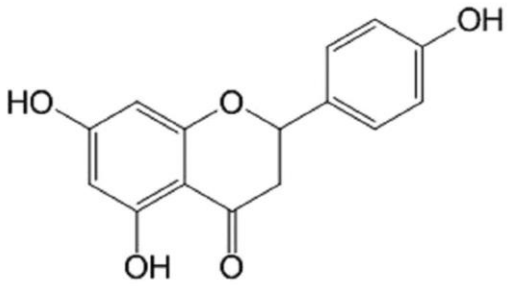

Figure 1.4 Chemical structure of Naringenin [66].

1.2 MELANOMA

1.2.1 Incidence and classification

Malignant melanoma is the most aggressive form of skin cancer and originates from melanocytes of the skin or mucous membranes [67]. Worldwide, the incidence of cutaneous melanoma has risen dramatically. It is estimated that about 1.7% of all newly diagnosed primary malignant tumors as well as 0.7% of all cancer deaths are caused by cutaneous melanoma annually. The most cases of melanoma are diagnosed in the USA and in Europe, indeed according to an American Cancer Society report are estimated 91 270 new cases of melanoma in the United States, while the European Cancer Information System (ECIS) estimated about 120 505 new cases of skin melanoma in European Union counties in 2018 [68]. Melanomas incidence and mortality rates in Europe are very different depending on the country, in Italy are estimated about 14 900 cases of melanoma in 2020 [69]. Although early-stages tumors at the time of diagnosis are treated by surgical excision, metastatic melanomas are very difficult to treat due to its high aggressiveness and resistance to common therapies [70,71]. Thus, new prognostic/diagnostic markers and druggable targets are needs to improve the accuracy of melanoma diagnosis and treatment.

Melanoma classification is very complex due to the high heterogeneity of this pathology, for this reason there are different types of classification based on different clinical or histopathological parameters. In relation to clinical and histological features, melanoma can be divided into 5 main subtypes [72]. The first subtype is nodular melanoma (NMM), that is composed of small nests and aggregates of cancer cells that together form the overall tumor nodule. It often occurs on the trunk and limbs of patients in the fifth or sixth decade of life and it is often ulcerated. This subtype does not have a RGP but only a VGP growth, and if not removed it easily metastasizes. Acral lentiginous melanoma (ALM) is uncommon in white people but it is the most common type of melanoma among asian, hispanic and african patients. Typically, it affects elderly patients. It is mainly localized on glabrous skin and adjacent skin of digits, palms and soles, and nail bed of the great toe or thumb. Lentigo maligna melanoma (LMM) correlates with long-term sun exposure and increasing age. It is characterized by RGP growth of cells that are localized to the basal layers of the epidermis, and it may evolve for decades before invading into the underlying dermis. The most common type is the superficial spreading melanoma (SSM), identified in 70% of cases. It is related to the intermittent exposure to the sun and may be due to episodes of severe sunburns in childhood. From the clinical point of view, this cancer shows a variety of colors and the lesion outline is usually sharply marginated with one or more irregular peninsula-like protrusions. The last subtype is desmoplastic melanoma (DM), which may be amelanotic and it can present as an erythematous or pale or flash-colored nodule or plaque arising in sun-damaged skin [70].

Another type is the traditional classification, which is based on Clark's method that describes the depth of invasion of melanoma cells in the various layers of the skin, identifying five different levels [73] (Figure1.5):

I. Melanoma cells are confined to the epidermis

II. Invasion into the superficial dermis

III. Invasion into the deep dermis

IV. Invasion into the reticular dermis

V. Invasion into the hypodermis

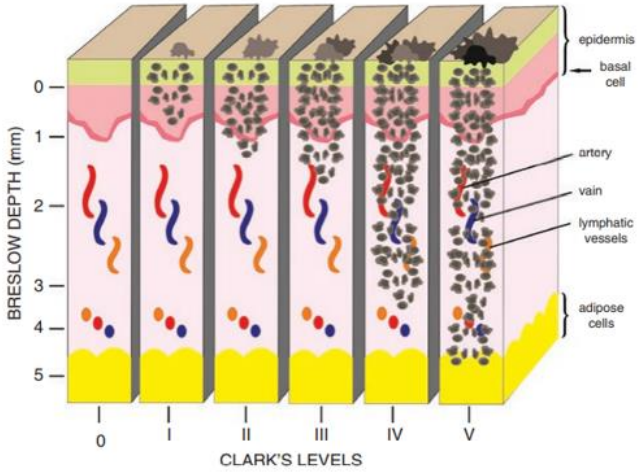

Figure 1.5: Schematic representation of Clark invasion levels and Breslow index [74].

A third method used for classifying melanoma is the Breslow index, which evaluates the depth of invasion in millimetres, measurements obtained with an ocular microtome. The stages in which melanoma is classified are 5 [75]:

I. ≥0.75mm

II. 0.76-1.5mm

III. 1.51-2.25mm

IV. 2.26-3mm

V. >3mm

Recently it has been created a new classification called TNM (tumor, nodes, metastases) staging system from The American Join Committee on Cancer, which combines the histologic information of the primary tumor, the presence and extent of regional lymph nodes disease and the presence and extent of distant metastasis [76].

- Tumor: size, depth of tumor growth (Clark's level and Breslow index), ulceration;
- Lymph nodes: presence of infiltrating cells;
- Metastasis: presence of metastatic dissemination.

Staging is important as it give clinicians the tools to assess patient prognosis and put together a treatment regimen that will give the patient the best possible chance for recovery or prolonged survival [77].

1.2.2 Risk factors and genetic alterations

Melanoma is a complex multifactorial disease, presenting genetic, clinical, histopathological and biological variants responsible for an unpredictable treatment efficacy. As said before, the main feature of melanocytes is to produce specific organelles, termed melanosomes, in which melanin pigment is synthesized and deposited. Melanosomes are subsequently transferred to keratinocytes for skin protection from UV radiations [78]. Nevertheless, exposure to UV rays is also the most important environmental risk factor for developing melanoma [70], both by excessive, intermittent exposures to solar UV radiations and subsequent sunburns, and the use of UVA-emetting indoor tanning beds. Specifically UVB induces DNA strand breaks and promotes inflammation, while UVA induces oxidative stress, which causes damage to DNA, lipids and proteins [68,79]. Other risk factors are: i) the presence and the number of melanocytic naevi, ii) family history of cutaneous melanoma [80], iii) multiple primary melanomas in a given individual, iv) immunosuppression, due both to genetic defects and ongoing therapies [81] and v) skin phototype [82]. There are also pathologies known as risk factors for melanoma, such as xeroderma pigmentosum [83], vitiligo [84] and albinism [85].

Melanoma is a complex disease involving numerous genes and displaying the highest rate of mutations among all cancers [86]. Not all variants of melanoma have the same mutational frequencies, but some recurring somatic mutations appear frequently in all types of melanomas. These driving mutations involve genes regulating different signaling pathways: proliferation (BRAF, NRAS, NF1), growth and metabolism (PTEN, KIT), resistance to apoptosis (TP53), senescence (TERT), cell identity (ARID2) and cell cycle (CDKN2A) [67,87,88] (Figure 1.6). The majority of melanomas arise from somatic mutations acquired in the course of life and only a handful of mutations may be inherited. Indeed it is estimated that only 10% of cases of melanoma has hereditary basis and that the cycline-dependent kinase inhibitor 2A (CDKN2A) mutation is the most commonly found in familial melanoma, determining a range of predisposition from 20 to 40% [89]. CDKN2A mutations lead to defects in the proteins $p14^{ARF}$ and $p16^{INK4A}$, which are important tumor suppressors that regulates the G1 checkpoint and stabilize p53 expression.

It has been estimated that 70% of melanoma cases are due to mutations in the MAPK pathway (Table 1): about 50% of melanoma cases are due to mutations in BRAF, while mutations in NRAS are responsible for an additional 15-20% of cases and in c-KIT for the 2% [77,87]. The most common mutation in BRAF is the V600E (>85% of BRAF mutations), which lead to constitutive activation of the MAPK pathway and correlates with the presence of superficial spreading melanoma (SSM). However, BRAF is mutated in up to 80% of benign naevi, therefore a BRAF mutation alone does not determine a malignant phenotype, but more mutations are needed to transform normal melanocytes into a malignant tumor [87,90]. The MAPK pathway is involved in controlling cell proliferation and survival, so when mutations lead to a constitutive activation of the pathway, cancer cells growth unchecked. Alterations of this pathway may not only be due to gene mutations but may be caused by a different regulation. In particular, it has been demonstrated that after UV radiations

ERK, JNK and P38 kinases are activated through phosphorylation of threonine and tyrosine in the activation site. Activation of these protein results in their translocation into the nucleus where they in turn phosphorylate transcription factors regulating cellular pathways such as proliferation, differentiation, development and cell death [91].

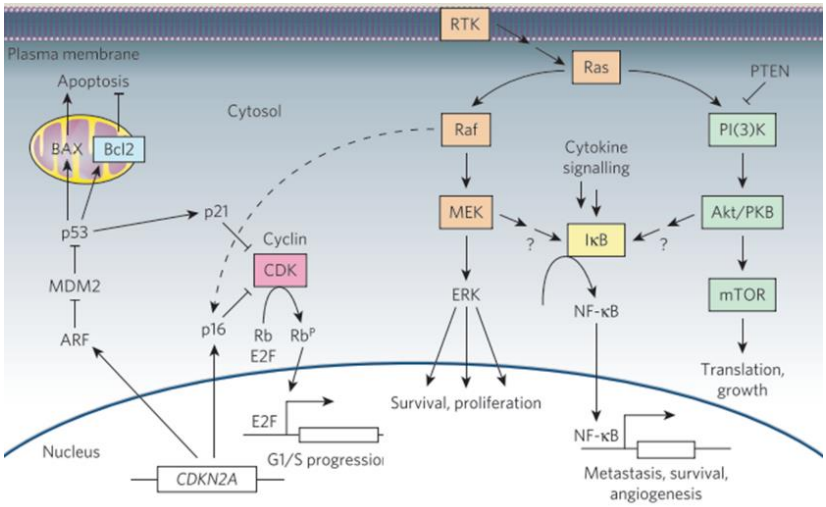

Figure 1.6: Schematic representation of the oncogenic pathways commonly misregulated in melanoma[67].

Table 1 | Selected genetic alterations in malignant melanomas

Gene type	Gene	Alteration frequency/type(s) in melanoma (%)
Oncogenes	*BRAF*	50–70% mutated
	NRAS	15–30% mutated
	AKT3	Overexpressed
Tumour suppressors	*CDKN2A*	30–70% deleted, mutated or silenced
	PTEN	5–20% deleted or mutated
	APAF-1	40% silenced
	p53	10% lost or mutated
Others	Cyclin D1	6–44% amplified
	MITF	10–16% amplified

Table 1: Frequency of genetic alterations in melanoma [67].

1.2.3 Progression

Melanoma originates from alterations in melanocytes. As a result of the progressive accumulation of spontaneous genomic mutations (except familial melanomas), also due to exposure to UV rays, melanocytes show an increase in proliferation that can be restricted to the epidermis (junctional naevus), the dermis (dermal naevus) or overlapping components of both (compound naevus) [67]. Naevi are benign alterations, since they are formed by melanocytes with limited proliferative capacity. Indeed, normally after acquiring an initial mutation, a melanocyte will undergo limited proliferation to form a naevus. Moreover, it has been hypothesized that the low levels of proliferation that occur within some naevi are counterbalanced by attritional factors such as apoptosis and immune system [78]. BRAF mutations seems to be present in 80% of cases [90,92], and some data suggest that this mutation is sufficient for naevogenesis [93]. Then, if naevi accumulate further genetic mutations may became dysplastic or atypical, characterized by an altered morphology of melanocytes with an

abnormal proliferation rate. Clinically, a dysplastic naevus is defined as a brownish patch of at least 5 mm in diameter, harbouring at least two of the following characteristics: variable pigmentation, asymmetry and/or irregular or indistinct borders [78]. Then naevus can progress to the radial-growth-phase (RGP) melanoma (Figure 1.7), an intra-epidermal lesion that may develop to the vertical-growth-phase (VGP) melanoma, a more dangerous stage in which the cells invades the underlying dermis [67]. At this stage, melanocytes invade the dermis forming niches of tumor cells and may subsequently infiltrate blood and lymphatic vessels and disseminate to local lymph nodes and distant sites. Not all melanomas develop through each of these individual phases, RGP or VGP can both developed directly from isolated melanocytes or naevi, and both can progress directly to metastatic melanoma [92].

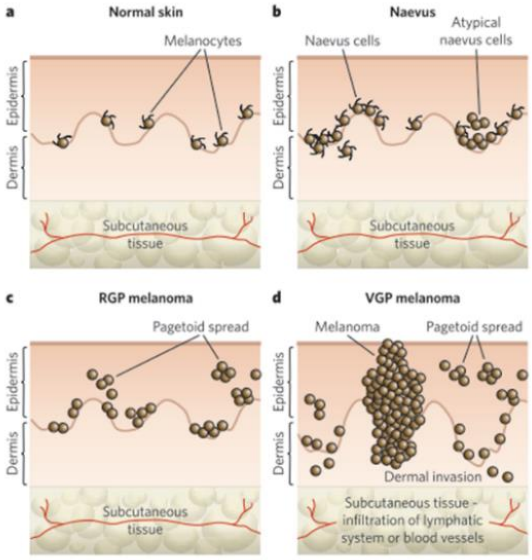

Figure 1.7: Progression of melanocyte transformation [67].

Several markers can be used to assess tumor progression, such as cadherins that are transmembrane glycoproteins involved in calcium-dependent adhesion. In the skin these molecules are expressed in different cell types: E-cadherin is the most expressed on the surface of keratinocytes, melanocytes and Langerhans cells [94], N-cadherin on the surface of fibroblasts and vascular endothelial cells of skin [95], while P-cadherin is found only in keratinocytes of the basal layer [94]. In human skin E-cadherin is involved in cellular adhesion of melanocytes and keratinocytes, and a reduced expression or lack of functionality of this protein leads to loss of cell-cell contacts and increase in tumor invasion. Indeed melanoma cells presents not only a down regulation of E-cadherin, but also an up-regulation of N-cadherin, this process termed as “cadherins switch” leads melanocytes to acquire new adhesive properties and altered spatial relationships that can facilitate proliferation, migration and invasion of melanoma cells [96,97]. Recently in a study that used matched tissue samples from primary and metastatic sites of melanoma, it has been observed that metastatic tumor showed a decrease in E-cadherin expression and an increase in N-cadherin expression compared to the primary tumor,

although the difference did not reach statistical significance [98]. The ability of neoplastic cells to invade the basal membrane and colonize other tissues is due to the loose of epithelial characteristics and the acquisition of a mesenchymal phenotype through a process known as the epithelium-mesenchymal transition (EMT). Another important marker involved in the EMT is Slug, a transcriptional repressor of E-cadherin [99]. Apart from these roles, Slug is also a survival molecule that promotes resistance to apoptosis in some cell contexts. In melanoma, it was shown that Slug functions as a melanocyte-specific factor required for the strong metastatic propensity of this tumor [100]. Even integrins may be use as tumor markers, because of their central role in mediating invasion and metastases. Numerous studies have shown a different expression of integrins in normal melanocytes and benign naevi compared to melanoma cells [101]. In particular, $\alpha_7\beta_1$integrin, binding laminin, has been detected in melanoma cells and not in normal melanocytes [102]. Similarly, $\alpha_4\beta_1$integrin is not express in primary and dysplastic naevi, while in melanoma the expression correlates with the progression from radial to vertical growth phase [103,104]. This integrin contributes to tumorigenesis and facilitate cells infiltration in blood and lymphatic vessels, promoting metastatization [105,106]. In according to these data, several studies have shown a direct correlation between $\alpha_4\beta_1$integrin expression, metastatic onset and reduction of disease-free survival [104].

1.2.4 Diagnosis

Since melanoma is characterized by high aggressiveness and mortality, early detection is needed to prevent the progression of the disease. A well-established guide to examine and interpret pigmented lesions for both health care professionals and patients has been the "ABCDE" criteria, which evaluates 5 macroscopic parameters: asymmetry, border, color, diameter and evolution [107]. Indeed melanoma is clinically recognized on the basis of morphological features such as raised surface, irregular shape, shades of color, sometimes superficial ulcerations, bleeding, inflammation, itching and pain. Moreover, various assistive optical devices, as dermatoscopes, are becoming part of routine clinical practice for a more detailed examination of the skin and in particular, pigmented lesions. Dermoscopy is a non-invasive diagnostic technique for *in vivo* observation of the epidermis. This device uses optic magnification associated with an incident light to permit visualization of morphological structures that are not visible to the naked eye [108]. A further technique is the Reflectance Confocal Microscopy (RCM), that allows non-invasive examination of native skin in real-time at a nearly histologic resolution. The reflectance confocal microscope emits a near-infrared, coherent laser beam that illuminated human skin. The image provides information on cells morphology of the skin lesion in the various layers, up to the dermal papillae [109].

The diagnosis of melanoma requires that a lesion be recognized as clinically atypical and biopsied. Once a lesion has been biopsied, a microscopic analysis is performed based on a variety of classic histopathological features. However, melanoma is a heterogeneous disease and some histologic variants are not easily recognizable by traditional hematoxylin and eosin (H&E) examination alone

[77]. So, there are other types of biomarkers commonly used for diagnostic and prognostic purpose: melanocytic markers and proliferative markers. Melanocytic markers are used to determine the melanocytic origin in case of ambiguous lesions, while proliferative markers are used to evaluate the cell cycle activity in a lesion [77]. The first are proteins involved in the typical processes of melanocytes, such as melanin synthesis, melanosomes biogenesis and melanocytes differentiation [110]. MART1 (Melanoma Antigen Recognized by T-cells-1) identifies a cytoplasmatic protein present during the process of melanosome differentiation [111]. This antigen was first detected in melanoma metastases and is now one of the most important melanocytic markers. Two different antibodies detect this antigen: MART1 and A103, generally referred to as Melan-A. Another melanocytic marker is HMB45, an antibody that recognised the glycoprotein gp100 (Pmel17) that is essential for melanin polymerisation, melanosome biogenesis and melanogenesis [77,111]. These two markers have some of the highest specificity, however they are also positive in few other types of skin lesions [110]. An additional marker for the identification of cancer cells with melanocytic origin is S100, an acidic calcium-binding protein that is present in the nucleus and cytoplasm. This marker is the most sensitive for melanocytic differentiation, it has a higher sensitivity than HMB-45 and MART1, but a low specificity for the melanoma because it is also positive in nerve sheath cells, myoepithelial cells, adipocytes, chondrocytes, Langerhans cells and associated tumors [112]. Finally, other common melanocytic markers used in melanoma diagnosis are: MITF (Micropthlamia Transcription Factor), a transcription factor necessary for the development of melanocytes during embryogenesis and the regulation of melanin synthesis, which produce a nuclear staning; tyrosinase, an enzyme that hydroxylates tyrosine in the first step of melanin synthesis and in melanomas can be seen as fine granular cytoplasmic staining; SOX10, a transcription factors involved in the regulation of embryonic development and determination of cell fate, essential in the formation of melanocytes [111,113]. Among the proliferation markers the most commonly used is Ki67, a protein involved in ribosomal transcription, expressed in the active phases of cell cycle and absent in G0. Its expression is associated with cell proliferation and is high elevated in the most aggressive melanomas [114,115].
Moreover, some additional techniques such as fluorescence in situ hybridization (FISH), comparative genomic hybridization (CGH) and sequencing and mass spectrometry (MS) may be utilized to improve the diagnosis [116]. In 2005, an interesting study shown the possibility of classifying melanomas by clinical-histopathological subtypes with 70% accuracy, analyzing alterations in the number of copies of DNA and individual somatic mutations [117]. So, in the future the detection of specific genetic alterations could therefore be used to improve the diagnosis and prognosis of the patients.

1.2.5 Therapies

If diagnosed in early stages melanoma is curable by surgical resection, while once it has progressed to the metastatic site the prognosis is highly unfavorable. Melanoma is an extremely aggressive

cancer, with high metastatic potential and high resistance to cytotoxic agents. Melanoma cells compared to other types of tumours have low levels of spontaneous apoptosis *in vivo*, and are relatively resistant to drug-induced apoptosis *in vitro* [71]. Metastatic melanoma is largely refractory to existing therapies and has a very poor prognosis, with a median survival rate of 6 months after diagnosis and 5-year survival rate of less than 5% [118].

At first, after melanoma surgical excision the most used pharmacological treatments were IFN-α, IL-2 and several chemotherapeutic drugs, including dacarbazine (DTIC) and paclitaxel, which unfortunately little contribute to overall patient survival [119]. In the last years, the identification of new signalling pathways that play central roles in melanoma initiation and progression has led to the development of targeted therapy and immunotherapy [67,77]. At the time, for patients with metastatic melanoma the first step is the evaluation of the functional state of BRAF, which is mutated in 40-50% of skin melanomas. For these patients are currently used combinations of BRAF/MEK inhibitors (vemurafenib/cobimetinib; dabrafenib/trametinib). However, though these drugs are highly effective for approximately half of patients with BRAF mutated melanomas, a majority of patients develop secondary resistance within a relatively short amount of time [77,120,121]. In these cases, or in patients who do not have BRAF mutations, the most effective treatment is the use of immunotherapeutic drugs, as anti PD-1 (nivolumab; pembrolizumab) or anti CTLA-4 (ipilimumab) [122,123]. Although immune checkpoint inhibitors have revolutionized the treatment of metastatic melanoma, a significant subset of patients still does not respond to these drugs, and many patients who do respond develop a secondary resistance [77]. Therefore, there is a great interest in finding new pharmacological targets for the development of new treatments for melanoma.

1.2.6 Melanosomes and role of pigmentation in melanoma

Melanin is synthetized from tyrosine which first is converted into L-DOPA by the enzyme tyrosinase (Figure 1.8). Two types of melanins are produced according to the availability of substrates and the function of melanogenetic enzymes: pheomelanins and eumelanins. Pheomelanins are brown, red and yellow pigments, formed by oxidation reactions involving cysteine residues [124]. On the contrary, the black and brown pigments eumelanins are synthetized in the absence of cysteine and with use of tyrosinase-related proteins (TRP1, TRP2/DCT) enzymes [125]. The production of dark melanins [DHI (5,6-dihydroxyindole) -melanins] maximizes photoabsorption, but at the same time increases cytotoxic effects, while light brown melanins [DHICA (5,6-dihydroxyindole-2-carboxylic acid) -melanins] have lower photoabsorption and toxic effects. Finally pheomelanins provide a very low photoabsorption, almost or completely zero, but do not produce cytotoxic effects [126–129].

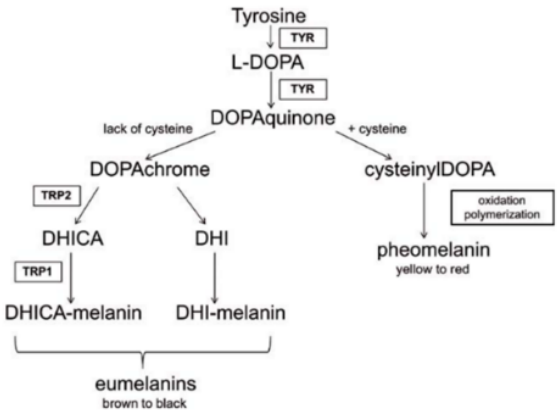

Figure 1.8: The simplified scheme of the melanin synthesis in melanocytes during melanogenesis [130].

Since many cytotoxic agents are formed during melanin synthesis, to avoid their interaction with other cytosolic components the process of melanization takes place in melanosomes. [131]. These organelles are lysosome-related organelles (LROs) as they have some common features with lysosomes such as a low luminal pH, numerous enzymes including lysosomal hydrolases and many membrane proteins [132–134]. Among the LROs melanosomes are specialised in biosynthesis, storage and transport of melanin in epidermal and ocular melanocytes and in pigment epithelia of the retina, iris and ciliary body of the eye [133]. Melanosome function depends on cell type: in retinal pigment epithelial cells melanosomes absorb stray light that did not interact with the retinal photoreceptors and probably trap free radicals [135], while in epidermal melanocytes melanosomes mediate the transfer of melanin to keratinocytes, leading to skin and hair pigmentation [136]. In addition to the determination of the phenotypic aspect, melanin is involved in a number of important functions [137], such as balance and auditory processing [138], absorption of drugs and toxic chemicals substances [139] and neurological development during embryogenesis [140–142]. However, the most important role is the protection against UV, which are cause of DNA damage, cellular aging and carcinogenesis [131].

As said before, keratinocytes need melanin for their own photoprotection. Physiologically, in keratinocytes UV radiations induce α-melanocyte stimulating hormone (α-MSH) secretion, which binds the melanocortin 1 receptor (MC1R) on melanocytes. The activation of this signaling pathway induces cell proliferation and melanin synthesis [143]. Therefore, melanocytes are able to respond to external signals by producing mature melanosomes, which will be transferred through cell extensions to neighbouring keratinocytes. Melanosomes develop following 4 sequential stages [144] (Figure 1.9) beginning with the formation of pre-melanosomes (stage I), that are membrane-delimited electron-lucent structures, similar to vacuoles and still without pigment. Stage II pre-melanosomes have a more elliptical structure, with intralumenal proteinaceus fibrils mainly formed by Pmel17 glycoproteins (and MART1, which regulates the formation of Pmel17 fibrils) that are present along their entire length. Once the fibrous striations are fully formed, melanin synthesis begins. Melanin is deposited on the fibrils, resulting in their thickening and blackening with maturation to stage III until

all internal structure is masked in stage IV. This accumulation of pigment on fibrils may avoid the spread of melanin during the transfer of organelles from melanocytes to keratinocytes. Early melanosomes (stage I and II) do not contain melanin and are usually located at the center of the cytoplasm, while late melanosomes (stage III and IV) that are strongly pigmented predominate in the distal dendrites of melanocytes, the main site of secretion [133]. Early and late melanosomes have different features, such as different proteins enrichment. For example Pmel17, a type I transmembrane glycoprotein also known as gp100, that serves as the structural foundation of the fibrils, is present mostly in early melanosomes, while the melanin biosynthetic enzymes tyrosinase, TRP1 and DCT are enriched in stage III and IV [133,145].

Interestingly, it has been observed that different melanins are synthesized in differential types of melanosomes, but both may be present in the same melanocyte [146]. The eumelanosomes are morphologically larger, elliptical and contain a fibrillar matrix, while pheomelanosomes are smaller, spherical and have a loose matrix organization [131,147].

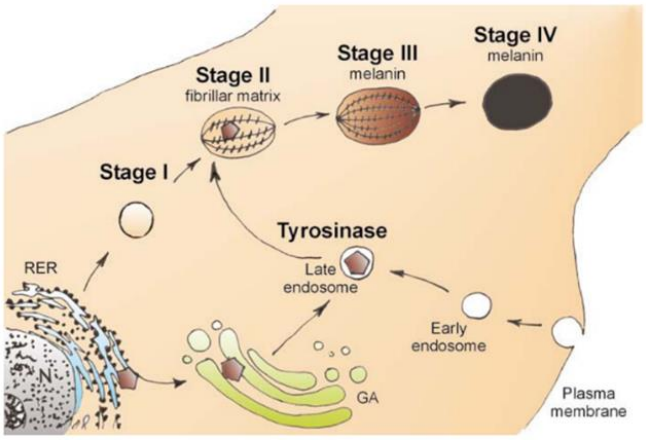

Figure 1.9: Scheme of the melanin synthesis in melanocytes during melanogenesis [130].

Melanoma cells retain the ability to produce and release melanosomes, indeed keratinocytes surrounding melanoma cells often show an abnormal distribution of melanin [148]. Changes in melanosomes biogenesis and pigment production are associated to cellular transformation in melanoma, indeed it has been observed that some melanocytes lose their ability to synthesize pigments and assume a disorganized structure [124,149,150]. Moreover, if on the one hand in healthy melanocytes melanin production protects from UV radiation and oxidative stress, on the other hand it has been observed that melanin can make melanoma cells resistant to therapy [151]. In according to these data, in patients with advanced melanomas the high production of melanin is inversely related to patient survival and disease-free survival [152]. Otherwise, in a recent study in mouse model it has been demonstrated that melanin synthesis by human melanoma cells inoculated in mouse inhibits their ability to spread and metastasize [153].

1.3 TUMOR MICROENVIRONMENT

1.3.1 Microenvironment

The TME (Tumor Microenvironment) is the cellular environment in which the tumor exists. Increasing evidence suggests that TME play an active role rather than simply acting as a by-stander in tumor progression. In fact, only through reciprocal communication, cancer cells and the microenvironment act in collusion leading to high proliferation and metastatic capability [154]. Apart from the tumor cells, the TME includes surrounding blood vessels, extracellular matrix (ECM), other non-malignant cells and signaling molecules.

The normal cells included: stromal cells, fibroblasts, immune cells (such as T lymphocytes, B lymphocytes, natural killer cells, natural killer T cells, tumor-associated macrophages, etc.), as well as pericytes and sometimes adipocytes. Stromal cells and fibroblasts secrete growth factors, such as hepatocyte growth factor (HGF), fibroblast growth factor (FGFs) and CXCL12 chemokine, which not only promote growth and survival of cancer cells but also function as a chemoattractant that stimulates the migration of other cells into the TME [155]. In addition, accumulating evidence have confirmed that tumor cells must recruit and reprogram the surrounding normal cells to serve as contributors to tumor progression, such as for fibroblasts that may be transformed into cancer-associated fibroblasts (CAFs) [154].

Other critical factors are chemokines and cytokines, which are secreted into the TME to recruit and activate various inflammatory cells, among these macrophages represent the majority. Cancer-related inflammatory microenvironment is important to induce cancer cell evasion from immune destruction, thus tissues with chronic inflammation generally exhibit high cancer incidence [154,156].

Another key component of TME is the ECM, composed of proteins, glycoproteins, proteoglycans, and polysaccharides with different physical and biochemical properties. ECM not only provide a physical scaffold for all the cells of the TME but also is abundance of growth factors. During cancer development ECM is commonly deregulated and becomes disorganized in later stages of tumor progression. For example, it has been observed that ECM is essential for the establishment and maintenance of tissue polarity and architecture, and abnormal ECM dynamics compromise the basement membrane and promote EMT, facilitating tissue invasion by cancer cells [157]. Moreover, abnormal ECM can dysregulate the behavior of stromal cells, promoting inflammation and angiogenesis processes. Interestingly, primary tumors with distinct metastatic potential differ in their ECM components. Indeed, the composition of the extracellular TME has been used a predictor of clinical prognosis [158].

Tumors also require the formation of a complex vascular network to meet the metabolic and nutritional needs for growth. For instance, stromal cells secreted VEGF, PDGF (platelet derived growth factor), bFGF (basic fibroblast growth factor) and IGF1 (insulin-like growth factor-1) to stimulate angiogenesis. When a quiescent blood vessel senses an angiogenic signal from growth factors or hypoxic conditions, heterogeneous new vessels with chaotic branching structures sprout

from the existing vasculature. However this new vasculature is often inadequate, leading to hypoxic and acidotic regions [159]. Furthermore, the tumor blood vessels exhibit an uneven vessel lumen and are usually leaky, which raises interstitial fluid pressure leading to unevenness of blood flow and nutrient, as well as drug distribution [158].

Although the composition of TME is heterogeneous in different tumor types, there are common features that contribute to chemoresistance and that may be use as therapeutic targets. Indeed, several recent studies have revealed that targeting chemokines and adhesion molecules, can improve the response of cancer cells to chemotherapy by increasing the access of drugs to the tumor [158].

Finally, cancer cells mainly rely on aerobic glycolysis rather than mitochondrial oxidative phosphorylation, generating lactate which contributes to acidic condition, ROS production and MAPK signaling activation [154]. All these TME conditions, including oxidative stress, low pH environment and nutrient deprivation contribute to genetic instability through the induction of enhanced mutagenesis and an impaired DNA damage pathway [160].

1.3.2 Melanoma microenvironment

Melanoma cells actively interact with the TME in a bidirectional manner, through direct cell-cell and cell-matrix communications, growth factors and secreted cytokines [161].

The interaction between keratinocytes and melanocytes of the epidermis contributes to the initial development of the tumor [162]. In human epidermis there is a constant ratio of keratinocytes to melanocytes 35:1 in the epidermal layer, and under normal conditions keratinocytes control melanocyte localization and proliferation through the secretion of grow factors and intercellular communication with adhesion molecules. The deregulation of this balanced system may induce melanocytic proliferation, leading to the transformation into naevus or melanoma [162]. An abnormal proliferation occurs when melanocytes downregulate the expression of cell adhesion molecules such as E-cadherin, P-cadherin, desmoglein, and connexins [163]. In melanocytes, E- cadherin is associated with cell-to-cell adhesion properties and loss of E-cadherin leads to an invasive phenotype often linked with transformed cells [164]. Not surprisingly, reintroduction of E-cadherin into melanoma cells renders them less motile, likely through a keratinocyte-regulated mechanism [96]. This protein can be downregulated by several mechanisms such as by the repressors Slug and Snail, that inhibit its transcription in melanoma cells. The switch from E-cadherin to N-cadherin allows melanoma cells to interact with other N-cadherin expressing cells such as fibroblasts and endothelial cells, increasing their motility due to less stringent cell interactions. Moreover, N-cadherin confers a survival advantages through repression of proapoptotic factors [161]. Another important class of proteins that are deregulated during melanoma progression are integrins, heterodimeric transmembrane proteins that promote the adhesion of cells to the ECM and play an important role in processes of proliferation, migration, invasion, angiogenesis and survival. Alterations in integrin expression allow melanoma

cells to dissociate from the primary site, alter the cytoskeleton, migrate through the contiguous stroma, and eventually disseminate through lymphatic or vascular vessels to distant organs [161].

During the early stages of tumor development, melanoma cells activate different mechanisms that allow them to migrate, invade, and survive outside the tumor niche (Figure 1.10). For example, compared to melanocytes, melanoma cells secreted bFGF, to promote proliferation and survival in an autocrine manner. Moreover, these cancer cells secreted PDFG, TGF-β (transforming growth factor) and VEGF that exercise paracrine functions in angiogenesis and stroma formation by inducing proliferation and activation of fibroblasts and endothelial cells [161].

An example of the continuous bidirectional cross-talk between tumor and microenvironment is the reciprocal activation between melanoma cells and stromal fibroblasts. Melanoma-secreted PDGF stimulates fibroblasts to produce and secrete IGF-1, which in turn stimulates the growth of cancer cells in a paracrine manner. Additionally, activated fibroblasts release bFGF and endothelin promoting melanoma growth (Ruiter 2002-melanoma stroma interactions: structural and functional aspects). Both melanoma and stromal cells also produce and secrete large quantities of MMPs (matrix metalloproteinases), enzymes involved in ECM degradation and tissue remodelling, thus promoting melanoma progression [161].

Finally, there are subcompartments within tumours itself with different microenvironmental milieu created by differential access to oxygen and nutrients. Therefore, melanoma cells within a tumour have different microenvironments [162].

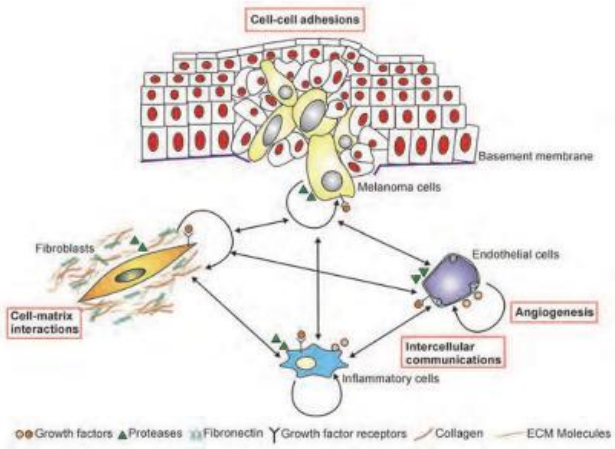

Figure 1.10: Interaction between melanoma cells and stromal microenvironment. These interactions promote changes in cell-cell, cell-matrix adhesions and in the process of angiogenesis [160].

1.3.3 CAFs

One of the most important components of the microenvironment are fibroblasts, whose physiologically are responsible for the deposition of the ECM, regulation of epithelial differentiation and control of inflammation and wound healing. Fibroblasts synthetize many components of the ECM such as type I, type III and type V collagen, fibronectin and contribute to the formation of the

basal membrane by secreting type IV collagen and laminin [165]. In the TME fibroblasts can be transformed into cancer-associated fibroblasts (CAFs). Both CAFs and normal fibroblasts express fibroblast-specific markers, such as fibronectin and vimentin, while molecules that are normally considered to be activation markers, including α-SMA (α-smooth muscle actin), S100A4, and FAP-α (fibroblast activation protein), are only expressed by CAFs [166,167]. Specifically, FAP is a serine protease with collagenolytic and dipeptidyl peptidase activities capable of degrading type I collagen, thus enhancing ECM remodeling and facilitating tumor growth and migration [168,169]; while α-SMA is an actin protein that promotes the contractile action of fibroblasts. This protein is known as a myofibroblast marker, indeed CAFs have similar properties to the activated myofibroblasts (fibroblast with features that are more typical of smooth muscle cells) found under inflammatory conditions or during wound healing [166]. CAFs exhibit both phenotypical and physiological differences compared to normal dermal fibroblasts, which under normal healthy conditions appear to be quiescent and function to maintain tissue homeostasis. Indeed, compared with normal fibroblasts, CAFs have increased rates of migration and proliferation capability [170]. For example, skin fibroblasts isolated from patients with breast cancer, malignant melanoma, familial polyposis coli, retinoblastoma and Wilms tumours show an increased proliferation rate in *vitro*, suggesting that CAFs possess an increased proliferative activity compared to fibroblast [165].

As mentioned, CAFs can derive from fibroblasts, indeed some experimental data indicate that cancer cells secrete high levels of TGF-β, which is chemotactic for fibroblasts and induces their transformation into CAFs (Figure 1.11). However, the original source of CAFs remain controversial. Other cell types that can be transformed into CAFs are epithelial cells, endothelial cells, cancer cells, myofibroblasts and human bone marrow-derived mesenchymal stem cells (hMSCs) [154].

Compared to normal fibroblast CAFs are able to: synthesize, deposit and remodel the ECM; secrete different cytokines and growth factors, which promote cancer cells growth and influence cell-cell interactions; promote angiogenesis and inflammation; modulate the immune system; influence drug access and therapy response [154,166,171]. Thus, CAFs promote cancer development from initiation, to primary and metastatic progression and favour drug resistance. *In vivo* experiment demonstrated that CAFs facilitate the invasiveness of otherwise non-invasive cancer cells when co-injected into mice [172] and xenografts of breast cancer cells co-injected in suspension with CAFs grew larger that xenografts infused with normal fibroblasts [173].

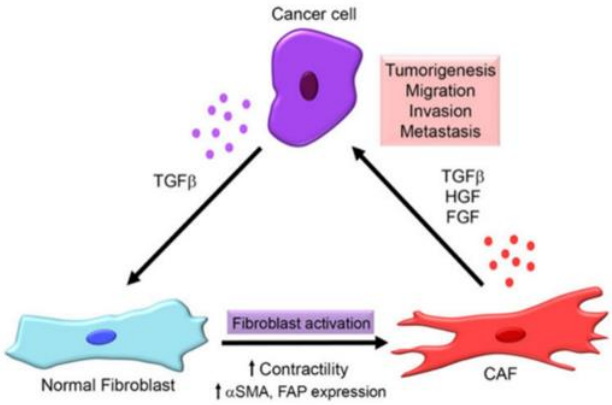

Figure 1.11: Interaction between neoplastic cells and CAFs in the TME [174].

As mentioned above, TGF-β has a role in the recruitment and transformation of fibroblasts, however it is a paradoxical growth factor in that it can both suppress and promote tumor progression in the proper cellular context. Before the initiation of cancer, and during the early stages of carcinogenesis, TGFβ probably functions as a tumour suppressor. Indeed, in normal tissues, the anti-proliferative and pro-apoptotic response of epithelial cells to TGFβ might limit the growth of normal epithelium and the emergence of malignant carcinomas. On the contrary, during advanced stages of cancer, TGFβ facilitates EMT of cancer cells, potentially promoting invasiveness and metastasis [165,175]. For example, CAFs-secreted TGF-β induces the expression of mesenchymal markers such as vimentin, fibronectin, MMP2 and MMP9 in breast cancer cells (Figure 1.11). So, CAFs expressed numerous protein involved in matrix remodelling, such as SNAIL, a transcriptional factor that responds to TGF-β and regulates EMT in cancer cells by suppressing E-cadherin expression [174]. Interestingly, it has been observed that melanoma-derived TGF-β has a growth inhibitory effect on epithelial cells and melanocytes, but melanoma cells themselves are resistant to these inhibitory effects. In addition, the paracrine secretion of TGF-β promotes increased deposition of ECM, angiogenesis, survival, immunosuppression, and transition to more aggressive phenotypes [161].

Recently Dror and collaborators [148] report that melanosomes participate in the communication between primary melanoma cells and their microenvironment, promoting the activation of dermal fibroblasts into CAFs (Figure 1.12). These activated fibroblasts not only show an increase in proliferation, motility, collagen contraction and upregulation of proliferation- and migration-associated genes and pro-inflammatory cytokines, but also increase melanoma cells proliferation and migration capability. Moreover, although in physiological conditions skin fibroblasts incorporate about 100 melanosomes, Dror et al. quantified 200–500 melanosomes per melanoma dermal fibroblast, indicating increased uptake under pathological conditions. Fibroblasts reprogramming into CAFs appeared to be mediate, at least in part, by miRNA-211, that targets IGF2R and leads to MAPK activation. Thus, it is supposed that melanoma forms a pro-metastatic dermal niche via melanosomes trafficking, promoting tumor invasion and progression [148].

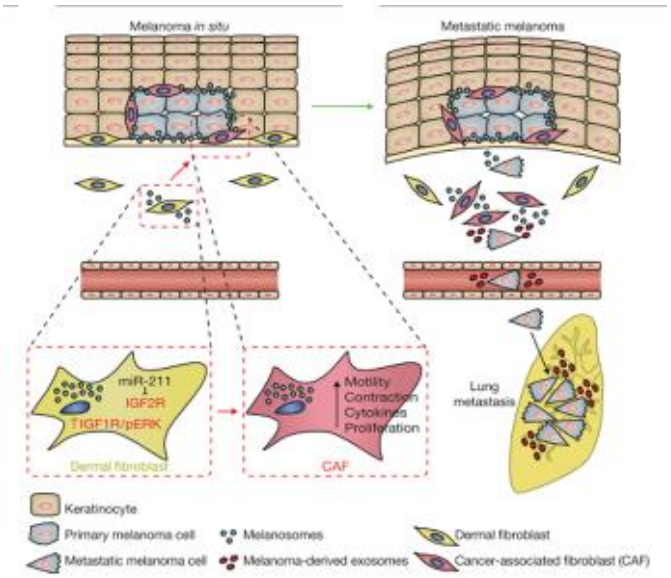

Figure 1.12: The melanosomes mediate the transformation of fibroblasts into CAFs favoring the tumor process [176].

1.4 THREE-DIMENSIONAL MODELS FOR MELANOMA

1.1.1 Multicellular spheroids

Three-dimensional cell cultures are models widely used in biomedical research and in the development of new drugs because they mimic better than two-dimensional culture the characteristics of the tumor *in vivo* and at the same time are considered a valid alternative to the use of animal models, that are much more complex and expensive. Three-dimensional models for melanoma can be divided into two categories: spheroids and skin equivalent [177]. Tumor spheroids can in turn be divided into: multicellular tumor spheroids, tumorospheres, spheres from partial tissue dissociation, and multicellular organotypic spheroids. Each of these models presents some specific characteristics that make it more or less suitable for different applications, such as hypoxia [178], cell metabolism [179] or invasion studies [180,181].

It is well known that spheroid models simulate better than 2D cultures many of the complex properties of the tumor *in vivo*, including cell-cell adhesion, barriers to mass transport, ECM deposition, cell-matrix adhesion, the sensitivity and resistance to drug and a necrotic core surrounded by a viable layer of quiescent and/or proliferating cells [182,177,183]. Indeed, it has been observed that the morphology of a spheroid presents three major layers [183] (Figure 1.13). The outer layer has the high proliferative capacity: cells are extremely active both in proliferation and metabolism, and nuclei are intact. More internally there is a quiescent layer, where cells have reduced metabolic functions that may be activated in the presence of nutrients, and smaller nuclei compared to those of the proliferative layer. Finally, the center of the spheroids with a diameter of more than 500μm is defined necrotic core and presents not-viable cells. This area is characterized by a lack of oxygen and nutrients due to their limited diffusion and by an accumulation of toxic substances due to cell metabolism that cannot be eliminated. For this reason there is a limited size that can be reached by spheroids [184]. Initially, during spheroids formation cells aggregates by interaction of cellular surface integrins with ECM fibers. Then cell-cell contact leads to an increase of E-cadherin expression, which accumulate on cellular surface and interact by homophilic bonds, forming solid aggregates [183,185,186]. The aggregation is also influenced by actin, that initially promotes contacts between adjacent cells, while after spheroids formation localized to cell periphery, giving compactness to the sphere [187,188].

Interestingly, 2D cultures of melanoma cells (primary, RGP or VGP and metastasis) fail to show differences among lines, while 3D spheroids show well distinct morphologic features and growth curves, reflecting the *in vivo* behaviour of the original tumor cells [177]. Tumor spheroids can also be enrich using different cell types such as fibroblasts, endothelial and immune cells, forming co-cultures models that allow to analyze the interactions between different cell populations [189]. For example, it has been generated spheroids composed with fibroblast and melanoma cells to study the role of stromal cells and factors in the growth and maintenance of tumors as well as their potential impact on treatment resistance [190]. Similarly, it has been demonstrated that a 3D model of fibroblasts,

keratinocytes, and melanoma cells, mimics the features observed in early melanoma stages, including loss of keratinocyte differentiation, melanoma cell invasion, and drug-induced increase of ABCB5 expression in external melanoma cells [191]. The insertion of all the components lead to the formation of a complex model called minitumor spheroid, which best summarizes the complex structure of the tumor *in vivo*.

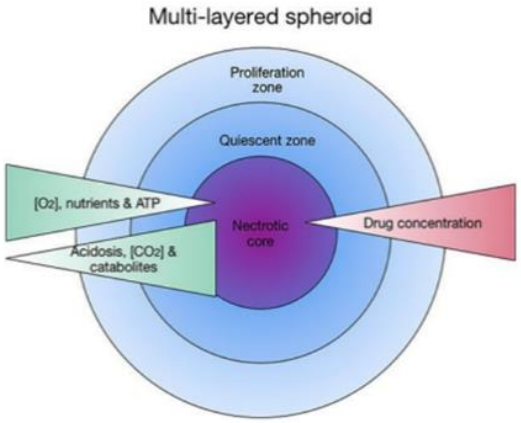

Figure 1.13: Schematic representation of a spheroid structure and gradient of concentrations of molecules through the layers [192].

1.1.1 Skin equivalents

Human skin equivalents (HSEs) are advanced three-dimensional *in vitro* models of reconstructed skin, consisting of primary cutaneous cells (keratinocytes, melanocytes and fibroblasts) and ECM components. For architecture and composition their closely resemble human skin, although they do not fully reproduce the complexity of the skin microenvironment. The main advantages are that artifacts due to 2D culture are minimal and it is possible to study the interactions between different cell populations. HSE consists of dermis and epidermis, of which the first is formed by viable fibroblasts included in rat tail or bovine type I collagen ECM, while epidermis is composed of melanocytes and keratinocytes, differentiated due to air exposure of the culture. The first step is dermis construction, that not only provides the scaffold of the model, but is also responsible for cell nutrition and gives the possibility of cell-cell interactions. Subsequently, onto the dermis are seeded keratinocytes, that stratify and contribute with fibroblasts to the formation of a functional basal membrane [193,194]. A different technique is based on the use of de-epidermised dermis (DED). DED derived from skin biopsy of a donor, that is deprived of the epidermal layer by overnight incubation in sodium chloride and digested with Dispase II to remove the basement membrane. Histologically, this model appears very similar to the skin *in vivo* and can be used as scaffold for primary keratinocytes, fibroblasts and melanoma cancer cells seeding [193].

The three-dimensional models of HSEs are used for numerous studies involving: skin barrier functionality, skin aging, UV radiation damage and photoprotection [194], bacterial infections [195],

irritation [196], skin diseases and wound healing [197]. Moreover, in HSEs it is possible to incorportate cancer cells, for example forming the melanoma skin equivalents (MSEs), which allow to study the development of melanoma in a microenvironment similar to the *in vivo* [177,193]. Interestingly, not only melanoma cells can be seeded together with primary keratinocytes on the reconstructed dermis, but tumor spheroids can also be incorporate within the dermis, to better mimic the original microenvironment of different melanoma subtypes [198,199]. It has been demonstrated that in MSEs melanoma cells from different stages of disease show the same properties of the tumor *in vivo*, so cells from a melanoma in situ are not able to invade the dermis, while cells of VGP or metastatic melanoma are able to invade the dermis [193,200]. Recently, MSE models have been used in pre-clinical studies to test efficacy, penetration and absorption of anti-tumor drugs, allowing also the simultaneous assessment of non-cancer cell toxicity in the microenvironment [188,201].

Giving that in the skin there are numerous cell types such as immune system cells, endothelial cells and adipocytes in the hypodermis, several researchers have tried to generate even more accurate and predictive models, as an higher skin equivalent containing the hypodermic components [202].

2. AIMS

Melanoma is most aggressive form of skin cancer and its incidence is rising steadily in western populations. Although early melanomas can be cured by surgical excision, metastatic are very difficult to treat due to its high aggressiveness and resistance to common therapies. Despite the great progress made on therapeutic strategy, only 5-10% of patients with metastatic melanoma achieve 5 years long-term survival due to cell resistance. Therefore, there is a great interest in finding new pharmacological targets for the development of more effective therapeutic treatments.

A factor that may be a mediator of melanoma progression is TPC2, a Ca^{2+} ionic channel activated by NAADP that localized on the membrane of intracellular acidic compartments, including melanosomes. This channel appears to be involved in several pathological conditions and in numerous aspects related to tumorigenesis and metastasization. In mouse melanoma cells, the inhibition of NAADP signaling strongly reduced the growth and invasiveness of both *in vitro* and *in vivo*. Although human melanoma cells with different phenotype and microenvironment showed conversely results, recently it has been observed that melanosomes, released by melanoma cells, are incorporated by normal fibroblasts and induce the transformation of fibroblasts into CAFs, promoting the formation of a dermal tumor primary niche that facilitates metastatic progression. Giving this evidence, we speculated that the prevention of melanosomes' release from early stage melanoma could impair the formation of the dermal tumor niche and then blockade the metastatic invasion. Since it has been observed that TPC2 is involved in the processes of cellular melanogenesis, we hypothesized that treating melanoma cells with Naringenin, a natural flavonoid that inhibits this channel, could affect both melanoma growth and invasiveness and the release of melanosomes and consequently fibroblasts transformation.

Therefore, TPC2 channel could be an interesting pharmacological target for the development of new therapies, to reduce the aggressiveness of melanoma by acting directly on cancer progression and tumor microenvironment, and Nar molecule may represent a potential innovative treatment for melanoma.

3. MATERIALS AND METHODS

3.1 CELL CULTURES

3.1.1 Melanoma cell cultures

Human melanoma cell lines (American Type Culture Collection, ATCC, USA) were maintained in standard culture conditions at 37°C and in a 5% CO_2 humidified atmosphere according to the manufacturer instructions. The table summarises the cell lines with their main characteristics and the culture conditions.

Cell line	Type of tumor	Mutations	Culture conditions
Lu1205	Mouse lung metastasis	BRAF V600E CDK4 K22Q PTEN deletion CDNK2A, CDNK2B deletion	MCDB 154CF, Lebovitz L-15 (Lonza) 2% Fetal bovine serum (FBS, EuroClone) 2mM L-Glutamine (Lonza) 1% Penicillin/Streptomycin/Amphotericin B (PSA, Lonza)
RPMI7951	Lymph node metastasis	BRAF V600E CDKN2A L16R PTEN deletion TP53 S166* TERT c.242_243CC>TT	EMEM (Sigma) 10% FBS, 2mM L-Glutamine 1% PSA
SH4	Pleural metastasis	BRAF V600E CDKN2A deletion	DMEM (Sigma) 10% FBS 4mM L-Glutamine 1% PSA
Skmel3	Lymph node metastasis	BRAF V600E TP53 R267W	McCoy's 5a Medium Modified 15% FBS, 1,5mM L-Glutamine 1% PSA
Skmel24	Lymph node metastasis	BRAF V600E CDKN2A deletion PTEN deletion TERT c.228C>T	EMEM 10% FBS, 2mM L-Glutamine 1% PSA
Skmel28	Primary VGF	BRAF V600E CDK4 R24C EGFR P753S PTEN T167A TERT c.161A>C TP53 L145R MC1R S83P/I155T	EMEM 15% FBS, 2mM L-Glutamine 1% PSA
WM115	Primary RGP	BRAF V600D PTEN deletion CDNK2A, CDNK2B deletion	EMEM 10% FBS 2mM L-Glutamine 1% PSA
WM266-4	Cutaneous metastasis	BRAF V600D PTEN deletion TERT c.250C>T MC1R R160W CDNK2A, CDNK2B deletion	EMEM 10% FBS, 2mM L-Glutamine 1% PSA
WM793-B	Primary VGF	BRAF V600E CDK4 K22Q	MCDB 154CF, Lebovitz L-15 2% FBS

			2mM L-Glutamine 1% PSA

3.1.2 Human fibroblasts and melanocytes isolation and cell cultures

Human fibroblasts were maintained in DMEM supplemented with 5% FBS, 4 mM L-Glutammine, and 1%PSA, while human melanocytes were cultured in Medium 254 containing HMGS-2 (Human Melanocyte Growth Supplement) and 1% PSA.

Fibroblasts and melanocytes were isolated from skin biopsies provided by the Surgical Room of Modena and Sassuolo (MO). The use of skin biopsies was approved by the ethical committee. Biopsies were quickly immersed in 70% alcohol and then in PBS. Any residues of subcutaneous tissue were eliminated and the tissue was cut into fragments of about 0.5 x 0.5 cm and placed in 1% antibiotic in base medium at 4°C for 1h. The fragments were incubated in dispase II (5mg/ml) overnight at 4°C, to separate dermis from epidermis. Then the epidermis was separated from the dermis: the derma fragments were transferred in petri dishes and incubated with culture medium (DMEM, 10% FBS, 1% PSA, 4mm L-Glutamine) at 37°C, in order to stimulate the spontaneous exit of the fibroblasts from the fragments; while the epidermis sheets were transferred in a solution of 0.25% trypsin, 0.02% EDTA in PBS and incubated for 25' at 37°C. Subsequently, the sheets were mechanically disrupted for 5' and the cell suspension was filtered in a 100µm cell strainer. After that, single cell suspension, formed by keratinocytes with a small percentage of melanocytes, was cultured in melanocytes culture medium, to promote its adhesion and proliferation.

3.1.3 Human Primary and Metastatic Melanoma Digestion

Primary melanoma biopsies were provided by the Dermatological Clinic of Modena and Sassuolo (MO). The use of melanoma biopsies was approved by the ethical committee. Immediately after surgical resection, primary or metastatic melanoma was digested using a Collagenase mix (type I and IV Collagenase, Gibco). Each Collagenase type was solubilized adding 1 ml of Hank's Balanced Salt Solution (HBSS, Sigma) with Mg^{2+} and Ca^{2+} directly to 1g vial and vortexed. Subsequently, a volume of HBSS, with Mg^{2+} and Ca^{2+}, was added to bring each collagenase solution to 100U/µl (1000X stock solution) and it was filtered to sterilize with a low protein binding filtration unit. Collagenase mix was generated with 50U/ml type I collagenase and 200U/ml type IV collagenase. Primary or metastatic melanoma biopsy was minced into 3-4 mm pieces with a sterile bistoury. Tissue pieces was washed several times with HBSS with Mg^{2+} and Ca^{2+}. Collagenase mix were then added and the tissue were incubated 30' at 37°C. After that, melanoma tissue pieces were mechanically dissociated by pipetting for 5'. This step was repeated again, and the solution was blocked with melanoma medium (RPMI, 10% decomplemented FBS, 2% Glutamine, 1% PSA). Cellular suspension was filtered with a cell strainer and centrifuged 12000 rpm for 8'. Pellet were then resuspended with RPMI medium and cells were counted with Burker camera. Cells were seeded directly to generate multicellular spheroids (liquid overlay method) and melanoma skin equivalent, or spotted on slices.

3.1.4 Citospin

100 000 primary and skin metastasis melanoma cells in 100µl PBS were spotted on slices. Cells were permeabilized with 0.1% Tritonx100 for 5' on ice, placed in a humidity chamber and used for immunohistochemistry of TPC2 (see paragraph 3.12).

3.1.5 Co-cultures

Co-cultures are prepared from a 1:1 mix of healthy human fibroblasts and melanoma cells. The cells were seeded on object-covered slides in a 6-well plate and were incubated at 37°C for 48h. Subsequently slides were fixed and used for immunofluorescence staining.

3.1.6 Spheroids formation

3D multicellular spheroids were obtained with the "liquid overlay method". 96-well plates (Biofil) were coated with 90µL of 1.5% agarose (Sigma) dissolved in the base medium of the cell line used. After agar polymerization, the plates were irradiated with UVB for 45' for sterilization. 5000 melanoma cells/well were seeded in 150µL of culture medium. After 48-72h spheroids were formed and monitored over time or used for other experiments.

For immunohistochemistry experiments, spheroids were washed in PBS and fixed with 4% paraformaldehyde (PFA) in PBS 4°C ON. Then after washing with PBS, spheroids were embedded in 4% agarose in bidistilled water. Polymerized agarose was divided in four pieces, and dehydrated. Briefly the sections were immersed in in increasing concentrations alcohol, from 50% to absolute. Finally, samples were put in xylol for clarification, embedded in paraffin and cut in sections of 4µm.

3.1.7 Naringenin treatment

Naringenin (Nar) (N5893-5G, Sigma) was dissolved in DMSO in a 500mM solution, from which several Nar dilutions were prepared in cellular culture medium, while control is 0,1% DMSO. Cells were treated with Nar for 48-72h and analysed.

3.1.8 DTIC treatment

Dacarbazine (DTIC) was used 300 mg/ml in cellular culture medium. Cells were treated for 24-48-72h and analysed.

3.1.9 Conditioned-medium treatment

SH4, WM793-B and melanocytes were seeded in petri dishes for 48h. Then conditioned medium was collected, added of 30% of fibroblasts culture medium and used immediately.

3.2 TRANSFECTION OF MELANOMA CELL LINES

Melanoma cell lines were plated to reach 70% confluence at the time of transfection. Cells were treated with antibiotic/FBS free basal medium supplemented with 0,1% bovine serum albumin (BSA, Sigma) for 8h. Then cells were transfected with 100nM scrambled or TPC2 siRNA (ON-TARGET plus Human TPC2 siRNA SMARTpool L-006508 and ON-TARGET plus Non-targeting Pool D-001810, Dharmacon Inc.) in combination with Lipofectamine (Invitrogen Corporation) and Opti-MEM (Gibco) following the manufacturer instructions. After 12h cells were re- transfected with the same conditions. After 48h from the second transfection, cells were lysed for protein analysis by western blotting.

To obtain spheroids, after 24h from the second transfection cells were seeded according to the liquid overlay method. After 72h spheroids were lysed and proteins expression was analysed using western blot.

3.3 MTT ASSAY

For 2D MTT assay, 5000cells/well were seeded in 96-well culture plates. After removal of the culture medium, cells were incubated with 50µL/well of 1mg/ml MTT (3-(4,5-dimethylthiazol-2-yl)-2,5-diphenyltetrazolium bromide) in basal medium at 37°C for 2h. Then, after removing the MTT solution, the salts are solubilized with 100µL/well of isopropanol. Finally, the staining was read at 540 nm in a spectrophotometer.

For 3D MTT assay, 5000 cells/well were seeded as 3D spheroids in 96-well culture plates. Then, cells were incubated with 5mg/ml MTT in PBS at 37°C for 4h and then dissolved with 100µl isopropanol with 0.04N HCl. Before reading in the spectrophotometer, disgregated spheroids were transferred into empty wells. The plate was read at 540 nm with a reference filter of 650 nm.

Results are expressed as viability percentage, as compared to control.

3.4 WOUND HEALING ASSAY

Melanoma cells were seeded in 12-well culture plates. After reaching 80% confluence cells were treated with 10µg/ml of mitomycin C (Sigma) in antibiotic/FBS free basal medium and incubated at 37°C for 2h. After washing with PBS, cells were cultured in antibiotic/FBS free basal medium supplemented with 0,1% BSA for 4h. Then, the medium was removed and for each well a line was drawn along the cell monolayer with a sterile plastic tip. After washing with PBS, cells were treated. For the analysis, cells were photographed at different time points, up to 72h from treatment. The result of each experiment was expressed as the mean of migrated cells from four different areas for condition.

3.5 TYPE I COLLAGEN INVASION ASSAY

Melanoma cells were seeded as 3D spheroids according to the liquid overlay method. After 72h, melanoma spheroids were implanted in a scaffold of type I collagen solution composed as following: DMEM, 200nM L-glutamine, 10% FBS, 2% sodium bicarbonate, 1,5 mg/ml of type I collagen previously extracted from rat tail and 1% PSA. Briefly, 100µl/well of collagen was deposited in a 96-well culture plates and allowed to polymerize for 40'. Then, spheroids were inserted into type I collagen matrix, taking care to maintain their position in the center of the well. The scaffold was overloaded with 100µl/well of melanoma culture medium. After 24h, spheroids were treated with different doses of Nar and monitored up to 144h. Pictures of the cellular invasion were taken at intervals of 24h and were analysed by using ImageJ (Wayne Rasband) and GIMP (The GIMP development team) software.

3.6 SPHEROIDS ANALYSIS

Pictures of spheroids were analysed by using ImageJ software. To calculate the areas, digital images were converted to 8 bits. Then, the binary images were subjected to a "clean-up" procedure to eliminate artefacts and with the application "Analyze particle" the interested area was measured. The **area** was calculated as number of total pixels and the **invasion area**, removing from the image selection the initial spheroid area to analyze only the invasion area. Similarly, for the **degree of compaction** was used the "average size" parameter. The **factor shape** was calculated with the following formula: perimeter squared/4π x area. The factor shape refers to a value that is affected by an object's shape but is independent of its dimensions. It gives a value of 1 for a perfect circle and larger values for more invasive spheroids. Each photo was analysed with 3 different "thresholds" to obtain an average value representing the picture. For each experiment, 3 photos/condition were analysed.

For the detection of the distance reached by cells migrated in type I collagen, pictures were analysed with GIMP software. Distance measurements were made from the edge of the spheroid in the four directions, taking as reference the cell that in this area was longer far from the spheroid core. The average of the four measurements, which indicates the distance reached by the cells in that picture, was made to obtain the **invasion distance**.

3.7 WESTERN BLOTTING

Celle were lysed on ice with a lysing solution composed as following: 150 mM Nacl, 15mM $MgCl_2$, 1mM EGTA, 50mM Hepes, 10% Glycerol and 1% Triton (pH 7.5), added with 0.2% PMSF (Sigma) and 15% protease inhibitors (Roche). The samples were mechanically disgregated using a 30Gx5/16 " needle of syringe and briefly sonicated and centrifuged. Protein lysates were quantified by the Bradford assay. Samples were diluted with 6x loading buffer, 2.5% β-mercaptoethanol and heated at 95°C for 5' in thermostatic block. For protein separation was used a 7.5% or 10% polyacrylamide gel (SDS-PAGE). The gel was obtained through polymerization of the running gel and stacking gel, the composition of which is described in the two tables below.

Running gel		
Acrylamide (Bio-Rad)	4.7 mL	6.25 mL
Tris-HCl 1.5M pH 8.8	6.25 mL	6.25 mL
Bidistilled H_2O	13.68 mL	12.12 mL
10% Sodium dodecyl sulfate (SDS)	250 µL	250 µL
10% Ammonium persulfate (APS) (Bio-Rad)	125 µL	125 µL

Stacking gel	
Acrylamide	1.25 mL
Tris-HCl 0.5M pH 6.8	3.15 mL

Bidistilled H_2O	7.95 mL
10% SDS	125 µL
10% APS	62.5 µL
TEMED	12.5 µL

The electrophoretic run was performed in a running buffer consisting of: 3.03g/L Tris Base, 14.42g/L Glycine, 1g/L SDS. The proteins were transferred to a nitrocellulose membrane (Bio-Rad) with transfer buffer (3.3g/L Tris, 14.4g/L Glycine, 20%methanol), at 100V for 1h at 4°C. Non-specific binding sites were saturated with blocking solution of 5% notfat dried milk in PBS-T (Phosphate Buffered Saline: 8g/L NaCl, 1.14g/L Na_2HPO_4, 0.2g/L KCl, 0.2g/L KH_2PO_4, 0.05%Tween20, pH 7.4) or TBS-T (Tris Buffered Saline: 80.6g/L NaCl, 24.22g/L TrisHcl pH 7.6, 0.1% Tween20) according to the primary antibody, for 2h in agitation at RT. Then the membranes were incubated with the following primary antibodies in 1% notfat dried milk in PBS-T or TBS-T in agitation at 4°C ON: **TPC2** (NBP1-30670, Novus Biologiclas) 1:300 in TBS-T; **N-Cadherin** (610920, BD Biosciences) 1:1000 in TBS-T; **E-Cadherin** (610181, BD Biosciences) 1:1000 in TBS-T; **α_7-Integrin** (SC-81807, Santa Cruz Biotechnology) 1:1000 in TBS-T; **α_4-Integrin** (SC-6589-R, Santa Cruz Biotechnology) 1:1000 in TBST-T; **HMB-45** (790-4366, Ventana); **Slug** (Histo Line Laboratories) 1:1000 in TBS-T; **α-SMA** (Sigma) 1:3000 in PBS-T; **SNAIL** (3895, Cell Signaling) 1:1000 in PBS-T; **FAP** (PA5-51057, Invitrogen) 1:1000 in PBS-T; **DCT** (PA5-105275, Invitrogen) 1: 1000 in PBS-T; **β-actin** (A5316, Sigma) 1:1000 in PBS-T; **α-tubulin** (Abcam) 1:1000 in PBS-T. After some washing in PBS-T or TBS-T, membranes were incubated with secondary antibodies conjugated with HRP (anti-mouse or anti-rabbit peroxidase conjugated antibody, Biorad) 1:3000 in 1% notfat dried milk in PBS-T or TBS-T at RT for 45'. After further washing in PBS-T or TBS-T, for the detection the HRP substrate enhanced luminol-based chemiluminescent (ECL Western Blotting Detection Reagents, Bio-rad) was used, and chemoluminescence was detected by the Chemidoc imaging system (Bio-rad). The band intensity was quantitatively determined using ImageJ software and protein levels' intensity was normalized to β-actin or α-tubulin expression.

3.8 QUANTIFICATION OF INTRACELLULAR AND EXTRACELLULAR MELANIN

For intracellular melanin determination, cells were harvested by trypsinisation using 0.05% trypsin (Gibco), 0.02% EDTA in PBS. Then, cells were washed with PBS and the pellets were lysed with 150µL of 1N NaOH containing 10% of DMSO at 80ºC for 2h. Samples were centrifuged at 12000g for 10' at room temperature (RT) and the absorbance was measured at 415nm in the spectrophotometer. To convert the absorbance values to the amount of melanin, a standard curve in 1N NaOH was obtained from 0 to 80µg/ml of synthetic melanin (Sigma) solution dissolved in 1N

NH_4OH. The amount of melanin was normalised on the total protein of the samples, quantified by Bradford assay.

For the determination of extracellular melanin, 200µL of the cell culture media were collected and centrifuged at 1200g 10'. Then, the media were transferred to a 96-well plate and the absorbance was read at 415nm using the spectrophotometer. The melanin content was determined from a standard curve in culture medium of synthetic melanin solution dissolved in 1N NH_4OH. The amount of melanin was normalised on the total protein of the cells of the plate, quantified by Bradford assay.

3.9 SKIN EQUIVALENTS

For skin equivalents construction, tissue culture inserts (Transwell, Costar) were incubated in a 12-well plate with 500µL of HBSS at 37°C for 30'. For dermal reconstructs, removed the HBSS solution, the acellular solution was added on the membrane of the transwell. This solution was prepared on ice, and included: type I collagen from rat tail (1.5 mg/ml), 10% FBS, 200nM L-Glutamine, 7.5% sodium bicarbonate and 1% PSA in DMEM. The inserts were incubated at RT for 30' to favour collagen polymerization and overlaid with 1ml/transwell of cell solution, composed of 150,000 human fibroblasts/ml mixed with acellular solution. The cell solution was incubated at 37°C for 1h, and after the addition of 10% FBS 1% PSA in DMEM above and below the inserts at 37°C for 4 days. For the construction of the epidermis, the medium was eliminated and dermis was incubated with HBSS at 37°C for 1h. Then, the dermis was overlaid with 350,000 keratinocytes/50µL of culture medium and incubated at 37°C for 1h before adding cell culture medium until complete immersion. After four day the medium was mainteined only in the outer chamber of the transwell, so that HSEs were exposed to air.

For MSE construction, 100,000 melanoma cells were added together with keratinocytes during the construction of the epidermis. Otherwise, for nodular melanoma subtypes, the spheroids have been inserted directly into the cellular component of the dermis.

After 14 days of air exposure, HSEs were washed in PBS and fixed in 4% formalin for 2h. Then, after a washing with HBSS, they were transferred into alcohol at increasing concentration, from 35% to absolute. Finally, the reconstructed skins were cut from the transwell and left in xylol for 15' to clarify the tissues. After clarification, the skins were embedded in paraffin and cut in sections of 4µm.

3.10 IMMUNOFLUORESCENCE

2D CULTUREs -The cells were seeded at 70% confluence on 12mm coverslips in 6-well culture plates. After two washes with PBS, the cells were fixed with 4% PFA in PBS 20', washed twice with PBS and permeabilized with 0.1% Tritonx100 for 5' on ice. The slides were blocked with 1% BSA in PBS at RT for 20' and incubated with the primary antibody: **HMB-45** (790-4366, Ventana) at RT for 1h; **DCT** (PA5-105275, Invitrogen) 1:200 in PBS at 37°C for 1h; **FAP** (PA5-51057, Invitrogen)

1:200 in PBS at 4°C overnight (ON); **α-SMA** (TA327604, Origene) 1:125 in PBS at RT for 1h. Then, after some washing in PBS-T, slides were incubated with the secondary antibody (anti-mouse Alexa Fluor 488- conjugated goat IgG or anti-rabbit Alexa Fluor 568-conjugated goat IgG) 1:500 in PBS at RT for 45'. Finally, after further washing in PBS-T, the nuclei were counter-stained with DAPI (Sigma) 1:2000 in PBS for 5'. The slides were finally washed three times with PBS and once with bidistilled water. The coverslips were mounted on slides with 50% of glycerol in bidistilled water and stored at -20°C until microscopy analysis. Samples were observed at fluorescence microscopy (ZOE Fluorescent Cell Imager, BIO-RAD).

HSEs- Paraffin embedded sections of HSEs were rehydrated. Briefly the sections were immersed in xylol for 10' and then in decreasing concentrations alcohol, from absolute to 50%, up to bidistilled water. The antigen unmasking was done with citrate buffer at 98°C for 20' and at RT for a further 20'. The slides were blocked with 1% BSA in PBS for 20' in a humidity chamber. Then, the following primary antibodies were added to the sections and incubated 1:100 in PBS at 4°C ON: **N-Cadherin** (610920, BD Biosciences), **E-Cadherin** (610181, BD Biosciences), **α_4-Integrin** (SC-6589-R, Santa Cruz Biotechnology) and **α_7-Integrin** (SC-81807, Santa Cruz Biotechnology). After washing three times with PBS-T, the sections were incubated with the secondary antibody (anti-mouse Alexa Fluor 488- conjugated goat IgG or anti-rabbit Alexa Fluor 568-conjugated goat IgG) 1:500 in PBS at RT for 45'. Finally, after further washing in PBS-T, the nuclei were counter-stained with DAPI 1:2000 in PBS for 5'. The slides were finally washed three times with PBS and once with bidistilled water. The coverslips were mounted on slides with 50% of glycerol in bidistilled water and stored at -20°C until microscopy analysis. Samples were observed at fluorescence microscopy (ZOE Fluorescent Cell Imager).

3.11 RETROSPECTIVE SELECTION OF MELANOMA PATIENTS

Melanoma patients were retrospectively evaluated. Cases were retrieved from the database of the Department of Dermatology of the University of Modena and Reggio Emilia. The study has been approved by the Institutional Review Board of Reggio Emilia. Inclusion criteria were: 1) pathology confirmed diagnoses of melanoma, 2) availability of relevant clinical data in patient records and 3) dermoscopic images. Dermoscopic images were acquired by means of a polarized dermoscope (DemLite Photo 3Gen® LLC, San Juan Capistrano, CA, USA). Demographic and clinical data were retrieved. Then, they have been grouped according to Breslow Index.

3.12 HEMATOXYLIN AND EOSIN STAINING

Paraffin embedded human primary melanomas were retrieved from the pathological anatomy of the university of Modena and Reggio Emilia. Primary melanomas, MSEs and spheroids slides were rehydrated. Briefly, the sections were immersed in xylol for 3' and then in decreasing concentrations

alcohol, from absolute to 50%, up to bidistilled water. Then, the slides were stained in a solution of haematoxylin for 2' and washed thoroughly with running water until all residues of hematoxylin have been removed. Subsequently, the slides were incubated in alcohol 75% and 95% for 1', and then immersed in a solution of eosin for 1'. Finally, the slides were incubated in solutions at increasing concentration of alcohol, sealed using the mounting medium (Eukitt, Bio-optica) and observed at microscopy.

3.13 IMMUNOHISTOCHEMISTRY

Paraffin embedded human primary melanomas were retrieved from the pathological anatomy of the university of Modena and Reggio Emilia. Primary melanomas, MSEs and spheroids sections were rehydrated. Briefly, the sections were immersed in xylol for 10' and then in decreasing concentrations alcohol, from absolute to 50%, up to bidistilled water. The antigen unmasking was done with citrate buffer at 98°C for 20' and at RT for a further 20'. The sections were placed in a humidity chamber and used for immunohistochemistry of **TPC2** (1:300, NBP1- Novus 86923, Novus Biologicals) according to UltraTek Alk-Phos Anti-Polyvalent Stain Kit instructions, using Fast Red as a chromogen (AMH080-IFU, Scytek Laboratories INC) or immunohistochemistry of **HMB-45** (ready to use, 790-4366, Ventana), **Melan-A** (ready to use, 790-2990, Ventana), **S100** (1:400, DakoCytomation) and **Ki67** (1:200 M7240, Dako Agilent) according to ultraView Universal DAB detection kit instructions (Ventana). Finally, the slides have been stained with hematoxylin, fixed with the mounting medium and observed at microscopy.

3.14 BIOINFORMATIC ANALYSIS

Normalized gene expression of skin cutaneous melanoma patients was obtained from the Broad Institute TCGA Genome Data Analysis Center (2016): TCGA data from Broad GDAC Firehose 2016_01_28 run; Broad Institute of MIT and Harvard Dataset. https://doi.org/10.7908/C11G0KM9. The statistical significance of the differential modulation of TPCN2 gene between subgroups of patients was inferred by Student's T-test.

3.15 STATISTICAL ANALYSIS

The results are calculated as the mean and the standard error of the mean (SEM). The statistical significance was calculated using Student's T-test and data with a p-value < 0.05 were considered significant, in particular: *$0.01< p < 0.05$; **$0.001< p < 0.01$; ***$0.0001 p < 0.001$; ****$p < 0.0001$. The statistical analysis was performed using the Graphpad Prism software.

4. RESULTS

4.1 Increase of TPC2 expression in primary human melanomas with higher Breslow Index

To evaluate the expression of TPC2 in malignant melanoma we analysed sections of primary melanomas at different stages according to the Breslow Index, which is based on the depth of skin infiltration of melanoma, defining the invasion levels in millimetres [75]. The first group had Breslow Index lower than 1mm, Clark's Level I-II and Mitotic Index lower than 1; the second presented Breslow Index between 1 and 2mm, Clark's Level III-IV and Mitotic Index between 1 and 2; the third showed Breslow Index higher than 2mm, Clark's Level IV-V and Mitotic Index higher than 5 (Figure 4.1a). These tumor subtypes had been characterised by dermoscopic images and histologic staining, which showed different clinical characteristics (Figure 4.1a). Then, we verified the expression of the melanocytic markers Melan-A and HMB45 to localize tumor cells. As expected, the depth of the tumor increases with the Breslow Index, passing from a first stage to purely superficial localization, to radial growth and vertical growth stages with invasion of the dermis (Figure 4.1b). TPC2 staining allowed us to observe that the channel is mainly present in the tumor area, where there is higher expression of Melan-A and HMB45. In addition, not only TPC2 expression is closely localized in the tumor area, but the number of tumor cells that are positive for TPC2 increases with the increase of the Breslow Index (Figure 4.1c). These data confirm the analysis of TPCN2 mRNA in the Cancer Genome Atlas (TCGA) that show a different expression between primary melanomas, with an increase expression that correlates with higher Breslow Index (Figure 4.1d).

a

	Breslow Index <1	Breslow Index 1≤x<2	Breslow Index ≥2
Clark's Level			
I	22,22%	0%	0%
II	61,11%	0%	0%
III	16,67%	70%	15,79%
IV	0%	30%	63,16%
V	0%	0%	21,05%
Mitotic Index	0,28 ± 0,23	1,44 ± 0,67	7,37 ± 2,47

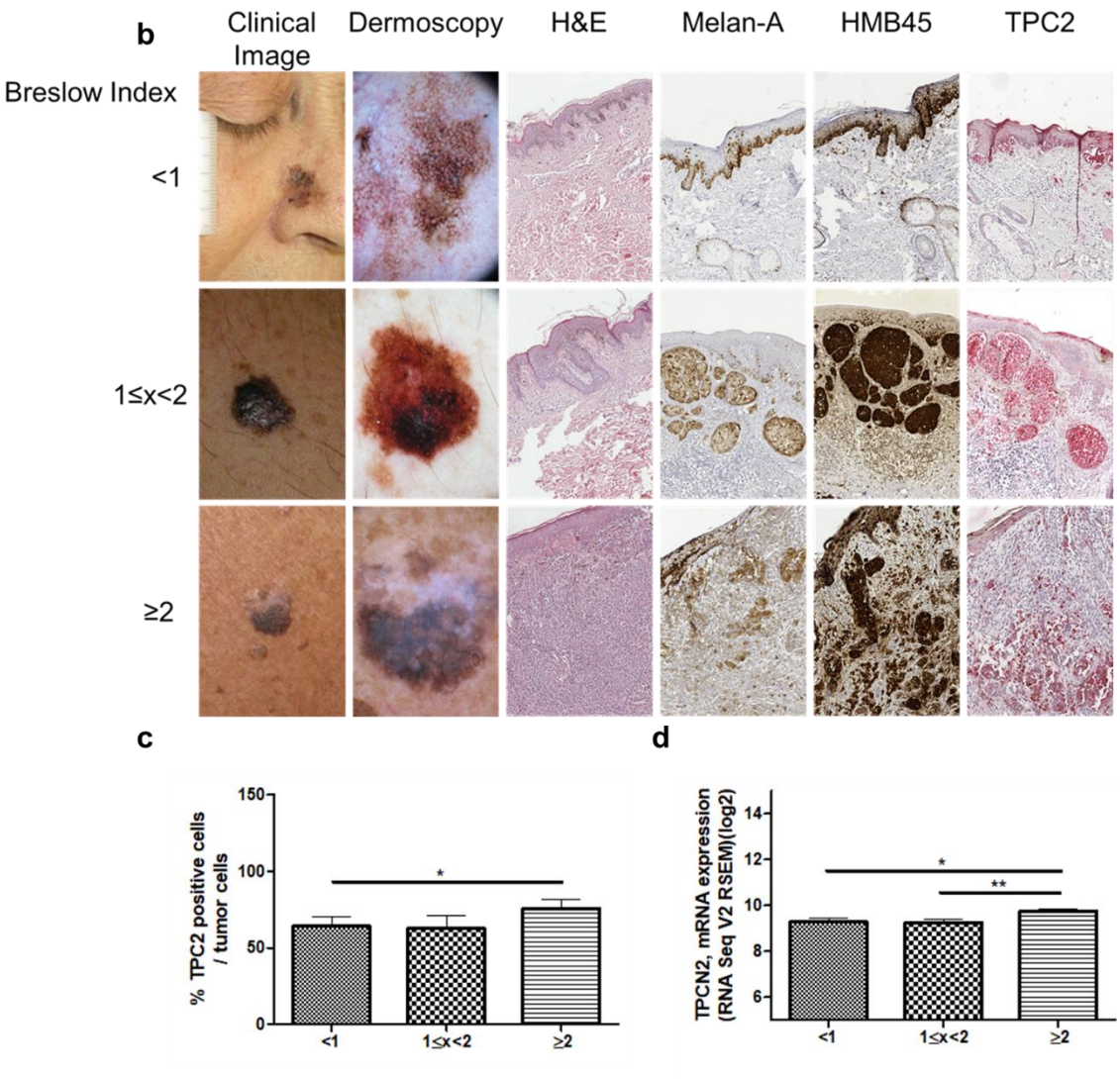

Figure 4.1 Increase of TPC2 protein and mRNA expression in primary human melanomas with higher Breslow Index. (a) Clark's Level and Mitotic Index of primary melanomas with different Breslow Index. (b) Representative clinical and demoscopic images, histologic staining with haematoxylin and eosin (H&E) and staining of Melan-A, HMB45 and TPC2 by IHC of skin sections of primary melanomas with different Breslow Index. (c) Percentage of TPC2 positive cells on tumor cells measured on melanoma sections. (d) Analysis of expression for TPC2 between primary patients in human skin cutaneous melanoma (SKCM). Normalized gene expression of skin cutaneous melanoma patients was obtained from the Broad Institute TCGA Genome Data Analysis Center (2016): TCGA data from Broad GDAC Firehose 2016_01_28 run; Broad Institute of MIT and Harvard Dataset. Data represent the mean and SEM, *0.01<p<0.05; ** 0.001<p<0.01;.

4.1.1 TPC2 expression in malignant and nodular melanoma

The subgroup of melanomas with Breslow Index higher than 2mm also included the nodular melanoma, for which a different origin is assumed. It is supposed that there has been no migration of cancer cells from the epidermal layer to the dermis, as happens in the melanoma with vertical growth, but that the melanocytes from which the tumor originates are already present in the dermis [203,204]. Indeed, nodular melanomas are typically characterized by melanoma well-circumscribed but unencapsulated with Melan-A and HMB45 positivity in the deep dermis and/or subcutaneous (Figure 4.2a).

To evaluate if these features are maintained in an *in vitro* model, primary malignant and nodular melanoma have been studied in 3D models. To better mimic the tumor microenvironment, two different types of MSEs have been constructed, taking into account the origin tissue of malignant and nodular melanoma. In the first model, malignant melanoma cells of tumor with Breslow Index higher than 2mm were seeded over the equivalent dermis along with keratinocytes during the construction of the epidermis. Due to their invasive capacity, melanoma cells migrated from the basal layer to the dermis, mimicking the behaviour of this type of tumor *in vivo*. For the second model, the nodular melanoma cell spheroid was inserted directly into the dermal equivalent. After 22 days, we observed that in MSEs with malignant melanoma cells, Melan-A and HMB45 are expressed at the dermal-epidermal junction, while in MSEs with nodular melanoma cells, the positivity to tumor makers is present, as expected, only at the dermal level (Figure 4.2b).

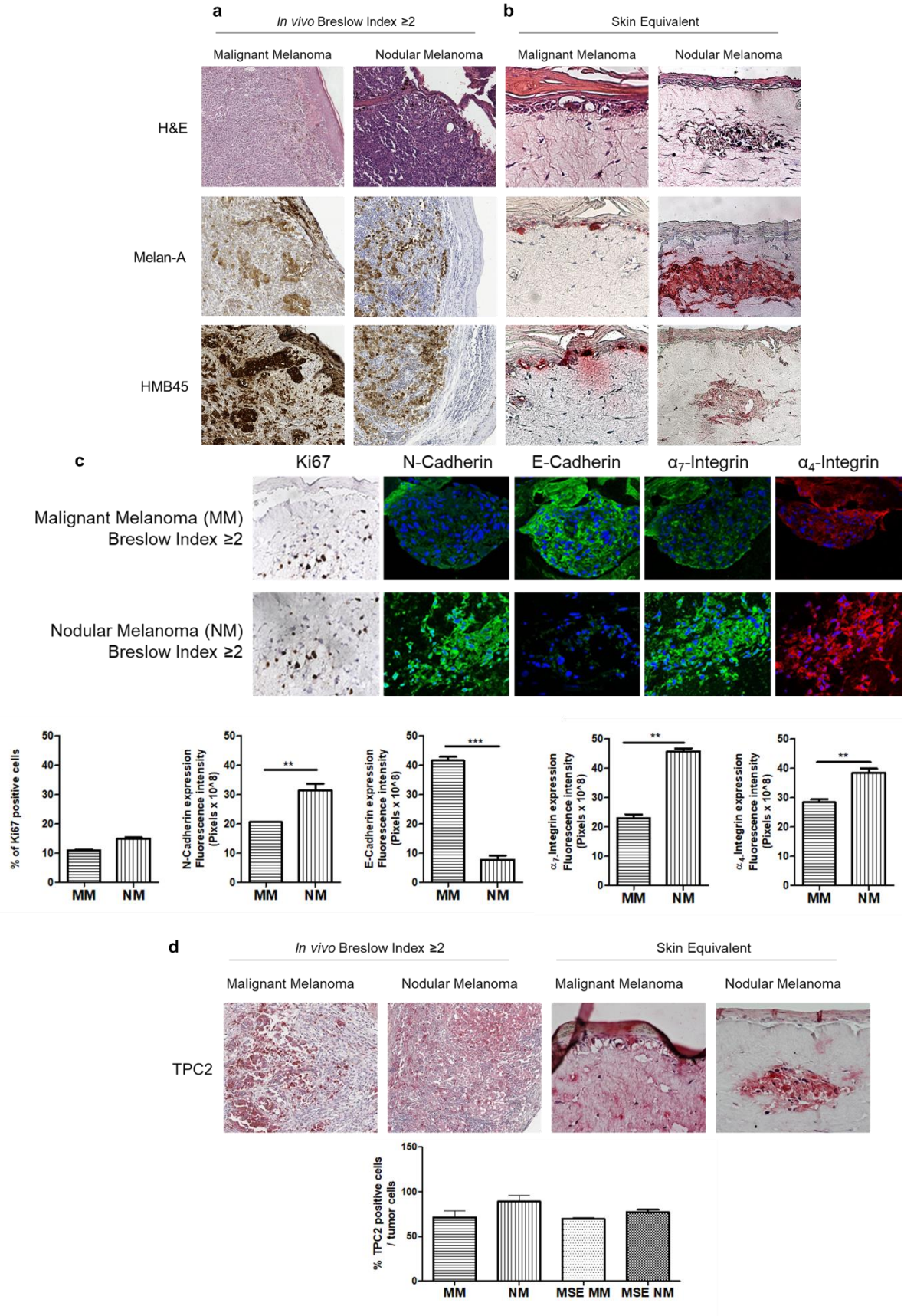

Figure 4.2 High TPC2 expression in skin sections and skin equivalents of malignant and nodular melanoma. (a) Histologic staining with H&E and staining of Melan-A and HMB45 by IHC of skin sections of primary malignant and nodular melanomas and (b) of skin equivalents with malignant or nodular melanoma cells (MSEs). (c) Expression of Ki67

by IHC and N-Cadherin, E-Cadherin, α_7-integrin and α_4-integrin by IF in sections of MSEs with malignant and nodular melanoma cells. Nuclei were stained with DAPI (blue). Percentage of Ki67 positive cells and proteins fluorescence intensity were detected and analysed using the ImageJ software. (d) Staining of TPC2 by IHC of skin sections of primary malignant and nodular melanomas and MSEs with malignant or nodular melanoma cells. Percentage of TPC2 positive cells on tumor cells measured on sections. Data represent the mean and SEM, **0.001<p<0.01; ***0.0001<p<0.001.

Subsequently, to characterize these two models of MSEs we analysed the expression of some tumor invasion markers. The stainings show that nodular MSE presents similar level of Ki67 positive cells, a higher expression of N-Cadherin, α_7-integrin and α_4-integrin and a reduced expression of E-Cadherin compared to malignant MSE (Figure 4.2c). Finally, we analysed TPC2 expression both in tumor tissue slices of patients and MSEs, observing an expression of the protein localized in tumor cells (Figure 4.2d), identified by Melan-A and HMB45. TPC2 expression appears to be higher in nodular melanoma, although not statistically significant, but still elevated in both types of cancer, which represent the most aggressive forms of melanoma and with the worst prognosis.

4.2 TPC2 expression in melanoma metastasis compared to primary tumor of the same patient

To evaluate the expression of TPC2 in different melanoma stages, first we analysed TPCN2 mRNA expression levels in the Cancer Genome Atlas (TCGA), observing a decrease expression in lymph nodes and other metastatic sites compared to primary tumors (Figure 4.3a). On the other hands, we analysed TPC2 protein expression in primary and cutaneous metastatic melanoma cells isolated from the same patient and we observed a greater number of TPC2 positive cells in the metastatic compared to the primary sample (Figure 4.3b).

To better assess the channel protein expression not only in tumor stages, but also in distinct microenvironment, we analysed sections of primary tumor and metastasis of different sites of the same patient by immunohistochemistry. TPC2 staining allowed us to observe that the channel is present in the tumor area, characterized by the expression of the melanocytic marker S100 (Figure 4.6a). Moreover, we noted that the number of TPC2 positive cells is variable in primary melanomas, such as in the different metastatic sites, however in the metastasis the expression is in general higher than in primary tumors, except for lung metastasis (Figure 4.3c).

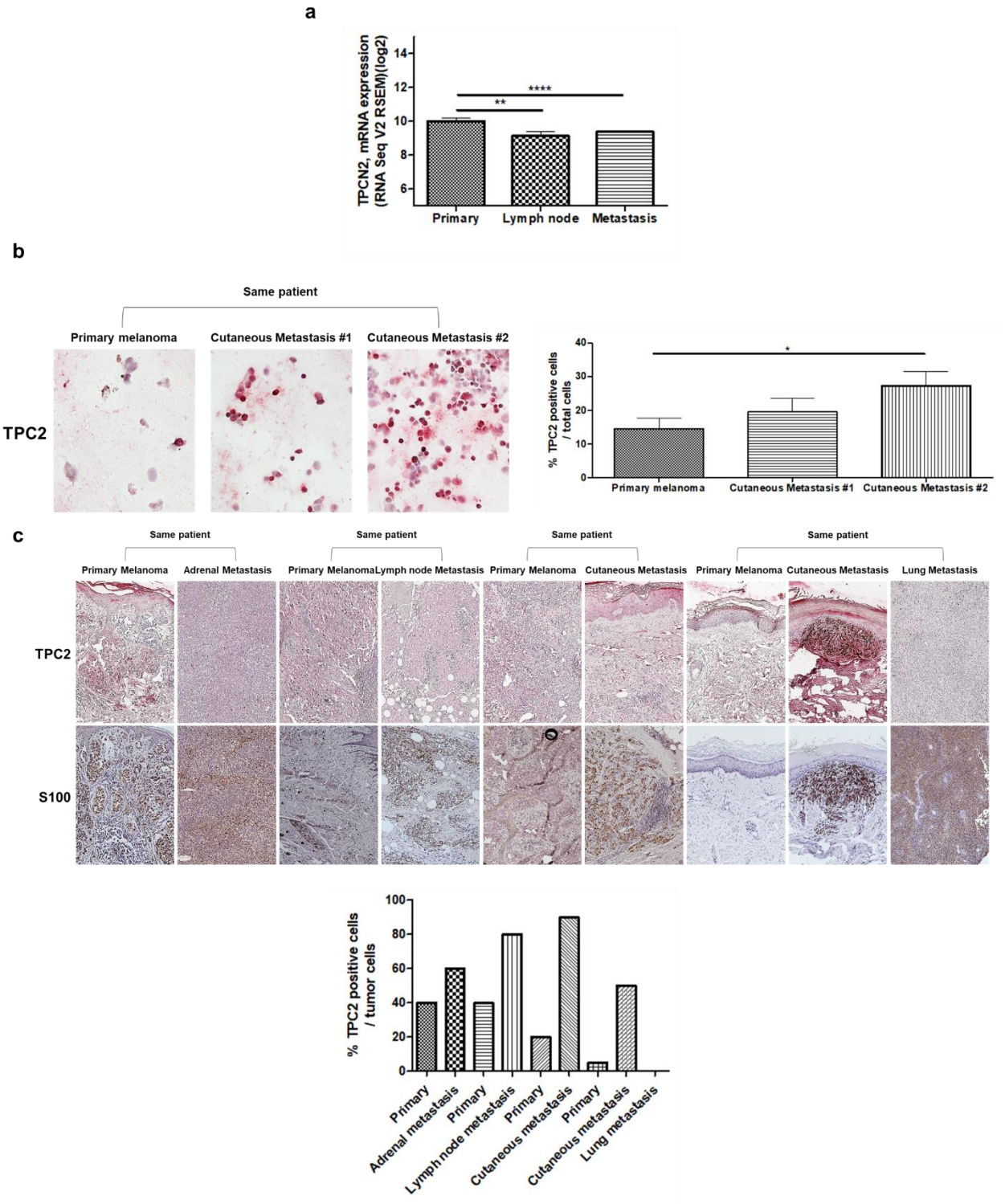

Figure 4.3 Decrease of TPCN2 mRNA expression and increase of TPC2 protein in melanoma metastasis compared to primary tumor of the same patient. (a) Analysis of expression for TPC2 between primary and metastatic patients in human skin cutaneous melanoma (SKCM). Normalized gene expression of skin cutaneous melanoma patients was obtained from the Broad Institute TCGA Genome Data Analysis Center (2016): TCGA data from Broad GDAC Firehose 2016_01_28 run; Broad Institute of MIT and Harvard Dataset. (b) Staining of TPC2 by IHC of primary and cutaneous metastatic melanomas cells of the same patient. The percentage of TPC2 positive cells was measured on total cells. (c) Staining of S100 and TPC2 by IHC of primary and metastatic melanomas sections. The percentage of TPC2 positive cells on tumor cells was measured on melanoma sections. Data represent the mean and SEM, *0.01<p<0.05, **0.001<p<0.01; ****p<000.1.

4.3 TPC2 expression in 2D and 3D melanoma cell cultures

TPC2 expression has also been evaluated in several commercial human melanoma cell lines with different degrees of aggressiveness: the WM115 cell line derived from primary RGP tumor; WM266-4 from skin metastasis of the same patient of the WM115; Skmel28 and WM793-B from primary VGP tumor; Lu1205 from mouse lung metastasis of the WM793-B; Skmel3, Skmel24 and RPMI7951 from lymph node metastases; SH4 from pleural metastasis. To better mimic the characteristics of the tumor *in vivo*, these cell lines have been used both in two-dimensional culture and in a three-dimensional model based on multicellular spheroids obtained with the liquid overlay method technique. From protein expression analysis we noted that TPC2 is expressed both in healthy melanocytes and in melanoma cell lines at different levels. In particular, TPC2 is less express in lymph node metastasis cell lines both in 2D and 3D cultures. Moreover, in both models the channel is more expressed in the metastatic lines WM266-4 and SH4, compared to the primary lines WM115, Skmel28, WM793-B and to healthy melanocytes (Figure 4.4a). These expression levels have also been confirmed in some human melanoma spheroids by IHC, in which we observed an increase TPC2 expression in SH4 and WM266-4 spheroids compared to WM115 and WM793-B spheres (Figure 4.4b).

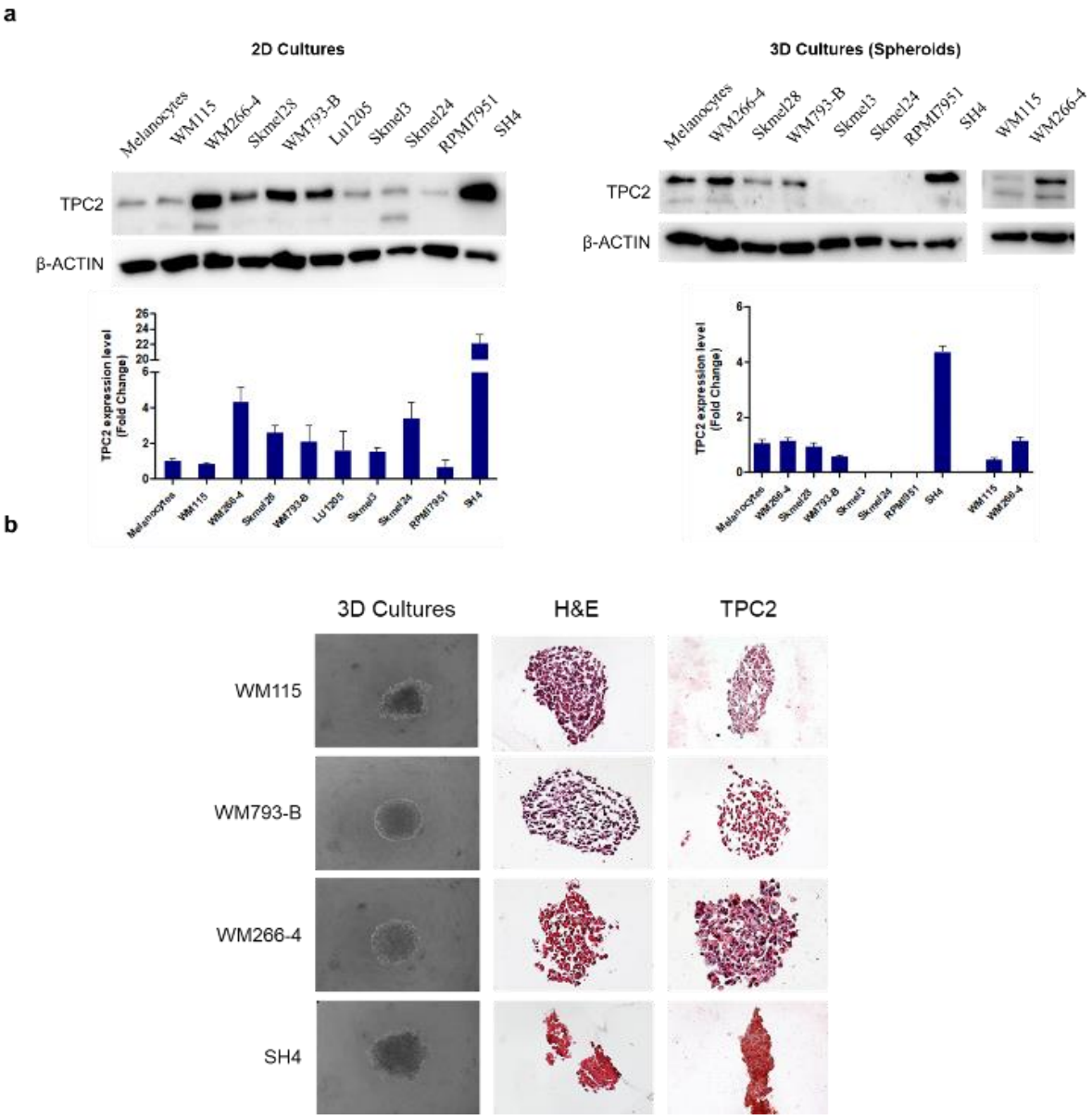

Figure 4.4 TPC2 expression in melanocytes and human melanoma cell lines of different degree of aggressiveness in two-dimensional and three-dimensional models. (a)TPC2 expression in melanocytes and human melanoma cell lines in 2D and 3D culture using western blot technique. The band intensity was quantitatively determined using ImageJ software and protein levels' intensity was normalized to β-actin expression. Data represent the mean and SEM of three independent experiments. (b) Clear field images of the morphology, histologic staining with H&E and TPC2staining by IHC of human melanoma cell lines spheroids. Data represent the mean and SEM of three independent experiments.

4.4 Decrease of cell proliferation and total spheroid area in melanoma cells after TPC2 inhibition

As TPC2 has been seen to play a role in cancer cell proliferation [32], we evaluated whether it also plays this role in melanoma cells using Nar, a natural inhibitor of this channel. Thus, to assess cell proliferation we treated WM115, WM793-B, WM266-4 and SH4 cell lines and performed the MTT assay. The WM793-B seems to be more sensitive than other lines at high concentrations of Nar, so

in this cell lines we performed treatments with lower doses. As shown in the graphs, by MTT assay control cells proliferate over time, while treated cells show a dose and time-dependent inhibition of growth (Figure 4.5).

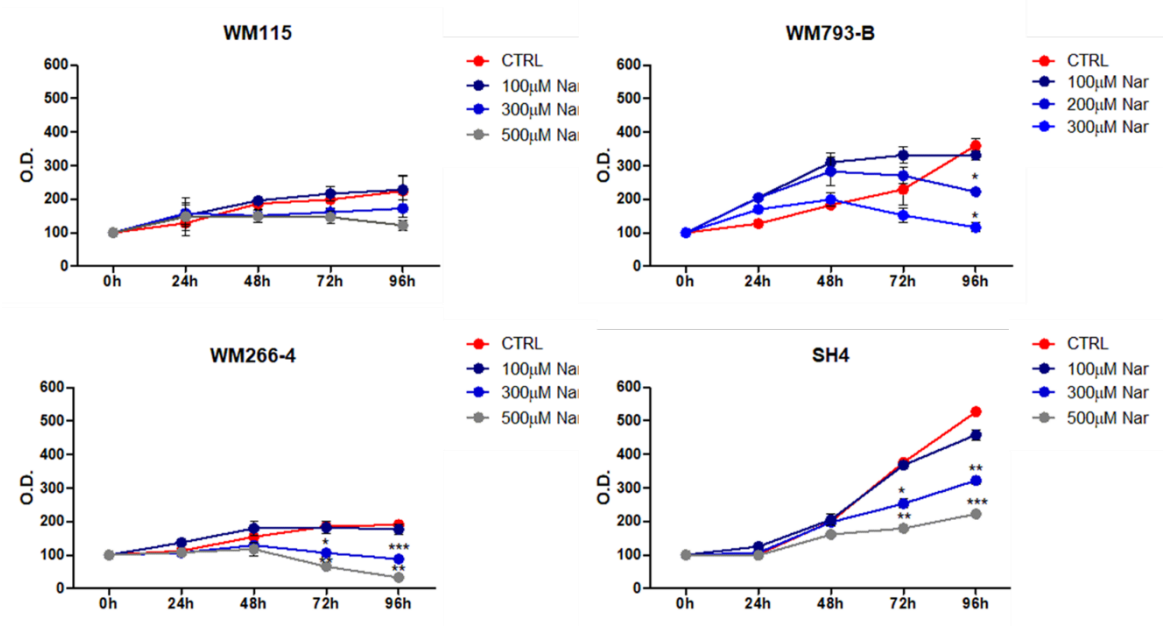

Figure 4.5 Inhibition of cell proliferation in melanoma cell lines after Nar treatment. Graphs show the MTT viability assay in two-dimensional cultures of WM115, WM793-B WM266-4 and SH4 cells after treatment with different doses of Nar. The vitality has been evaluated by O.D. at different times, up to 96h from treatment with Nar. Five wells were analysed, for each condition. Data represent the mean and SEM of three independent experiments, *0.01<p<0.05; **0.001<p<0.01; ***0.0001<p<0.001.

To better resemble *in vivo* architecture and tumor microenvironment, we focused on the three-dimensional tumor models, melanoma spheroids, using the same melanoma cell lines as previous experiments. After Nar treatment WM115, WM793-B and WM266-4 spheroids show a dose and time dependent reduction of total spheroid area. On the contrary, after Nar treatment in SH4 spheroids no decrease of the area of the spheroid has been observed compared to control, but the spheres seem to be less compact (Figure 4.6).

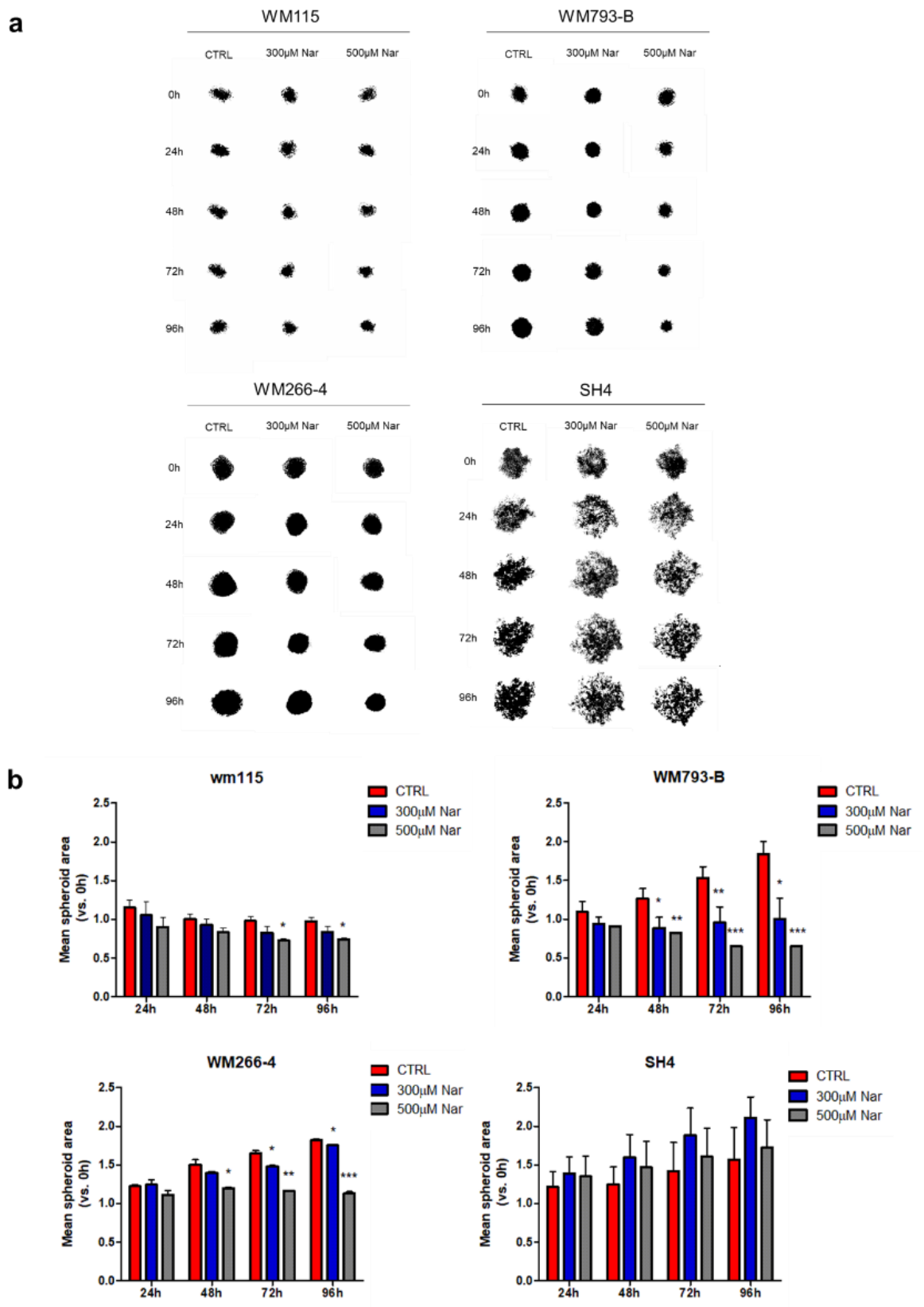

Figure 4.6 Reduction of spheroids area in melanoma spheroids after Nar treatment. (a) The multicellular spheroids of WM115, WM793-B, WM266-4 and SH4 cell lines were treated with different doses of Nar. Images were taken from the time of treatment up to 96h. (b) The total area of the spheroid was calculated using the ImageJ software. Four spheres were analysed for each condition. Data represent the mean and SEM of three independent experiments, *0.01<p<0.05; **0.001<p<0,01; ***0.0001<p<0.001.

To better understand the role of TPC2 in SH4 spheroids proliferation, we performed the same experiments after TPC2 silencing (Figure 4.7a). In these conditions we observed that control spheroids proliferate over time, while silenced spheres show a significantly slower proliferation rate (Figure 4.7b) and smaller total spheroid area (Figure 4.7c).

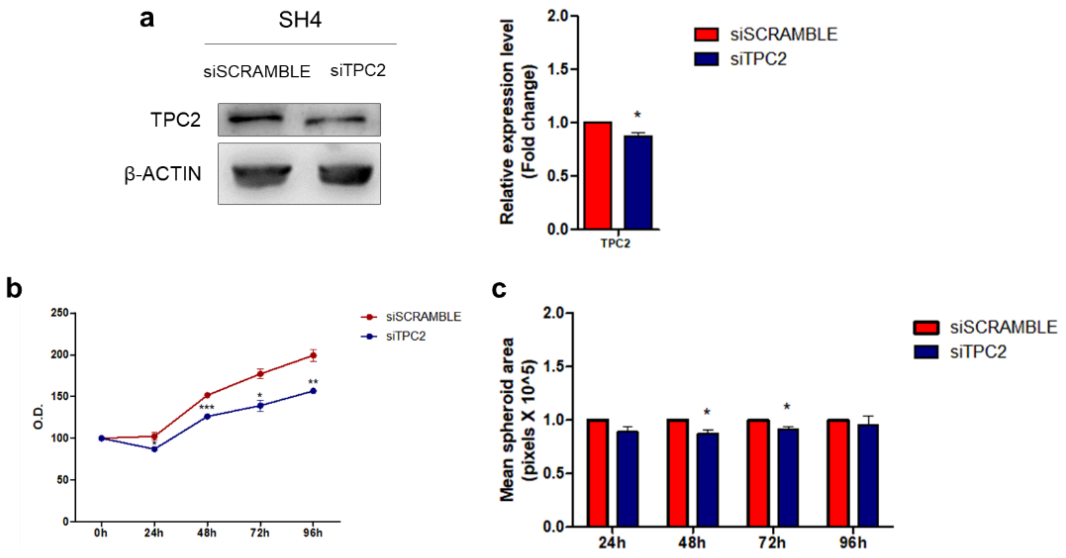

Figure 4.7 Reduction of cell proliferation and total spheroids area of SH4 spheroids after TPC2 silencing. The SH4 cells were transfected with scrambled or TPC2 siRNA. (a) After 48h the expression of TPC2 was evaluated by western blot. The band intensity was quantitatively determined using ImageJ software and protein levels' intensity was normalized to β-actin expression. The values have been normalized to the value obtained from cells with siRNA scramble. SH4 transfected cell lines were plated according to the "liquid overlay methods" to obtain multicellular spheroids: (b) the graph shows the MTT viability assay, the vitality has been evaluated by O.D. at different times, analyzing five wells for each condition; (c) the total spheroid area was calculated using the ImageJ software. Four spheres were analysed for each condition. Data represent the mean and SEM of three independent experiments, *0.01<p<0,05; **0.001<p<0.01; ***0.0001<p<0.001.

4.5 Decrease invasive and migratory capacities of melanoma cells after TPC2 inhibition

Since several studies have shown a role of TPC2 in the invasion process of different types of cancer [32,33,46,47], we hypothesized a role also in melanoma. So, we evaluated the involvement of the channel in tumor progression in WM115 RGP primary, in WM793-B VGP primary and in WM266-4 and SH4 metastatic melanoma cell lines assessing their invasive and migratory capabilities in 2D and 3D culture systems.

First of all, in 2D cell cultures, we observed a dose and time dependent reduction of migratory capacity in both primary and metastatic melanoma cell lines after Nar treatment, by scratch assay (Figure 4.8).

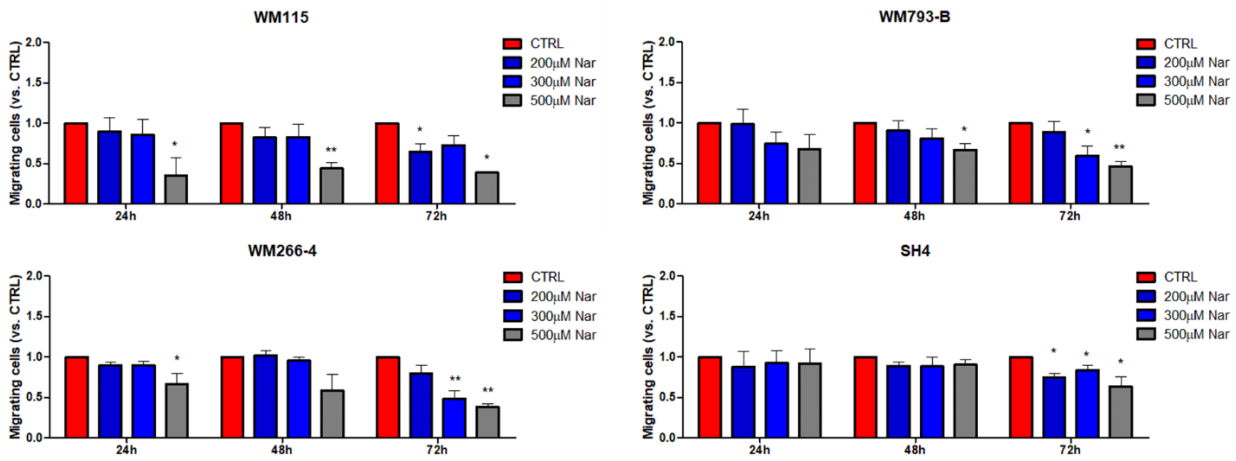

Figure 4.8 Reduction of migratory capacity in melanoma cells after Nar treatment. WM115, WM793-B, WM266-4 and SH4 cells were treated with different doses of Nar in serum-free medium. The cells migrated into the scraped area were evaluated, and four different areas for condition were counted. The data represent the mean and SEM of three different experiments, *0.01<p<0,05; **0.001<p<0.01.

In addition, after TPC2 silencing in 2D VGP primary and metastatic cell lines, there is a decrease of different tumor progression markers, N-Cadherin, α_7-integrin, α_4-integrin and slug, which promote EMT, while the expression of E-Cadherin, a tumor suppressor protein is increased (Figure 4.9a). To confirm these results in 3D culture systems, we treated WM266-4, WM793-B and SH4 spheroids with Nar and we observed again a reduced expression of N-Cadherin, α_7-integrin, α_4-integrin and slug and an increase of E-Cadherin, even if the expression of TPC2 does not significantly change after treatment (Figure 4.9b).

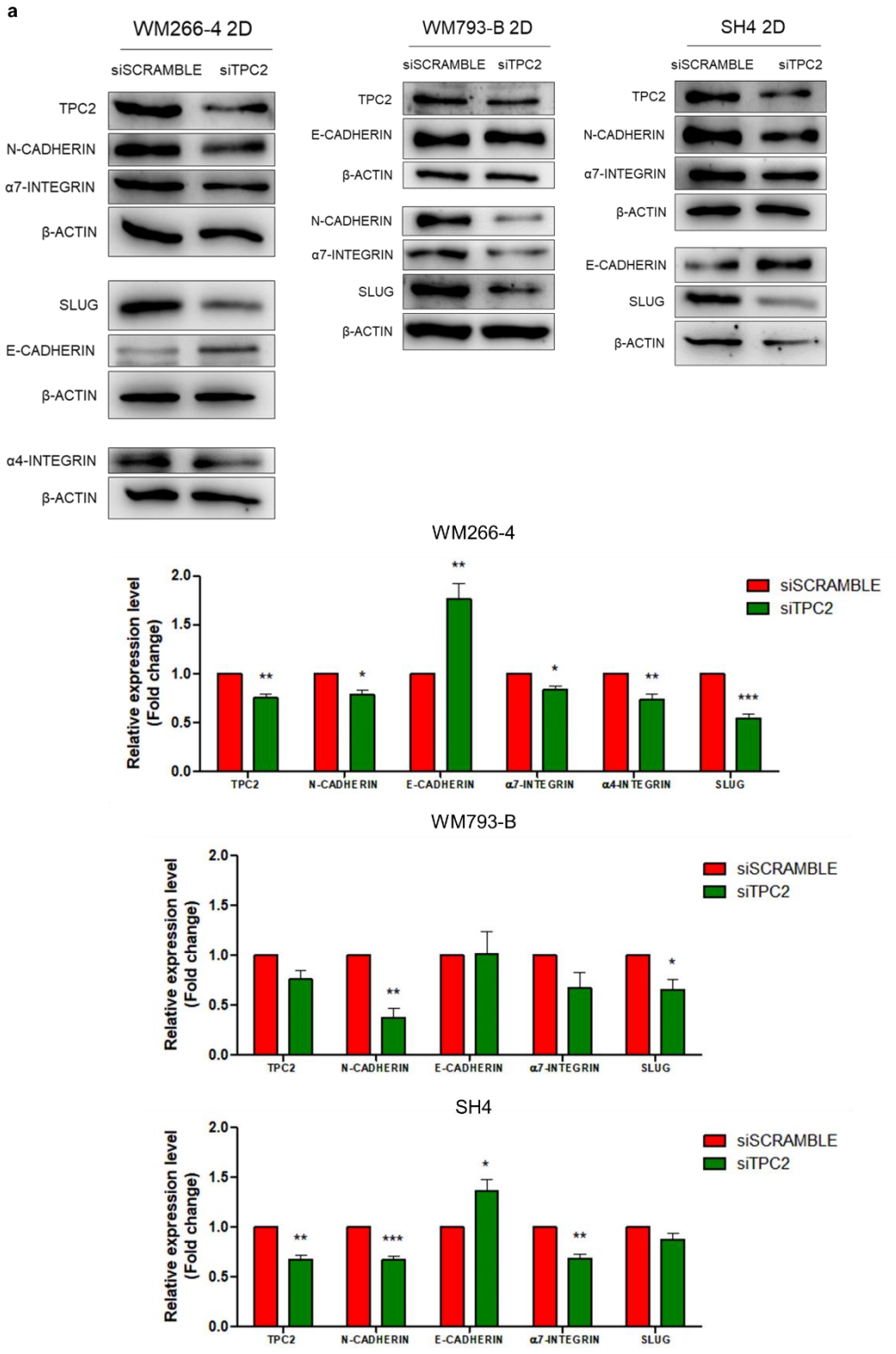
a
WM266-4 2D
siSCRAMBLE
siTPC2
TPC2
N-CADHERIN
α7-INTEGRIN
β-ACTIN
SLUG
E-CADHERIN
β-ACTIN
α4-INTEGRIN
β-ACTIN
WM793-B 2D
siSCRAMBLE
siTPC2
TPC2
E-CADHERIN
β-ACTIN
N-CADHERIN
α7-INTEGRIN
SLUG
β-ACTIN
SH4 2D
siSCRAMBLE
siTPC2
TPC2
N-CADHERIN
α7-INTEGRIN
β-ACTIN
E-CADHERIN
SLUG
β-ACTIN
WM266-4
Relative expression level (Fold change)
siSCRAMBLE
siTPC2
TPC2
N-CADHERIN
E-CADHERIN
α7-INTEGRIN
α4-INTEGRIN
SLUG
WM793-B
Relative expression level (Fold change)
siSCRAMBLE
siTPC2
TPC2
N-CADHERIN
E-CADHERIN
α7-INTEGRIN
SLUG
SH4
Relative expression level (Fold change)
siSCRAMBLE
siTPC2
TPC2
N-CADHERIN
E-CADHERIN
α7-INTEGRIN
SLUG

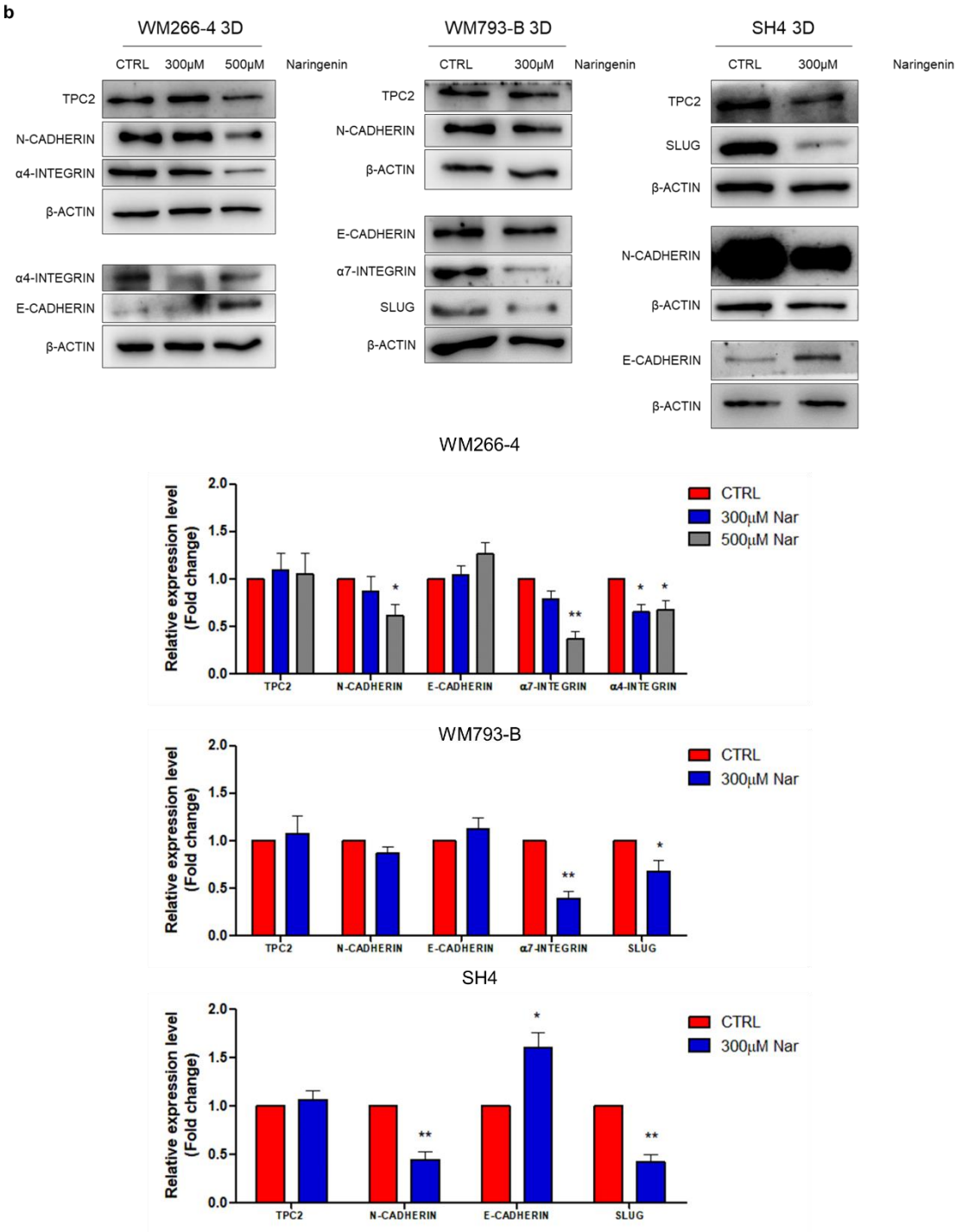

Figure 4.9 Decrease expression of tumor invasion markers in melanoma cell lines after TPC2 silencing or Nar treatment. (a) 2D cultures of WM266-4, WM793-B and SH4 were transfected with scrambled or TPC2 siRNA. (b) 3D cultures WM266-4, WM793-B and SH4 were treated with 300-500μM of Nar. The expression of TPC2, N-Cadherin, E-Cadherin, α_7-integrin, α_4-integrin and slug was evaluated by western blot. The band intensity was quantitatively determined using ImageJ software and protein levels' intensity was normalized to β-actin expression. The values have been normalized to the value obtained from cells with siRNA scramble or CTRL. Data represent the mean and SEM of three independent experiments, *0.01<p<0.05; **0.001<p<0.01; ***0.0001<p<0.001.

To better clarify the role of TPC2 in tumor migration and invasion and in order to mimic an *in vivo* condition, in which tumor cells invade the extracellular matrix and surrounding tissues, primary RGP

melanoma WM115 spheroids were implanted in type I collagen and treated with Nar (Figure 4.10a). This experiment allowed to monitor the aggressiveness of cancer cells and it was possible to observe that Nar treated spheres show a lower invasion capacity over time. In particular, the analysis of the images shows a reduction of the total spheroid area, invasion area, invasion distance, factor shape and degree of compaction (Figure 4.10b). Finally, to confirm a role of TPC2 in WM115 spheroids invasion process, we evaluated the expression of some tumor invasion markers. After TPC2 silencing, WM115 spheroids show a reduction of N-Cadherin and α_7-integrin expression (Figure 4.10c).

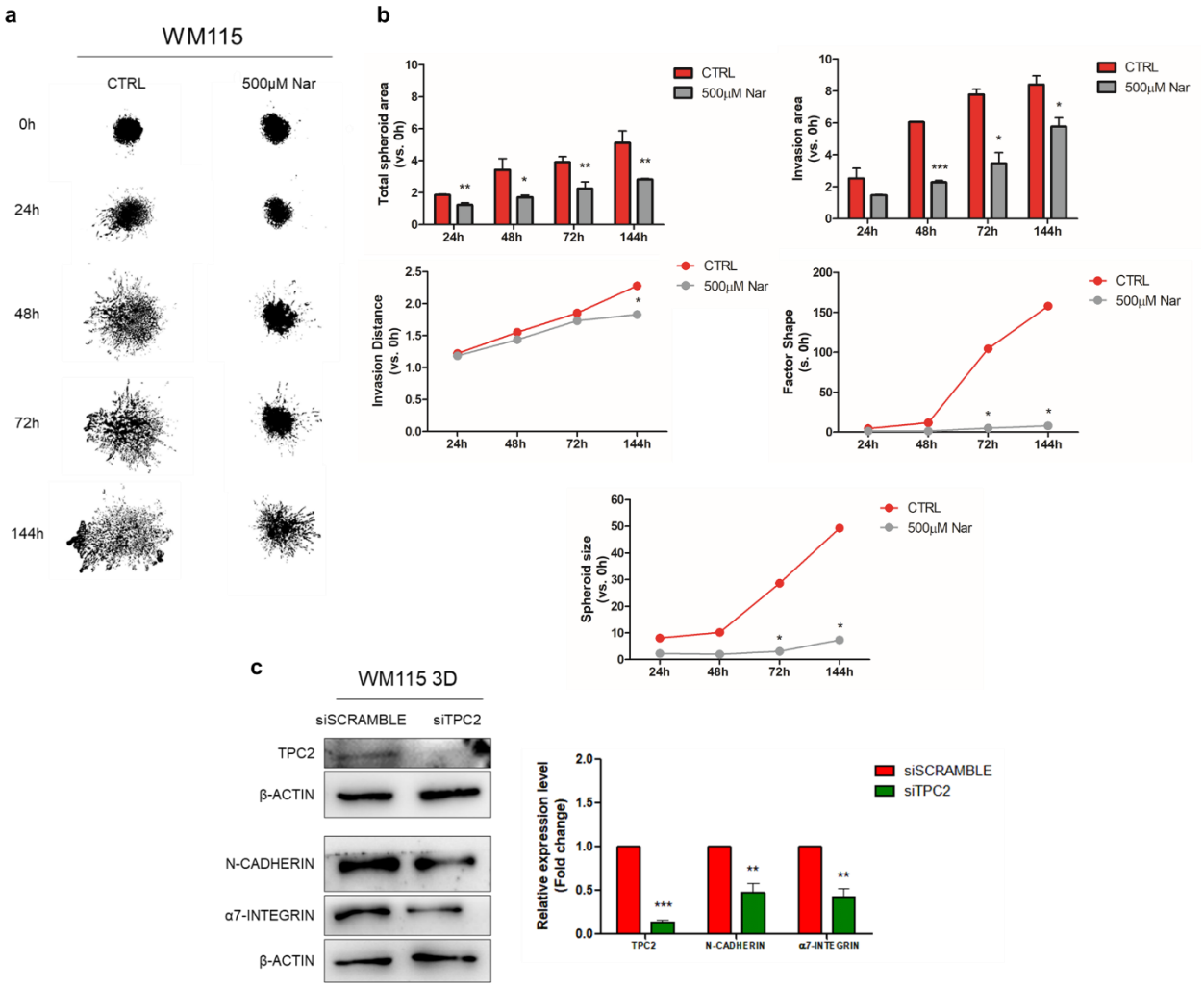

Figure 4.10 Reduction of invasion in type I collagen after Nar treatment and decrease expression of tumor invasion markers after TPC2 silencing in RGP primary melanoma spheroids. (a) WM115 multicellular spheroids were transferred into type I collagen matrix and treated with 500µM Nar. The images were taken from the time of treatment up to 144h. (b) Total spheroid area, invasion area, factor shape and the degree of compaction were calculated using the ImageJ software. The spheroid invasion distance was calculated using the software GIMP while. Four spheres were analysed for each condition. (c) The WM115 multicellular spheroids were transfected with scrambled or TPC2 siRNA. After 48h the expression of TPC2, N-Cadherin and α_7-integrin was evaluated by western blot. The band intensity was quantitatively determined using ImageJ software and protein levels' intensity was normalized to β-actin expression. The values have been normalized to the value obtained from cells with siRNA scramble. Data represent the mean and SEM of three independent experiments, *0.01<p<0.05; **0.001<p<0.01; ***0.0001<p<0.001.

4.6 Decrease of melanosomal exocytosis in melanoma cells after TPC2 inhibition

Recently, it has been hypothesized that melanoma cells promote dissemination through melanosomes. In particular, melanosomes, released by melanoma cells, are incorporated by normal fibroblasts and promote the formation of the dermal tumor primary niche [148]. Giving this data, and evidence of TPC2 involving in exocytosis process [25], we wanted to investigate whether the TPC2 affects the release of melanosomes by melanoma cells. First, to evaluate the presence of melanosomes in SH4 and WM793-B tumor cell lines we analysed the expression of the melanosomal markers HMB45 and DCT [111,133]. By western blots and immunofluorescence, we observed that both SH4 and WM793-B cells express the markers, in particular HMB45 protein is higher in SH4 compared to WM793-B, while DCT is similarly expressed in both cell lines, lower than in healthy melanocytes (Figure 4.11a).

Then, to assess the role of TPC2 in melanosomes release, we analysed the expression of the melanosomal markers after Nar treatment. SH4 treated cells show a significantly increases of HMB45 and a weaker increase of DCT (Figure 4.11b); similarly, in WM793-B cells we observed an increases expression of HMB45 and DCT after Nar treatment (Figure 4.11c).

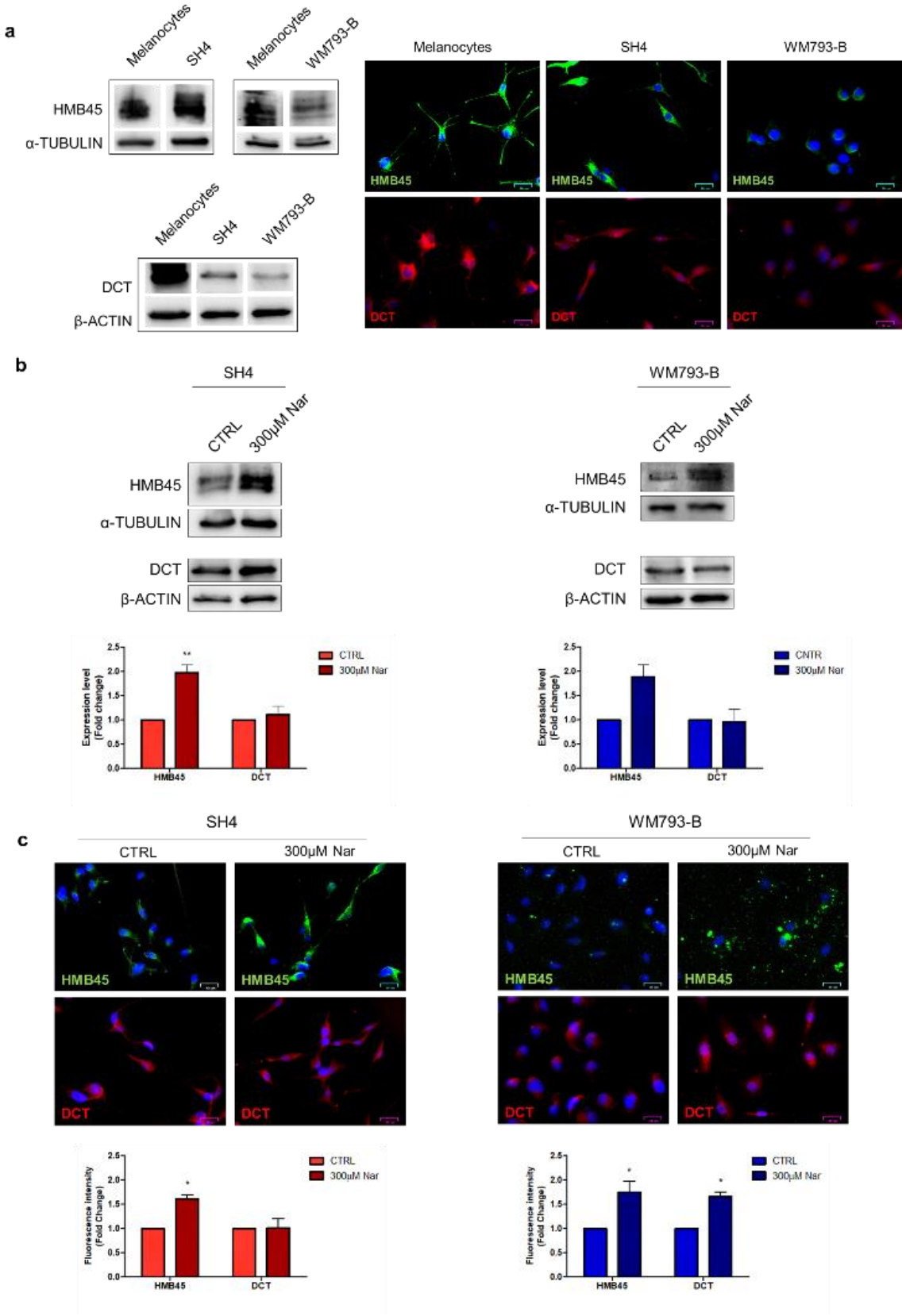

Figure 4.11 Increase expression of HMB45 and DCT in melanoma cells after Nar treatment. (a) HMB45 and DCT expression under basal conditions in melanocytes, SH4 and WM793-B cells by western blot. The expression of HMB45 (green) and DCT (red) was observed by IF in melanocytes, SH4 and WM793-B cells. Nuclei were stained with DAPI

(blue). (b) SH4 and WM793-B cells were treated with 300μM of Nar. The expression of HMB45 and DCT was evaluated by western blot. The band intensity was quantitatively determined using ImageJ software and protein levels' intensity was normalized to β-actin or α-tubulin expression. The values have been normalized to the value obtained from CTRL cells. (c) The expression of HMB45 (green) and DCT (red) was observed by immunofluorescence in SH4 and WM793-B cells treated with 300μM of Nar. Nuclei were stained with DAPI (blue). Fluorescence intensity was detected and analysed using the ImageJ software. Data represent the mean and SEM of three independent experiments, *0.01<p<0.05; **0.001<p<0.,01. Scale 25μm.

However, since this melanosomes increase in cell cytoplasm may be due to a fewer melanosomes released in culture medium or to an higher melanosomes synthesis and release, we evaluated the amount of intracellular and extracellular melanin after Nar treatment. Interestingly, both SH4 and WM793-B cells show an increase in the amount of intracellular melanin, visible as dark pigmentation in light microscopy (Figure 4.12a) and a lower release of melanin in culture medium after Nar treatment (Figure 4.12b).

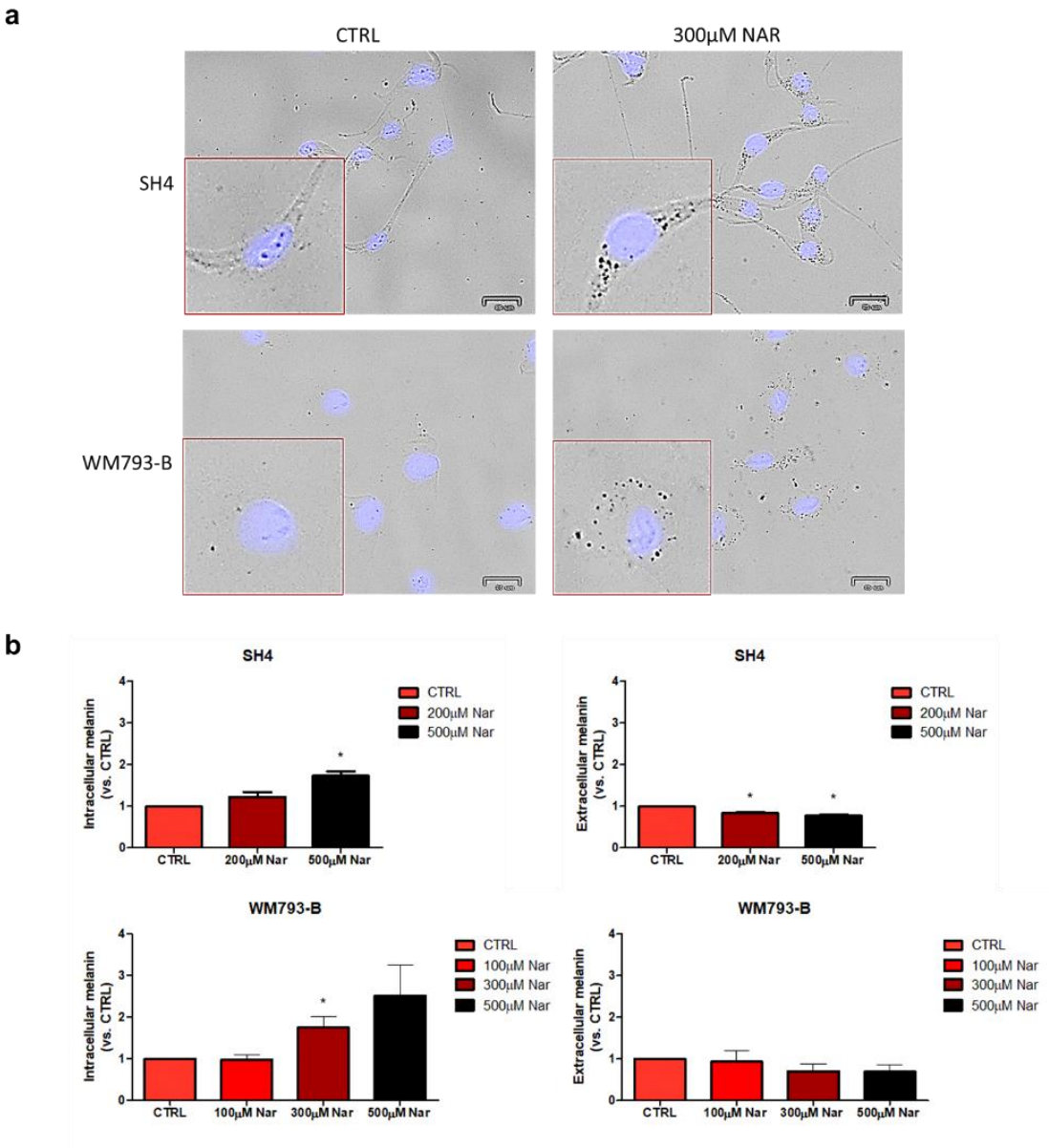

Figure 4.12 Increase in intracellular melanin and decrease in release of extracellular melanin in melanoma cells after Nar treatment. SH4 and WM793-B cells were treated with different doses of Nar. (a) Dark pigmentation was observed in light microscopy and nuclei were stained with DAPI (blue). (b) The amount of intracellular and extracellular melanin was evaluated by reading the absorbance to the spectrophotometer and normalized on control. Data represent the mean and SEM of three independent experiments, *0.01<p<0.05. Scale 25µm.

4.7 Incorporation of melanosomes in fibroblasts treated with melanoma-conditioned medium

As said before, it has been hypothesized that melanosomes, released by melanoma cells, are incorporated by normal fibroblasts and responsible for their transformation into CAFs, thus promoting the formation of a dermal pro-tumor niche [148]. For this reason, we wanted to confirm this process of melanosomes incorporation by treating human primary fibroblasts with SH4 and WM793-B cells conditioned medium. By immunofluorescence we observed that control fibroblasts do not express melanosomal markers, while fibroblasts treated with melanoma-conditioned media express both HMB45 and DCT in the cytoplasm (Figure 4.13).

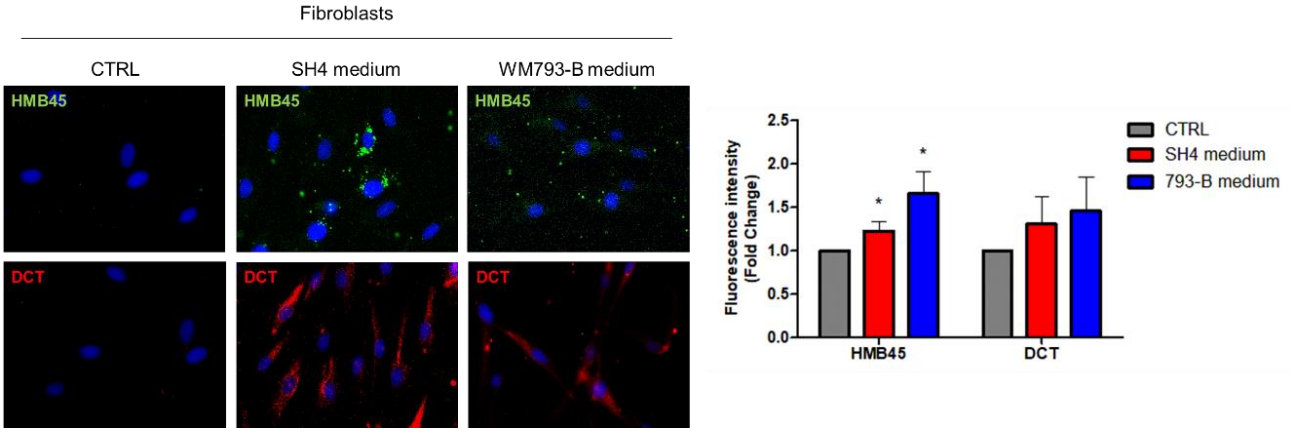

Figure 4.13 Expression of HMB-45 and DCT in fibroblasts treated with melanoma-conditioned medium. Fibroblasts were treated with conditioned medium of SH4 or WM793-B melanoma cells. The expression of HMB45 (green) and DCT (red) was observed by immunofluorescence in fibroblasts. Nuclei were stained with DAPI (blue). Fluorescence intensity was detected and analysed using the ImageJ software. Data represent the mean and SEM, *0.01<p<0.05. Scale 25µm.

4.8 Transformation of fibroblasts treated with melanoma-conditioned medium in CAFs

Since one of the characteristics of CAFs is to acquire a higher proliferative capacity than normal fibroblasts [161,170], to verify whether treatment with melanoma conditioned medium induced fibroblasts transformation into CAFs, we evaluated cells proliferation after treatment with the conditioned medium of SH4, WM793-B cell lines and melanocytes. By MTT assay, after 144h we did not observe any differences in fibroblasts proliferation (Figure 4.14a), only an increase after 144h of treatment with WM793-B conditioned medium, but not significative. Another characteristic of CAFs is to acquire a higher migratory and invasive capacity than healthy fibroblasts [170], thus to verify

fibroblasts transformation we also evaluated cell migration by scratch assay. Fibroblasts treated with SH4 and WM793-B cell lines-conditioned medium show an increase migratory capacity compared to those treated with melanocytes-conditioned medium (Figure 4.14b). Moreover, to confirm the data obtained by scratch assay we evaluated the expression of SNAIL, a protein involved in EMT process [174]. By western blot we noted an increase protein expression in fibroblasts treated with melanoma-conditioned medium compared to melanocytes-conditioned medium (Figure 4.14c).

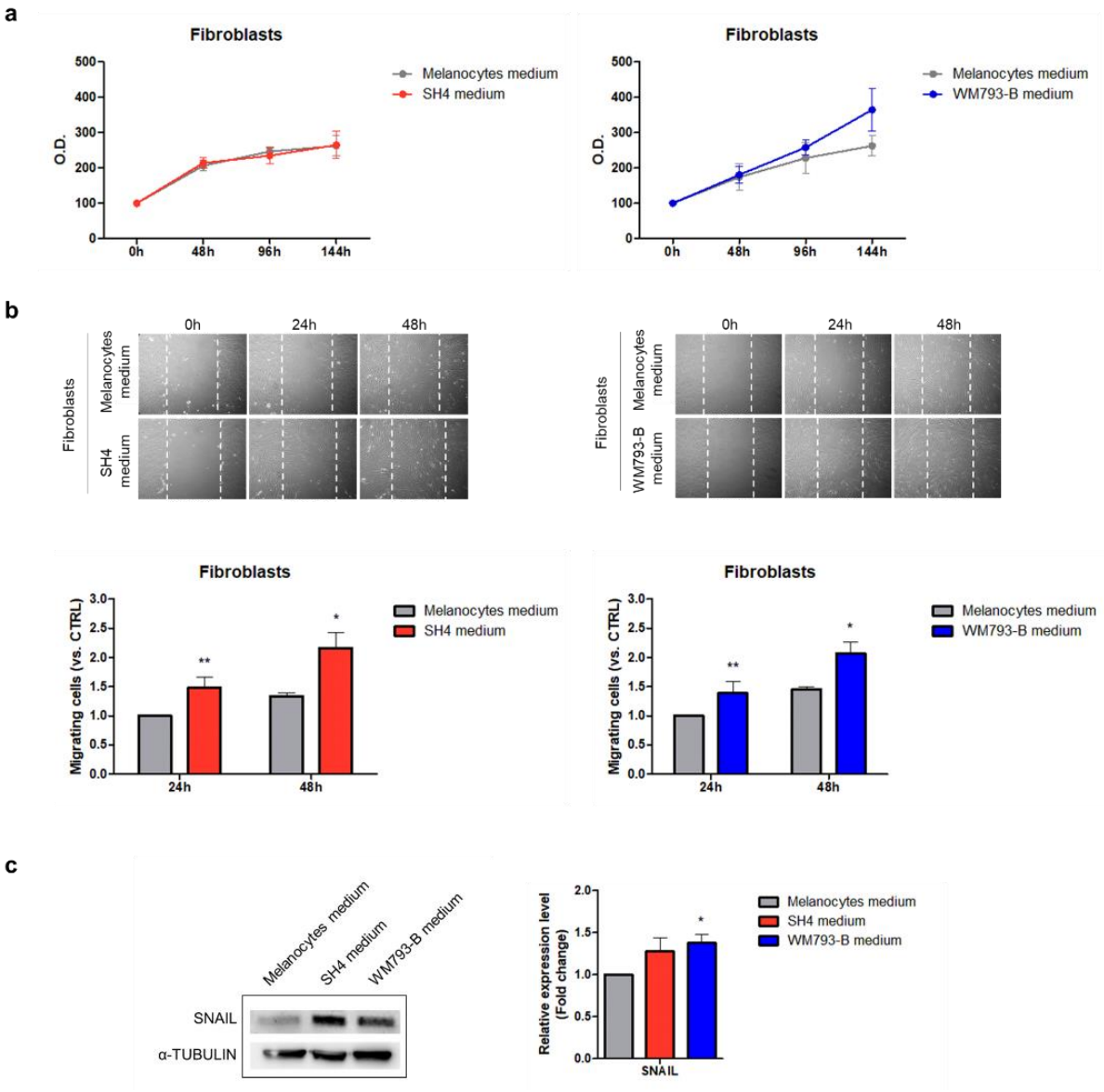

Figure 4.14 Analysis of cell proliferation and increase of migration capacity in fibroblasts treated with melanoma-conditioned medium. Fibroblasts were treated with conditioned medium of melanocytes, SH4 and WM793-B melanoma cells. (a) Graphs show the MTT viability assay of fibroblasts after treatment. The vitality has been evaluated by O.D. at different times, up to 144h from treatment. Five wells were analysed, for each condition. (b) For migration analysis four image were taken from the treatment up to 48h, for each condition. The cells migrated into the scraped area were evaluated, and four different areas for condition were counted. (c) SNAIL expression was evaluated in treated fibroblasts by western blot. The band intensity was quantitatively determined using ImageJ software and protein levels' intensity was normalized to α-tubulin expression. Data represent the mean and SEM of three independent experiments, *001<p<0.05; **0.001<p<0.01.

Subsequently, even to assess fibroblasts transformation we evaluated the expression of two specific markers of CAFs: FAP and α-SMA. By protein analysis we observed that fibroblasts incubated with SH4 conditioned medium show a higher expression of FAP and α-SMA, while those treated with WM793-B conditioned medium show a higher α-SMA expression although not statistically significant, while FAP expression does not change (Figure 4.15a). To better mimic the tumor microenvironment, the same markers were analysed by immunofluorescence in a co-culture of fibroblasts and melanoma cells. Both α-SMA and FAP are more expressed in fibroblasts growth in co-culture with the SH4 or WM793-B melanoma cells compared to fibroblasts growth alone (Figure 4.15b).

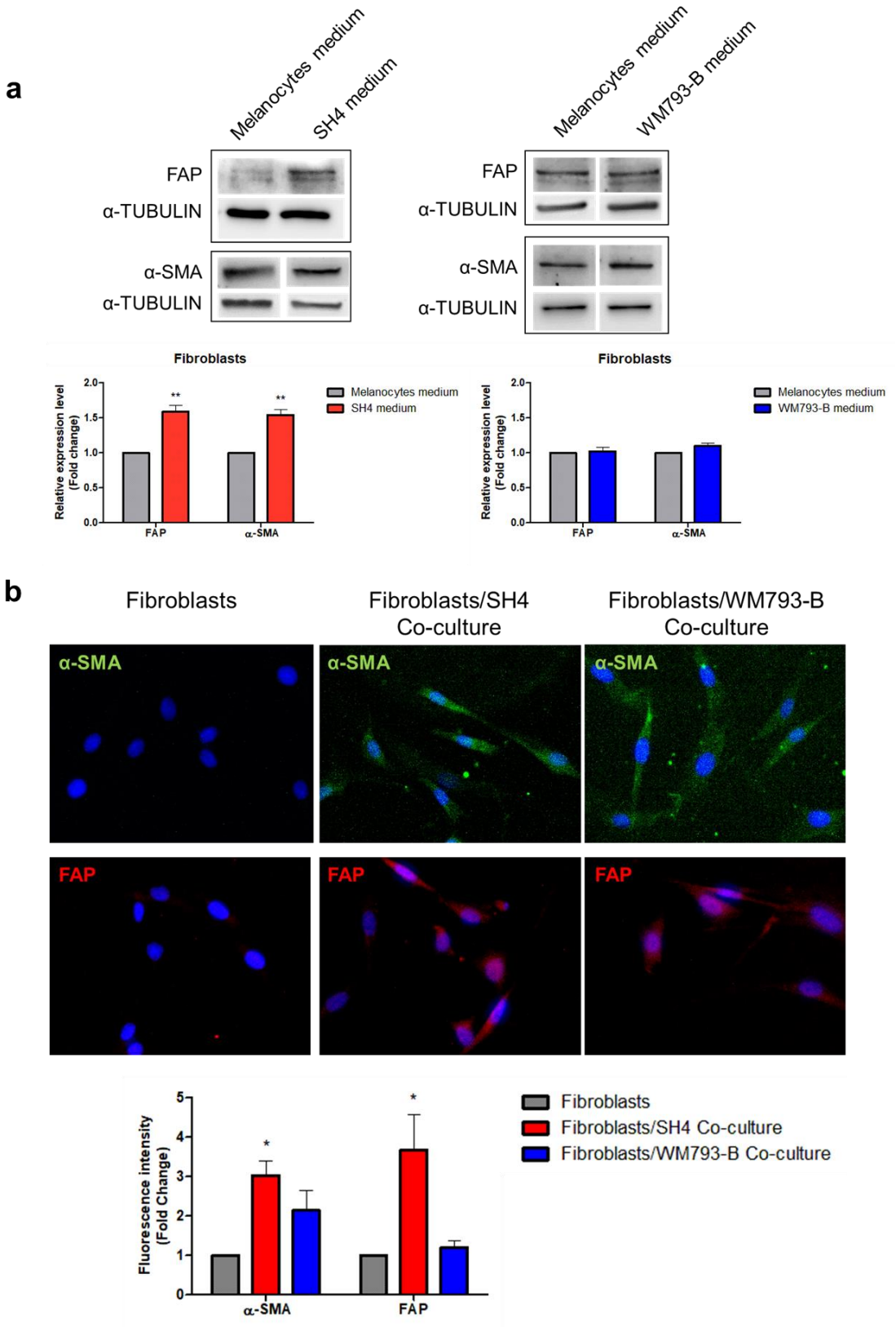

Figure 4.15 Increase expression of CAFs markers in fibroblasts treated with melanoma-conditioned medium or co-culture condition. (a) Fibroblasts were treated with conditioned medium of melanocytes, SH4 and WM793-B melanoma cells. The expression of FAP and α-SMA was evaluated by western blot. The band intensity was quantitatively determined using ImageJ software and protein levels' intensity was normalized to α-tubulin expression. (b) Fibroblasts were co-cultured with SH4 or WM793-B melanoma cells. The expression of α-SMA (green) and FAP (red) was observed by

immunofluorescence. Nuclei were stained with DAPI (blue). Fluorescence intensity was detected and analysed using the ImageJ software. Data represent the mean and SEM of three independent experiments, *0.01<p<0.05. Scale 25µm.

4.9 Analysis of fibroblast behaviours cultured with conditioned medium of Nar pre-treated melanoma cells

Since we have hypothesized that melanosomes of the conditioned medium are responsible of the transformation of fibroblasts into CAFs, and that Nar affects melanosomes release by melanoma cells, then we hypothesized that Nar treatment of melanoma cells may prevents fibroblasts transformation. So, we analysed the migration capacity of fibroblasts cultivated with conditioned medium of SH4 and WM793B cells pre-treated with Nar, observing a decreased fibroblasts migratory capacity Nar pre-treatment of melanoma cells (Figure 4.16).

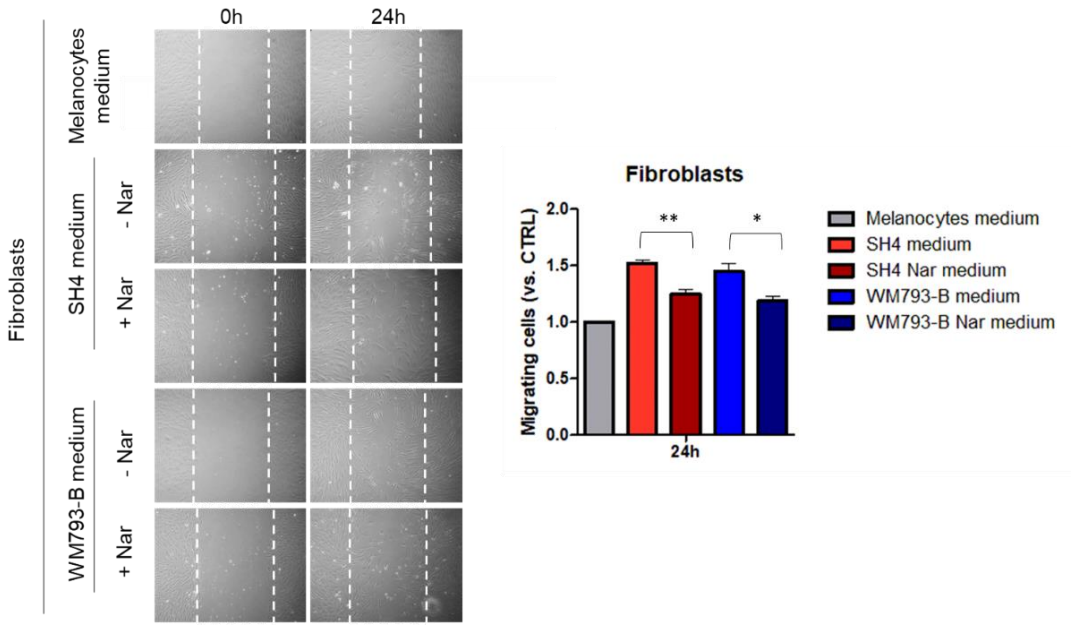

Figure 4.16 D**ecrease of migration capacity in fibroblast cultured with conditioned medium of Nar pre-treated melanoma cells.** Fibroblasts were treated with conditioned medium of melanocytes, SH4 and WM793-B melanoma cells pre-treated or not with Nar. The images represent the migratory capacity of treated fibroblasts. For each condition four image were taken. The cells migrated into the scraped area were evaluated, and four different areas for condition were counted. The data represent the mean and SEM of three different experiments, *0.01<p<0,05; **0.001<p<0.01.

4.10 Decrease of total spheroids area in TPC2 silenced melanoma spheroids after DTIC treatment

Since, not only it has been observed that the expression of PD-L1 is regulated by TPC2 [51], but also that TPC2 expression regulates authopagy, a key process in resistance to BRAF inhibitors [205] and the

channel is overexpressed after Vemurafenib (BRAF inhibitor) treatment in A375 BRAF V600E mutated melanoma cells [51], we hypothesized that TPC2 modulation may influence melanoma responses to drug inhibitors. First of all, after DTIC treatment RPMI7951, WM266-4 and SH4 cell lines show a decrease TPC2 expression (Figure 4.17a). Moreover, not only WM266-4 spheroids present a reduction of total spheroids area after TPC2 silencing, and in the same way after DTIC treatment, but interestingly we observed a synergistically reduction of total area in melanoma spheroids after TPC2 silencing and DTIC treatment (Figure 4.17b).

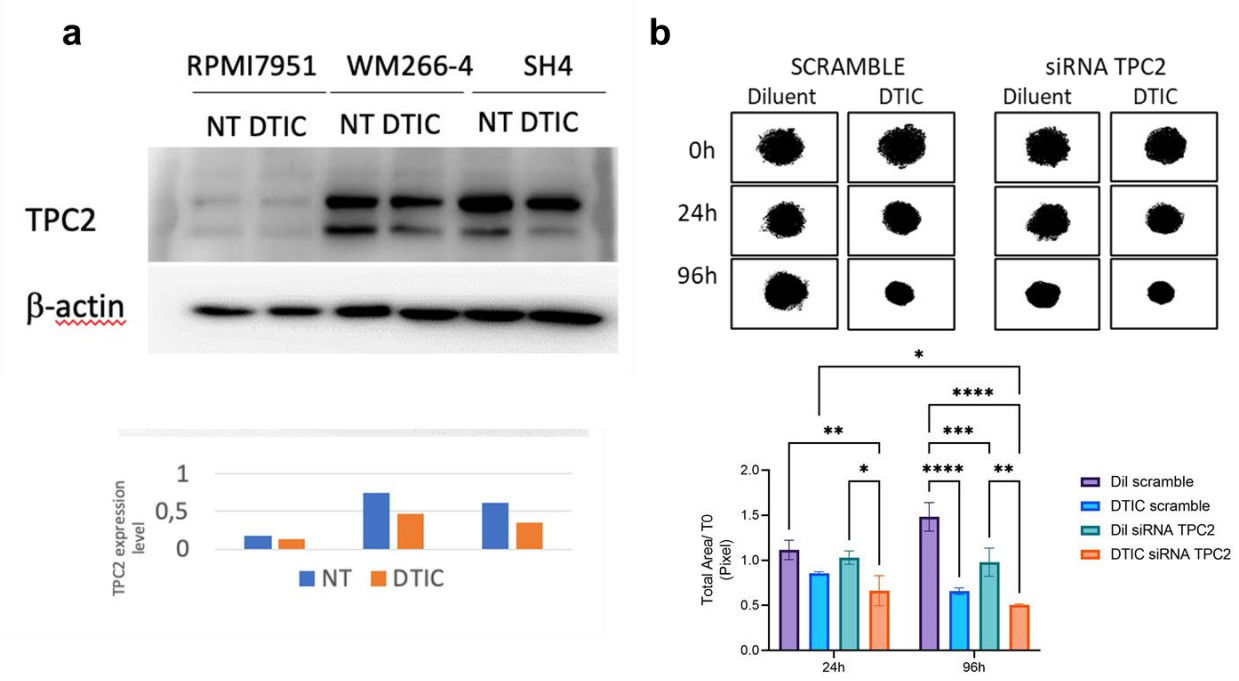

Figure 4.17 Decrease expression of TPC2 in melanoma cell lines after DTIC treatment and reduction of total spheroids area in TPC2 silenced melanoma spheroids after DTIC treatment. (a) RPMI7951, WM266-4 and SH4 melanoma cells were treated with DTIC. TPC2 expression was evaluated by western blot. The band intensity was quantitatively determined using ImageJ software and protein levels' intensity was normalized to β-actin expression. (b) The WM266-4 cells were transfected with scrambled or TPC2 siRNA. The transfected cell lines were plated according to the "liquid overlay methods" to obtain multicellular spheroids and treated with DTIC. Images were taken from the time of treatment up to 96h. The total spheroid area was calculated using the ImageJ software. The data represent the mean and SEM of three different experiments, *0.01<p<0.05; **0.001<p<0.01; ***0.0001<p<0.001; ****p<0.0001.

5. DISCUSSION AND CONCLUSIONS

Malignant melanoma is a complex multifactorial disease, presenting genetic, clinical, histopathological and biological variants, which make it the most aggressive form of skin cancer. Worldwide, the incidence of cutaneous melanoma has risen dramatically, and although early-stages tumors may be treated by surgical excision, metastatic melanomas are very difficult to treat due to its high aggressiveness and resistance to common therapies [70,71]. Despite the great progress made on therapeutic strategy such as the recent advancements in BRAF/MEK target therapies and immunotherapeutic drugs, only 5-10% of patients with metastatic melanoma achieve 5 years long-term survival due to cell resistance [118]. Therefore, there is a great interest in finding new pharmacological targets for the development of new treatments for melanoma.

Recently, it has been hypothesized a role of TPC2 in melanoma progression, indeed among different cancer cell lines it has been shown that TPCN2 mRNA expression is higher in HCC (hepatocellular carcinoma) and melanoma [206]. In detail, regarding primary melanomas the analysis in the TCGA showed an increase expression that correlates with melanoma depth and with TPC2 protein analysis in skin sections. In addition, VGP melanoma cell lines express high level of TPC2 compared to RGP tumor cells, suggesting a role of this cation channel in tumor progression. Interestingly, nodular melanomas, which present different clinical and histopathological features than malignant melanomas [207], show slightly higher TPC2 level than malignant melanomas with high Breslow Index. This subtype is assumed to originate from melanocytes of the dermis, and MSE models with nodular melanoma cells show high level of tumor invasion markers, such as α_4-integrin, α_7-integrin and N-Cadherin and low expression of E-Cadherin, suggesting that this subtype is more invasive and aggressive than malignant melanoma. Although this group presents different biomolecular markers [207], the fact that TPC2 is highly expressed in both types may suggest an important role of this channel in tumor growth and invasion through the dermis. In other cancer types TPCN2 is differently expressed: in bladder cancer it is found to be significantly associated with increased survival [208]; in prostate cancer it is one of a six gene signatures that predict postoperative biochemical recurrence [209] and in half of all oral squamous cell carcinomas that presents the amplification of 11q13, the overexpression of TPC2 results in a poor outcome of patients [210].

More contrasting results came from metastasis analysis, because if the analysis in the TCGA show a decrease TPCN2 expression in melanoma metastasis [51] both in lymph node and other metastatic sites, on the other hand TPC2 protein level seems to be higher in different melanoma metastasis. This decrease of TPC2 mRNA in metastasis and the increase in TPC2 protein may be explain by a different post-translational modifications that stabilize the protein, such as N-glycosylation, which can affect protein folding, stability and function [16]. Furthermore, it is possible that the metastases analysed in the database come from treated patients, which could affect the level of channel expression. Indeed, in this thesis project we observed that DTIC treatment reduces TPC2 expression

in different melanoma cell lines. In particular, skin sections of cutaneous metastasis show high channel level compared to primary melanoma of the same patient, and similarly results were obtained with skin metastasis and RGP human primary melanoma cell lines of the same patients by western blot. Differently, lymph node metastasis shows a high diffuse staining in patient tissue section, while 2D and 3D models of lymph node metastasis cell lines show low level of TPC2 expression compared to healthy melanocytes. Finally, in lung metastasis we did not observe TPC2 expression in patient tissue section, although 2D and 3D models of cell line derived from pleural effusion show high level of protein. Taken together, these experiments showed that TPC2 expression is increased in cutaneous metastasis compared to primary melanoma, although further investigation are required to assess if TPC2 expression correlates with specific metastatic sites, given a great heterogeneity between different tumor microenvironments.

To evaluate the role of TPC2 in melanoma we used Nar, a molecule that strongly inhibits the activities of this channel [31,50]. Literature data showed that Nar molecule had low toxicity in normal fibroblasts, with IC50 of 1090µM at 24h [211], andsimilar results were obtained by other researchers, showing that this flavonoid exhibited strong inhibitory effects against cancer lines and very weak activity in normal cells [212]. Therefore, considering the low toxicity, in *in vitro* experiments we used analogous Nar concentrations (300-500µM) that could then be replicated "in a clinical setting". Investigating TPC2 function in tumor growth, we observed that 2D melanoma cell lines show reduced proliferation rate after TPC2 blocking with different doses of Nar. Similarly, in 3D models we observed a reduction of total spheroid area after Nar treatment, although we noted that RGP primary melanoma spheroids continue to compact over time. Since initially during spheroids formation cells aggregates by interaction of cellular surface integrins with ECM fibers and cell-cell interactions by E-Cadherin homophilic bonds [183,185,186], we may suppose that RGP primary cells during the formation of the spheres increase the expression of adhesion molecules, that are basically highly expressed in this tumor subtype, forming very compact spheres. On the contrary, pleural metastasis spheroids are less compact, probably because 3D models reflect the *in vivo* behaviour of the original tumor cells, such as distinct morphologic features [177]. While after Nar treatment RGP, VGP and skin metastasis show a dose and time dependent reduction of total area, in pleural metastasis we do not observe any effects. On the other hand, after TPC2 silencing pleural metastasis spheroids show reduce cell proliferation rate and total area. Because TPC2 silencing modulated spheroids growth, it is possible that in this contest Nar does not affect the proliferation rate acting on other pathway, even if also in breast, gastric, liver and prostate cancer *in vitro* studied show an antiproliferative effect of Nar [55,56]. A role of TPC2 in the inhibition of cell proliferation has been identified also in other cancer types, such as in 4T1 mouse mammary cancer cells [32] and B16F0 and B16F10 mouse melanoma cells [33,213,214], moreover Müller et al. identified TPC2 as a cancer driver. The findings show that genetic deletion of the channel reduces the proliferation of liver cancer cells *in vitro* and successfully stops tumour growth in an ectopic mice model [215].

In regard to tumour progression, we observed a reduction of tumor migration capacity in RGP and VGP primary cells, skin metastasis and pleural metastasis after TPC2 silencing or Nar treatment. Moreover, RGP primary tumor spheroids, that is supposed to be the less aggressive subtype, in type I collagen matrix show lower invasive capacity after TPC2 blocking. In line with our data, it has been observed that TPC2 negative regulates migration processes in mammary, bladder, liver cancers and mouse melanoma *in vitro* models [32,33] and reduces formation of lung metastases in *in vivo* mouse models of mammary and melanoma cancer cells, respectively 4T1 and B16F0 [33,46]. In addition, in MNT-1 human melanoma cells TPC2 knockout or Nar treatment decreases cell proliferation, migration and invasion [50], probably via regulation of MIFT protein levels, a transcription factor that regulates genes involved in cell cycle progression and differentiation, a role sustained throughout the process of melanogenesis and in melanoma [206]. In particular, Netcharoensirisuk et al. in TPC2-/- MNT-1 cells find increase GSK3β protein levels and an increase proteasomal degradation of MIFT. On the contrary, in CHL1 human metastatic melanoma cell line TPC2 inhibition increases the metastatic traits. TPC2 knockout impairs cell adhesion to type I collagen matrix, increases invasion capability and induces the expression of bona fide YAP/TAZ target genes. Thus indicates an activation of YAP/TAZ, which are target genes of the HIPPO signaling pathway, that is involved in several biological processes including proliferation, survival, differentiation and in mechanisms of tumor progression [51,52]. D'Amore et al., differently to Netcharoensirisuk et al, observed an increased expression of MITF in TPC2-/- CHL-1 cells. The three lines used in these studied presented completely different features: MNT-1, derived from lymph node metastasis, are highly pigmentated and with BRAF mutation; CHL-1, derived from pleural effusion, are amelanotic and BRAF wt; B16F0, derived from mouse primary melanoma, are highly pigmented and BRAF wt. In our experiments, also the cell lines derived from primary tumors are all BRAF mutated, but present different aggressiveness, distinct metastatic sites, and different pigmentation (Table 1 Materials and Methods), therefore the different role of TPC2 may depend on some of these characteristics. Thus, the opposite role played by TPC2 in different melanoma cell lines may be indicative that the function of this ion channel could be pro-tumoral or anti-tumoral according to the cell phenotype such as pigmentation, genomic mutations, and microenvironment. To better assess the role of this channel in different cellular contests, the channel could be pharmacologically inactivated or activated by different specific antagonists/agonists respectively, such as Ned-19 (a NAADP-antagonist), flavonoid compounds MT-8 and UM-9 [50], Tetrandrine and Verapamil (Ca^{2+} channel blocker) or by NAADP, PI(3,5)P2, TPC2-A1-N and TPC2-A1-P agonists [216]

TPC2 involvement in tumor invasion has been confirm also by the analysis of tumor invasion markers in VGP primary tumor, skin and pleural metastasis. Indeed, after TPC2 silencing or Nar treatment, all the lines present a decrease expression of α_7-integrin and α_4-integrin, important component of melanoma microenvironment. Because these proteins normally promote cells adhesion to ECM, alterations in the expression of integrins allow melanoma cells to dissociate from the

primary site, alter the cytoskeleton, migrate through the stroma and lymphatic or vascular vessels and disseminate to distant sites [161]. Numerous studies have shown a different expression of integrins in normal melanocytes and benign naevi compared to melanoma cells [101], for example $\alpha_7\beta_1$-integrin has been detected in melanoma cells and not in normal melanocytes [217], while $\alpha_4\beta_1$-integrin is not expressed in primary and dysplastic naevi, while in melanoma the expression correlates with the progression from RGP to VGP [103,104]. According to this data, the decrease expression of α_7 and α_4-integrin after TPC2 blocking may suggest a role of this channel in tumor invasion process. Interestingly, in a mammary cancer cell line TPC2 blocking alters endolysosomal system and leads to an accumulation of the protein in early endosomes, inhibiting the normal recycling of β_1-integrin and the formation of β_1-integrin polarized lamellopodia [46]. Although in this contest total protein levels of β_1-integrin are not significantly modified after TPC2 blocking, but mammary cells express TPC2 only in lysosomes and late endosomes, since they have not melanosomes, it is possible that in melanoma cells TPC2 regulates both integrins expression and recycling acting on endolysosomal system.

Similar to integrins, TPC2 blocking modifies the expression of other adhesion molecules, decreasing N-Cadherin and increasing E-Cadherin expression. These adhesion molecules have been related to melanoma progression, indeed E-Cadherin is associated with cell-to-cell adhesion properties in melanocytes and loss of expression leads to an invasive phenotype often linked with transformed cells [164]. The switch from E-Cadherin to N-Cadherin allows melanoma cells to interact with other N-Cadherin expressing cells such as fibroblasts and endothelial cells, increasing their motility due to less stringent cell interaction, conferring survival advantages through repression of proapoptotic factors [161]. Recently in a study that used matched tissue samples from primary and metastatic sites of melanoma, it has been observed that metastatic tumor show a decrease in E-Cadherin expression and an increase in N-Cadherin expression compared to the primary tumor, although the difference do not reach statistical significance [98].

Finally, also the expression of slug, a transcriptional repressor of E-Cadherin [99] involved in the EMT, decreases in melanoma cells after TPC2 blocking. In melanoma, it has been shown that Slug functions as a melanocyte-specific factor required for the strong metastatic propensity of this tumor [100]. Therefore, Cadherin switch from E- to N- suggests a role of TPC2 in the regulation of the epithelium-mesenchymal transition, and in melanoma progression, in agreement with the increase TPC2 expression in primary melanoma with higher Breslow Index.

Cellular transformation in melanoma is associated to changes in melanosomes biogenesis and pigment production, indeed it has been observed that some melanocytes lose their ability to synthesize pigments and assume a disorganized structure [124,149,150]. Since TPC2 is involved in exocytosis process [25] and in B16F10 mouse melanoma cells Nar treatment increases intracellular melanin concentration and melanogenic proteins [64,65], it is possible that TPC2 plays a role not only in melanogenesis but also in melanosomes releases, regulating tumor progression. To analysed

melanosomes expression we used two melanocytic markers: HMB45, an antibody that recognizes Pmel17, a type I transmembrane glycoprotein also known as gp100, which is expressed in early melanosomes (stage I and II) and DCT (TRP2), a protein that modulates the activity of tyrosinase that mainly localize in strongly pigmented late melanosomes (stage III and IV) [133]. As expected, healthy melanocytes and melanoma cells express both HMB45 and DCT, moreover after Nar treatment melanosomal markers expression and intracellular melanin amount increase. As said before, a role of Nar in melanogenesis has already been assess in B16-F10 mouse melanoma cells. In this contest, Nar increases intracellular melanin concentration, melanogenic proteins levels and enhances phosphorylation of Akt and GSK3β protein, which inactivates the kinase activity of GSK3β, resulting in the elevation of intracellular β-Catenin levels. β-Catenin promotes melanogenesis by up-regulating the melanocyte differentiation-related proteins, such as MITF and tyrosinase [64]. Differently, in MNT-1 human melanoma cells, Nar increases melanin production with a different mechanism, because in TPC2 knockout melanoma cells MITF level is reduced, the expression of proteins involved in melanogenesis or regulated by MITF such as DCT, Rab27a, or PMEL is unchanged, while GSKβ level is increased [50]. Interestingly, flavonoids have been reported to affect MITF expression through interference with Wnt signalling. Thus, in human melanoma cells growth inhibition by flavonoids is associated with disruption of Wnt signalling and decreased MITF levels [218]. In the end, in MNT-1 melanin production is independently of MITF through direct interference with tyrosinase activity in melanosomes, by indirect interference with the melanosomal proton pump: decreased driving force for the pump due to absent or reduced TPC2 activity, resulting in reduced proton uptake by melanosomes, leading to less acidic melanosomal pH, increased tyrosinase activity, and eventually increased melanin production [206]. According with this data Ambrosio et al. in TPC2 knockout MNT-1 cells show an increase of melanin and less acid and larger melanosomes, but no increase in the number per cell [41]. Since, in our analysis after Nar treatment we observe an increase not only of melanin, but also of DCT and HMB45, it suggests a MIFT regulation of melanogenesis and/or a block of melanosomes releases. Since after Nar treatment melanoma cells show a lower release of melanin in culture medium, we can assume that TPC2 blocking also inhibits the process of maturation of melanosomes and/or the release of melanin.

Recently, it has been shown that dermal fibroblasts have the ability to uptake melanosomes secreted by melanocytes, demonstrating that these organelles are not only transferred to keratinocytes in healthy skin [219]. Although in physiological conditions skin fibroblasts incorporate about 100 melanosomes, Dror et al. quantified 200–500 melanosomes per melanoma dermal fibroblast, indicating increased uptake under pathological conditions. In melanoma, it has been hypothesized that melanosomes, released by melanoma cells, are incorporated by normal fibroblasts and responsible for their transformation into CAFs, thus promoting the formation of a dermal pro-tumor niche [148]. Indeed, we observed that fibroblasts treated with conditioned medium of SH4 and WM793-B cells express both HMB45 and DCT in the cytoplasm, confirming the melanosomes incorporation.

In the same way, fibroblasts treated with the conditioned medium of MNT-1 melanoma cells show the expression of two melanosomal markers, HMB45 and GPNMB, which show that even in this context the treated fibroblasts incorporate melanosomes released into the medium by melanoma cells [148]. Some of the characteristics of CAFs are to acquire a higher proliferative, migratory and invasive capacity than normal fibroblasts [161,170], indeed fibroblasts isolated from patients with breast cancer, melanoma and retinoblastoma, show an increased in proliferation rate *in vitro* [165]. Of note, the treatment with conditioned medium of SH4 and WM793-B cells increase fibroblast migration capability and expression of SNAIL, a protein involved in the process of cell migration, although it does not affect fibroblast proliferation. Similarly, Dror et al. show that fibroblasts cultured with the conditioned medium of MNT-1 melanoma cells increase proliferative and migratory capacity compared to those treated with melanocytes-conditioned medium [148]. Moreover, we observed that fibroblasts incubated with SH4 conditioned medium show a higher expression of FAP and α-SMA, while those treated with WM793-B conditioned medium show a higher α-SMA expression, while FAP expression does not change. In addition, both α-SMA and FAP are more expressed in fibroblasts growth in co-culture with the SH4 or WM793-B melanoma cells compared to fibroblasts growth alone. Since, these two proteins are specifically expressed by CAFs [166,167], FAP a serine protease that helps to reorganize the matrix and α-SMA an actin that promotes the contractile action of fibroblasts, we can suppose that melanoma-conditioned medium induce fibroblasts transformation.

As in MNT-1 cells, fibroblasts reprogramming into CAFs appeared to be mediate, at least in part, by the melanosomal miRNA-211, as in our cells lines melanosomes of the conditioned medium are incorporated by normal fibroblast and melanoma-conditioned medium has induced fibroblasts transformation, we may hypothesize that also SH4 and WM793-B melanosomes are responsible of fibroblasts transformation. Therefore, since Nar affects melanosomes release by melanoma cells, Nar treatment may prevent fibroblasts transformation. Indeed, fibroblasts cultivated with conditioned medium of SH4 and WM793-B cells pre-treated with Nar show reduces migratory capacity.

Therefore, these data suggest that Nar-treatment can regulate melanoma cell EMT processes as well as melanosome maturation and release, suggesting this molecule as a new potential treatment for melanoma towards a personalized medicine. Although a limitation of this study is the lack of *in vivo* models both in term of toxicity and efficacy of Nar treatment, literature data show that Nar has already been used in B16F10 *in vivo* mouse studies via intraperitoneal injection [220] and oral administration [221]. Moreover, clinical trials evaluating the safety and pharmacokinetics of Nar in healthy adults show that Nar ingestion has no related adverse events or alteration in blood safety markers [222]. Of course, further experiments are needed to assess if these concentrations are efficacy against cancer cells, without causing undue toxicity *in vivo*. Finally, according to melanoma heterogeneity it is possible that even lower doses of Nar can be used for carcer treatment.

Observing that DTIC treatment seems to reduce TPC2 protein expression and to synergistically inhibit total spheroids area in TPC2 silenced melanoma cell lines, we supposed that TPC2 modulation

may influence melanoma responses to drug inhibitors. Thus, these experiments suggest that Nar may act as a chemosensitiser. In the same way, in different type of advanced cancers, it has been observed that Nar is beneficial in a combinatorial setting to alleviate multi-drug resistance [223]. For example, combining Nar with Paclitaxel synergistically increased cytotoxicity in prostate cancer cells [174], while in combination with histone deacetylase inhibitors synergistically suppressed neuroblastoma tumor progression [224] and with 5-fluorouracil synergistically enhanced colorectal cancer cell death [225].

Summarizing, the results obtained in this study show that TPC2 is differently express in primary and metastatic melanomas, probably according to specific tumor features like stage and microenvironment. In the same way, the opposite role played by TPC2 in different melanoma cell lines showed in some studies, may be indicative that the function of this ion channel could be specific according to the cell phenotype such as pigmentation, genomic mutations, and microenvironment.

In conclusion, this channel proves to be an interesting pharmacological target for the development of new personalized therapies and suggest Nar as a new potential treatment for melanoma.

6. BIBLIOGRAPHY

1. Calcraft, P. J. *et al.* NAADP mobilizes calcium from acidic organelles through two-pore channels. *Nature* **459**, 596–600 (2009).
2. Feijóo-bandín, S. *et al.* Two-pore channels (TPCs): Novel voltage-gated ion channels with pleiotropic functions. **6950**, (2017).
3. Morgan, A. J., Platt, F. M., Lloyd-evans, E. & Galione, A. Molecular mechanisms of endolysosomal Ca2+ signalling in health and disease. *Biochem. J* **374**, 349–374 (2011).
4. Jin, X. *et al.* Targeting Two-Pore Channels : Current Progress and Future Challenges. *Cell Press* **41**, (2020).
5. Rietdorf, K. *et al.* Two-pore Channels Form homo- and heterodimers. *J. Biol. Chem.* **286**, 37058–37062 (2011).
6. She, J., Zeng, W., Guo, J. & Chen, Q. Structural mechanisms of phospholipid activation of the human TPC2 channel. 1–17 (2019).
7. Walseth, T. F. *et al.* Photoaffinity Labeling of High Affinity Nicotinic Acid Adenine Dinucleotide Phosphate (NAADP) -Binding Proteins in Sea Urchin Egg * □. *J. Biol. Chem.* **287**, 2308–2315 (2012).
8. Lin-moshier, Y. *et al.* Photoaffinity Labeling of Nicotinic Acid Adenine Dinucleotide Phosphate (NAADP) Targets in Mammalian. *J. Biol. Chem.* **287**, 2296–2307 (2012).
9. Pitt, S. J., Lam, A. K. M., Rietdorf, K. & Galione, A. Reconstituted Human TPC1 Is a Proton-Permeable Ion Channel and Is Activated by NAADP or Ca 2 +. **7**, (2014).
10. Pitt, S. J., Donnell, B. R. & Sitsapesan, R. Exploring the biophysical evidence that mammalian two-pore channels are NAADP-activated calcium-permeable channels. *J. Physiol.* **594**, 4171–4179 (2016).
11. Wang, X. *et al.* TPC Proteins Are Phosphoinositide- Activated Sodium-Selective Ion Channels in Endosomes and Lysosomes. *Cell* **151**, 372–383 (2012).
12. Cang, C. *et al.* mTOR Regulates Lysosomal ATP-Sensitive Two-Pore Na + Channels to Adapt to Metabolic State. *Cell* **152**, 778–790 (2013).
13. Rybalchenko, V. Membrane Potential Regulates Nicotinic Acid Adenine Dinucleotide Phosphate (NAADP) Dependence of the pH- and Ca 2 ⁒ -sensitive Organellar Two-pore Channel TPC1. *J. Biol. Chem.* **287**, 20407–20416 (2012).
14. Jha, A., Ahuja, M., Patel, S., Brailoiu, E. & Muallem, S. Convergent regulation of the lysosomal two-pore channel-2 by Mg2+, NAADP, PI(3,5)P2 and multiple protein kinases. **33**, 501–511 (2014).
15. Pitt, S. J. *et al.* TPC2 Is a Novel NAADP-sensitive Ca 2+ Release Channel , Operating as a Dual Sensor of Luminal pH and Ca 2+. *J. Biol. Chem.* **285**, 35039–35046 (2010).
16. Hooper, R., Churamani, D., Brailoiu, E., Taylor, C. W. & Patel, S. Membrane Topology of NAADP-sensitive Two-pore Channels and Their Regulation by N-linked Glycosylation. *J. Biol. Chem.* **286**, 9141–9149 (2011).
17. Ramos, I., Reich, A. & Wessel, G. M. Two-pore channels function in calcium regulation in sea star oocytes and embryos. *Co. Biol.* 4598–4609 (2014) doi:10.1242/dev.113563.
18. Arredouani, A. *et al.* Nicotinic Acid Adenine Dinucleotide Phosphate (NAADP) and Endolysosomal Two-pore Channels Modulate Membrane Excitability and Stimulus-Secretion Coupling in Mouse Pancreatic betaCells *. *J. Biol. Chem.* **290**, 21376–21392 (2015).

19. Hamilton, A. *et al.* Adrenaline Stimulates Glucagon Secretion by Tpc2- Dependent Ca 2 + Mobilization From Acidic Stores in Pancreatic a -Cells. *Diabetes* **67**, 1128–1139 (2018).

20. Notomi, T. *et al.* Role of lysosomal channel protein TPC2 in osteoclast differentiation and bone remodeling under normal and low-magnesium conditions. *J. Biol. Chem.* **292**, 20998–21010 (2017).

21. Aley, P. K. *et al.* Nicotinic acid adenine dinucleotide phosphate regulates skeletal muscle differentiation via action at two-pore channels. *PNAS* **108**, (2010).

22. Zhang, Z., Lu, Y. & Yue, J. Two Pore Channel 2 Differentially Modulates Neural Differentiation of Mouse Embryonic Stem Cells. *PLoS One* **8**, (2013).

23. Tugba Durlu-kandilci, N. *et al.* TPC2 Proteins Mediate Nicotinic Acid Adenine Dinucleotide Phosphate (NAADP) - and Agonist-evoked Contractions of Smooth Muscle. *J. Biol. Chem.* **285**, 24925–24932 (2010).

24. Garcia-Rua, V. *et al.* Endolysosomal two-pore channels regulate autophagy in cardiomyocytes. *J. Physiol. Physiol.* **11**, 3061–3077 (2016).

25. Davis, L. C. *et al.* NAADP Activates Two-Pore Channels on T Cell Cytolytic Granules to Stimulate Exocytosis and Killing. *Curr. Biol.* **22**, 2331–2337 (2012).

26. Hockey, L. N. *et al.* Dysregulation of lysosomal morphology by pathogenic LRRK2 is corrected by TPC2 inhibition. *Co. Biol.* 232–238 (2015) doi:10.1242/jcs.164152.

27. Kayala, K. M. N., Dickinson, G. D., Minassian, A., Walls, K. C. & Green, K. N. PRESENILIN-NULL CELLS HAVE ALTERED TWO-PORE CALCIUM CHANNEL EXPRESSION AND LYSOSOMAL CALCIUM; IMPLICATIONS FOR LYSOSOMAL FUNCTION. *Brain Res.* 8–16 (2013) doi:10.1016/j.brainres.2012.10.036.PRESENILIN-NULL.

28. Grimm, C. *et al.* High susceptibility to fatty liver disease in two-pore channel 2-deficient mice ¨. *Nat. Commun.* (2014) doi:10.1038/ncomms5699.

29. Sakurai, Y. *et al.* Two pore channels control Ebola virus host cell entry and are drug targets for disease treatment. *Science (80-.).* **347**, 995–998 (2016).

30. Favia, A. *et al.* VEGF-induced neoangiogenesis is mediated by NAADP and two-pore channel-2–dependent Ca2+ signaling. *PNAS* 4706–4715 (2014) doi:10.1073/pnas.1406029111.

31. Pafumi, I. *et al.* Naringenin Impairs Two-Pore Channel 2 Activity And Inhibits VEGF-Induced Angiogenesis. *Nature* (2017) doi:10.1038/s41598-017-04974-1.

32. Sun, W. & Yue, J. TPC2 mediates autophagy progression and extracellular vesicle secretion in cancer cells. *Exp. Cell Res.* **370**, 478–489 (2018).

33. Favia, A. *et al.* NAADP-Dependent Ca2+ Signaling Controls Melanoma Progression, Metastatic Dissemination and Neoangiogenesis. *Sci. Rep.* **6**, 1–12 (2016).

34. Lin, J. Y. & Fisher, D. E. Melanocyte biology and skin pigmentation. *Nature* **445**, 843–850 (2007).

35. Grønskov, K., Ek, J. & Brondum-nielsen, K. Oculocutaneous albinism. *Orphanet J. Rare Dis.* **8**, 1–8 (2007).

36. Yamaguchi, Y. & Hearing, V. J. Melanocytes and Their Diseases. *Cold Spring Harb. Perspect. Med.* 1–18 (2014).

37. Sulem, P. *et al.* Two newly identified genetic determinants of pigmentation in Europeans. *Nat. Genet.* **40**, 835–837 (2008).

38. Chao, Y. *et al.* TPC2 polymorphisms associated with a hair pigmentation phenotype in humans result in gain of channel function by independent mechanisms. (2017) doi:10.1073/pnas.1705739114.

39. Bellono, N. W., Escobar, I. E. & Oancea, E. A melanosomal two-pore sodium channel regulates pigmentation. *Nat. Publ. Gr.* 1–11 (2016) doi:10.1038/srep26570.

40. Patwardhan, A. & Delevoye, C. Ions switch off darkness : Role of TPC2 in melanosomes. *Pigment Cell Melanoma Res.* (2016) doi:10.1111/pcmr.12510.

41. Ambrosio, A. L., Boyle, J. A., Aradi, A. E., Christian, K. A. & Di, S. M. TPC2 controls pigmentation by regulating melanosome pH and size. *PNAS* **113**, 1–6 (2016).

42. Smith, D. R., Spaulding, D. T., Glenn, H. M. & Fuller, B. B. The relationship between Na+/H+ exchanger expression and tyrosinase activity in human melanocytes. *Exp. Cell Res.* **298**, 521–534 (2004).

43. Sturm, R. A., Box, N. F. & Ramsay, M. Human pigmentation genetics: the difference is only skin deep. *BioEssays* **20**, 712–721 (1998).

44. Lin-moshier, Y. *et al.* The Two-pore channel (TPC) interactome unmasks isoform-specific roles for TPCs in endolysosomal morphology and cell pigmentation. *PNAS* **111**, 13087–13092 (2014).

45. Alharbi, A. F. & Parrington, J. Endolysosomal Ca 2 + Signaling in Cancer : The Role of TPC2 , From Tumorigenesis to Metastasis. *Front. Cell Dev. Biol.* **7**, 1–7 (2019).

46. Nguyen, P. *et al.* Two-Pore Channel Function Is Crucial for the Migration of Invasive Cancer Cells. *Cancer Res.* **2**, 1427–1439 (2017).

47. Jahidin, A. H., Stewart, T. A., Thompson, E. W., Roberts-thomson, S. J. & Monteith, G. R. Differential effects of two-pore channel protein 1 and 2 silencing in MDA-MB-468 breast cancer cells. *Biochem. Biophys. Res. Commun.* **477**, 731–736 (2016).

48. Mathew, R. & White, E. Role of autophagy in cancer. *Nat. Rev. Cancer* **7**, 961–967 (2010).

49. Janse van Rensburg, H. *et al.* The Hippo Pathway Component TAZ Promotes Immune Evasion in Human Cancer through PD-L1. *Cancer Res.* 1457–1471 (2018) doi:10.1158/0008-5472.CAN-17-3139.

50. Netcharoensirisuk, P. *et al.* Flavonoids increase melanin production and reduce proliferation, migration and invasion of melanoma cells by blocking endolysosomal/melanosomal TPC2. *Sci. Rep.* **11**, 1–14 (2021).

51. D'amore, A. *et al.* Loss of two-pore channel 2 (TPC2) expression increases the metastatic traits of melanoma cells by a mechanism involving the hippo signalling pathway and store-operated calcium entry. *Cancers (Basel).* **12**, 1–18 (2020).

52. Thompson, B. J. YAP/TAZ : Drivers of Tumor Growth , Metastasis , and Resistance to Therapy. *BioEssays* **1900162**, 1–16 (2020).

53. Gattuso, G. *et al.* Flavonoid Composition of Citrus Juices. *Molecules* 1641–1673 (2007).

54. Erlund, I. Review of the flavonoids quercetin , hesperetin , and naringenin . Dietary sources , bioactivities , bioavailability , and epidemiology. *Nutr. Res.* **24**, 851–874 (2004).

55. Joshi, R., Kulkarni, Y. A. & Wairkar, S. Pharmacokinetic, pharmacodynamic and formulations aspects of Naringenin: An update. *Life Sci.* **215**, 43–56 (2018).

56. Salehi, B. *et al.* The therapeutic potential of naringenin: A review of clinical trials. *Pharmaceuticals* **12**, 1–18 (2019).

57. Alam, M. A. *et al.* Effect of Citrus Flavonoids , Naringin and Naringenin , on Metabolic Syndrome and Their. 404–417 (2014) doi:10.3945/an.113.005603.404.

58. Mukai, R., Shirai, Y., Saito, N., Yoshida, K. & Ashida, H. Subcellular localization of flavonol aglycone in hepatocytes visualized by confocal laser scanning fluorescence microscope. *Cytotechnology* 177–182 (2009) doi:10.1007/s10616-009-9206-z.

59. Straub, I. *et al.* Citrus fruit and fabacea secondary metabolites potently and selectively block TRPM3. 1835–1850 (2013) doi:10.1111/bph.12076.

60. Waheed, A. *et al.* Naringenin inhibits the growth of Dictyostelium and MDCK-derived cysts in a. *Br. J. Pharmacol.* **171**, 2659–2670 (2014).

61. Saponara, S. *et al.* Naringenin as large conductance Ca 2+ - activated K + (BK Ca) channel opener in vascular smooth muscle cells. 1013–1021 (2006) doi:10.1038/sj.bjp.0706951.

62. Li, Q. *et al.* Naringenin exerts anti-angiogenic effects in human endothelial cells : Involvement of ERR α / VEGF / KDR signaling pathway. *Fitoterapia* **111**, 78–86 (2016).

63. Benkerrou, D. *et al.* A perspective on the modulation of plant and animal two pore channels (TPCs) by the flavonoid naringenin. *Biophys. Chem.* **254**, 106246 (2019).

64. Huang, Y., Yang, C. & Chiou, Y. Citrus flavanone naringenin enhances melanogenesis through the activation of Wnt / B -catenin signalling in mouse melanoma cells. *Phytomedicine* **18**, 1244–1249 (2011).

65. Ohguchi, K., Akao, Y. & Nozawa, Y. Stimulation of Melanogenesis by the Citrus Flavonoid Naringenin in Mouse B16 Melanoma Cells. *Biosci. Biotechnol. Biochem* **70**, 1499–1501 (2006).

66. Liu, X. *et al.* The citrus flavonoid naringenin confers protection in a murine endotoxaemia model through AMPK-ATF3-dependent negative regulation of the TLR4 signalling pathway. *Nat. Publ. Gr.* 1–14 (2016) doi:10.1038/srep39735.

67. Gray-schopfer, V., Wellbrock, C. & Marais, R. Melanoma biology and new targeted therapy. *Nat. Insight Rev.* **445**, (2007).

68. Wrobel, S., Przybyło, M. & Stepien, E. The Clinical Trial Landscape for Melanoma Therapies. *J. Clin. Med.* 1–14 (2019) doi:10.3390/jcm8030368.

69. I numeri del cancro in italia. (2021).

70. Rastrelli, M., Tropea, S., Rossi, C. R. & Alaibac, M. Melanoma : Epidemiology , Risk Factors , Pathogenesis , Diagnosis and Classification. **1012**, 1005–1011 (2014).

71. Soengas, M. S. & Lowe, S. W. Apoptosis and melanoma chemoresistance. 3138–3151 (2003) doi:10.1038/sj.onc.1206454.

72. Clark, W. *et al.* A Study of Tumor Progression : The Precursor Lesions of Superficial Spreading and Nodular Melanoma. *Hum. Pathol.* **15**, 1147–1165 (1984).

73. Clark, H., From, L., Bernardino, E. & Mihm, M. C. The Histogenesis Malignant and Biologic Behavior of Primary Human Melanomas of the Skin. *Cancer Res.* (1969).

74. Champsas, G. & Papadopoulos, O. The Role of the Sentinel Lymph Node Biopsy in the Treatment of Nonmelanoma Skin Cancer and Cutaneous Melanoma. *Non-Melanoma Ski. Cancer Cutan. Melanoma* 647–704 (2020).

75. Breslow, A. Thickness , Cross-Sectional Areas and Depth of Invasion in the Prognosis of Cutaneous Melanoma. *Ann. Surg.* 902–908 (1970).

76. Gershenwald, J. *et al.* Melanoma Staging: Evidence-Based Changes in the American Joint

Committee on Cancer Eighth Edition Cancer Staging Manual. *CA Cancer J Clin* **67**, (2017).

77. Davis, L. E. *et al.* Current state of melanoma diagnosis and treatment. *Cancer Biol. Ther.* **20**, 1366–1379 (2019).

78. Shain, A. H. & Bastian, B. C. From melanocytes to melanomas. *Nat. Publ. Gr.* **16**, 345–358 (2016).

79. Sample, A. & He, Y. Mechanisms and prevention of UV- - induced melanoma. *Photodermatol Photoimmunol Photomed.* 13–24 (2018) doi:10.1111/phpp.12329.

80. Berwick, M., Erdei, E. & Hay, J. Melanoma Epidemiology and Public Health. *Dermatol. Clin.* **27**, 1–14 (2009).

81. Collins, L., Quinn, A. & Stasko, T. Skin cancer and immunosuppression. *Dermatol. Clin.* **37**, 83–94 (2019).

82. Dasgupta, A. & Katdare, M. Ultraviolet Radiation-Induced Cytogenetic Damage in White, Hispanic and Black Skin Melanocytes: A Risk for Cutaneous Melanoma. *Cancers (Basel).* 1586–1604 (2015) doi:10.3390/cancers7030852.

83. Paszkowska-Szczur, K. *et al.* Xeroderma pigmentosum genes and melanoma risk. *Int. J. Cancer* **1101**, 1094–1100 (2013).

84. Rodrigues, M. Skin Cancer Risk (Nonmelanoma Skin Cancers/Melanoma) in Vitiligo Patients. *Dermatol. Clin.* **35**, 129–134 (2017).

85. Rayner, J. *et al.* Germline and somatic albinism variants in amelanotic/hypomelanotic melanoma: Increased carriage of TYR and OCA2 variants. *PLoS One* 1–18 (2020) doi:10.1371/journal.pone.0238529.

86. Lawrence, M. S. *et al.* Mutational heterogeneity in cancer and the search for new cancer-associated genes. *Nature* 0–4 (2013) doi:10.1038/nature12213.

87. Scolyer, R. A., Long, G. V & Thompson, J. F. Evolving concepts in melanoma classification and their relevance to multidisciplinary melanoma patient care. **5**, (2011).

88. Read, J., Wadt, K. A. W. & Hayward, N. K. Melanoma genetics. *Cancer Genet.* 1–14 (2016) doi:10.1136/jmedgenet-2015-103150.

89. Goldstein, A. M. *et al.* Features associated with germline CDKN2A mutations: a GenoMEL study of melanoma-prone families from three continents. *J. Med. Genet.* (2007) doi:10.1136/jmg.2006.043802.

90. Pollock, P. *et al.* High frequency of BRAF mutations in nevi. *Nat. Genet.* **12**, 2002–2003 (2002).

91. Bode, A. M. & Dong, Z. Mitogen-Activated Protein Kinase Activation in UV-Induced Signal Transduction. *Sci. stke* 38–40 (2003).

92. Miller, A. J. & Mihm, M. C. Melanoma. *N. Engl. J. Med.* 51–65 (2006).

93. Shain, H. *et al.* The Genetic Evolution of Melanoma from Precursor Lesions. *N. Engl. J. Med.* (2015) doi:10.1056/NEJMoa1502583.

94. Tang, A. *et al.* E-cadherin is the major mediator of human melanocyte adhesion to keratinocytes in vitro. *J. Cell Sci.* **992**, 983–992 (1994).

95. Hsu, M., Wheelock, M., Johnson, K. & Herlyn, M. Shifts in cadherin profiles between human normal melanocytes and melanomas. *J Investig Dermatol* **1**, (1996).

96. Hsu, M. *et al.* E-Cadherin Expression in Melanoma Cells Restores Keratinocyte-Mediated Growth Control and Down- Regulates Expression of Invasion-Related Adhesion Receptors.

Am. J. Pathol. **156**, 1515–1525 (2000).

97. Li, G., Satyamoorthy, K. & Herlyn, M. N-Cadherin-mediated Intercellular Interactions Promote Survival and Migration of. *Cancer Res.* 3819–3825 (2001).

98. Yan, S., Holderness, B. M., Li, Z. & Seidel, G. D. Epithelial – Mesenchymal Expression Phenotype of Primary Melanoma and Matched Metastases and Relationship with Overall Survival. **6456**, 6449–6456 (2016).

99. Bolos, V. *et al.* The transcription factor Slug represses E-cadherin expression and induces epithelial to mesenchymal transitions : a comparison with Snail and E47 repressors. *Co. Biol.* **129**, (2016).

100. Fenouille, N. *et al.* The Epithelial-Mesenchymal Transition (EMT) Regulatory Factor SLUG (SNAI2) Is a Downstream Target of SPARC and AKT in Promoting Melanoma Cell Invasion. *PLoS One* **7**, (2012).

101. Arias-mejias, S. M. *et al.* The role of integrins in melanoma : a review. 525–534 (2020) doi:10.1111/ijd.14850.

102. Kramer, R., Vu, M., Cheng, Y. & Ramos, D. Integrin expression in malignant melanoma. *Cancer Metastasis Rev* **10**, (1991).

103. Albelda, S. M. *et al.* Integrin Distribution in Malignant Melanoma : Association of the ÃŸ3 Subunit with Tumor Progression1. (1990).

104. Schadendorf, D. *et al.* Tumour progression and metastatic behaviour in vivo correlates with integrin expression on melanocytic tumours. *J. Pathol.* **70**, (1993).

105. Rebhun, R. B. *et al.* Constitutive Expression of the α 4 Integrin Correlates with Tumorigenicity and Lymph Node Metastasis of the B16 Murine Melanoma 1. **12**, 173–182 (2010).

106. Vizkeleti, L. *et al.* Altered integrin expression patterns shown by microarray in human cutaneous melanoma. *melanoma Res.* (2017).

107. Abbasi, N. *et al.* Early diagnosis of cutaneous melanoma: revisiting the ABCD criteria. *JAMA* (2004).

108. Russo, T. *et al.* Dermoscopy pathology correlation in melanoma. *J. Dermatol.* 507–514 (2017) doi:10.1111/1346-8138.13629.

109. Shahriari, N., Grant-Kels, J., Rabinovitz, H., Oliviero, M. & Scope, A. Reflectance confocal microscopy may enhance the accuracy of histopathologic diagnosis : A case series. *J. Cutan. Pathol.* 830–838 (2019) doi:10.1111/cup.13548.

110. Prieto, V. G. & Shea, C. R. Use of immunohistochemistry in melanocytic lesions. *J. Cutan. Pathol.* **35**, 1–10 (2008).

111. Ohsie, S. J., Sarantopoulos, G. P., Cochran, A. J. & Binder, S. W. Immunohistochemical characteristics of melanoma. *J. Cutan. Pathol.* **35**, 433–444 (2008).

112. Cochran, A. & Wen, D. S-100 protein as a marker for melanocytic and other tumours. *Pathology* (1985).

113. Ordóñez, N. G. Value of melanocytic-associated immunohistochemical markers in the diagnosis of malignant melanoma : a review and update ☆. *Hum. Pathol.* **45**, 191–205 (2014).

114. Ladstein, R. G., Bachmann, I. M., Straume, O. & Akslen, L. A. Ki-67 expression is superior to mitotic count and novel proliferation markers PHH3 , MCM4 and mitosin as a prognostic

factor in thick cutaneous melanoma. *BMC Cancer* **10**, (2010).

115. Nielsen, P., Riber-Hansen, R. & Steiniche, T. Immunohistochemical double stains against Ki67/MART1 and HMB45/MITF: promising diagnostic tools in melanocytic lesions. *J. Dermatopathol.* **33**, (2011).

116. Kim, R. & Meehan, S. Immunostain use in the diagnosis of melanomas referred to a tertiary medical center: a 15-year retrospective review. *J. Cutan. Pathol.* (2017).

117. Curtin, J. *et al.* Distinct Sets of Genetic Alterations in Melanoma. *N. Engl. J. Med.* 2135–2147 (2005).

118. Cummins, D. *et al.* Cutaneous Malignant Melanoma. *Mayo clin proc* **81**, 500–507 (2006).

119. Tarhini, A. & Agarwala, S. Cutaneous melanoma : available therapy for metastatic disease. **19**, 19–25 (2006).

120. Chapman, P. *et al.* Improved Survival with Vemurafenib in Melanoma with BRAF V600E Mutation. *ne* 2507–2516 (2011).

121. Scolyer, R. & Prieto, V. Melanoma Pathology: Important Issues for Clinicians Involved in the Multidisciplinary Care of Melanoma Patients. *Surg. Oncol. Clin. N. Am.* 2021 (2011).

122. Larkin, J. *et al.* Five-Year Survival with Combined Nivolumab and Ipilimumab in Advanced Melanoma. *new* (2019) doi:10.1056/NEJMoa1910836.

123. Carreau, N. & Pavlick, A. Nivolumab and ipilimumab: immunotherapy for treatment of malignant melanoma. *Futur. Oncol L. Engl* (2019).

124. Hearing, V. J. Biochemical Control of Melanogenesis and Melanosomal Organization. *J. Investig. Dermatology Symp. Proc.* **4**, 24–28 (1999).

125. Kobayashi, T. *et al.* Modulation of melanogenic protein expression during the switch from eu- to pheomelanogenesis. *J cell Sci.* **108**, (1995).

126. Ou-yang, H., Stamatas, G. & Kollias, N. Spectral Responses of Melanin to Ultraviolet A Irradiation. *J. Invest. Dermatol.* **122**, 492–496 (2004).

127. Pawelek, J. & Lerner, A. 5,6-Dihydroxyindole is a melanin precursor showing potent cytotoxicity. *Nature* (1978).

128. Urabe, K. *et al.* The inherent cytotoxicity of melanin precursors: a revision. (1994).

129. Schmitz, S., Thomas, P., Allen, T., Poznansky, M. & Jimbow, K. Dual Role of Melanins and Melanin Precursors as Photoprotective and Phototoxic Agents: Inhibition of Ultraviolet Radiation_Induced Lipid Peroxidation. *Photochem Photobiol* (1995).

130. Cichorek, M. & Skoniecka, A. Heterogeneity of neural crest-derived melanocytes. (2015) doi:10.2478/s11535-013-0141-1.

131. Cichorek, M., Wachulska, M., Stasiewicz, A. & Tymińska, A. Skin melanocytes : biology and development. 30–41 (2013) doi:10.5114/pdia.2013.33376.

132. Orlow, S. J. Melanosomes Are Specialized Members of the Lysosomal Lineage of Organelles. *J. Invest. Dermatol.* **105**, 3–7 (1995).

133. Raposo, G. & Marks, M. S. Melanosomes — dark organelles enlighten endosomal membrane transport. *Nature* **8**, (2007).

134. Bhatnagar, V., Anjaiah, S., Puri, N., Darshanam, B. & Ramaiah, A. pH of melanosomes of B 16 murine melanoma is acidic: its physiological importance in the regulation of melanin biosynthesis. *Arch Biochem Biophys* **307**, (1993).

135. Futter, C. E. The molecular regulation of organelle transport in mammalian retinal pigment epithelial cells. (2006) doi:10.1111/j.1600-0749.2006.00303.x.

136. Seiberg, M. Keratinocyte – Melanocyte Interactions During Melanosome Transfer. *Pigment Cell Res.* 236–242 (2001).

137. Ortonne, J. & Prota, G. Hair melanins and hair color: ultrastructural and biochemical aspects. *J Invest Dermatol* **101**, (1993).

138. Creel, D., Boxer, L. & Fauci, A. Visual and auditory anomalies in Chediak-Higashi syndrome. *Electroencephalogr Clin Neurophysiol* **55**, (1983).

139. Lindquist, N. Accumulation of drugs on melanin. *Acta Radiol Diagn* **325**, (1973).

140. Riley, V. Unique Properties of Melanocytes. *Pigment Cell* (1975).

141. Creel, D. *et al.* Abnormalities of the central visual pathways in Prader-Willi syndrome associated with hypopigmentation. *N. Engl. J. Med.* **314**, (1986).

142. King, R. *et al.* Brown Ocuuiocutaneous Albinism: Clinical, Ophthalmological, and Biochemical Characterization. *Ophthalmology* **92**, (1985).

143. Williams, P., Olsen, C., Hayward, N. & Whiteman, D. Melanocortin 1 receptor and risk of cutaneous melanoma: a meta-analysis and estimates of population burden. *Int J Cancer.* **129**, (2011).

144. Seiji, M., Fitzpatrick, T., Simpson, R. & Birbeck, M. Chemical Composition and Terminology Of Specialized Organelles (Melanosomes and Melanin Granules) in Mammalian Melanocytes. *Nature* **197**, (1963).

145. Raposo, G., Tenza, D., Murphy, D. M., Berson, J. F. & Marks, M. S. Distinct Protein Sorting and Localization to Premelanosomes , Melanosomes , and Lysosomes in Pigmented Melanocytic Cells 7. **152**, 809–823 (2001).

146. Costin, G. & Hearing, V. J. Human skin pigmentation : melanocytes modulate skin color in response to stress. *FASEB J.* (2007) doi:10.1096/fj.06-6649rev.

147. Schiaffino, M. V. SIGNALING PATHWAYS IN MELANOSOME BIOGENESIS AND PATHOLOGY. *Int J Biochem Cell Biol* **42**, 1094–1104 (2010).

148. Dror, S. *et al.* Melanoma miRNA trafficking controls tumour primary niche formation. *Nat. Cell Biol.* **18**, (2016).

149. Sakai, C., Kawakami, Y., Law, L., Furumura, M. & Hearing, V. Melanosomal proteins as melanoma-specific immune targets. *melanoma Res.* **7**, (1997).

150. D'Orazio, J. A. D. *et al.* Topical drug rescue strategy and skin protection based on the role of Mc1r in UV-induced tanning. *Nature* **443**, 340–344 (2006).

151. Brożyna, A. A., Jóźwicki, W., Roszkowski, K. & Filipiak, J. Melanin content in melanoma metastases affects the outcome of radiotherapy. **7**, 17844–17853 (2016).

152. Brozyna, A., Jozwicki, W., Carlson, J. & Slominski, A. Melanogenesis Affects Overall and Disease-Free Survival in Patients with Stage III and IV Melanoma. **44**, 2071–2074 (2014).

153. Sarna, M., Krzykawska-serda, M., Jakubowska, M. & Zadlo, A. Melanin presence inhibits melanoma cell spread in mice in a unique mechanical fashion. *Sci. Rep.* 1–9 (2019) doi:10.1038/s41598-019-45643-9.

154. Yuan, Y., Jiang, Y., Sun, C. & Chen, Q. Role of the tumor microenvironment in tumor progression and the clinical applications. *Oncol. Rep.* 2499–2515 (2016) doi:10.3892/or.2016.4660.

155. Hanahan, D. & Coussens, L. M. Accessories to the Crime : Functions of Cells Recruited to the Tumor Microenvironment. *Cancer Cell* **21**, 309–322 (2012).

156. Grivennikov, S. I., Greten, F. R. & Karin, M. Immunity , Inflammation , and Cancer. *Cell* **140**, 883–899 (2010).

157. Lu, P., Weaver, V. M. & Werb, Z. The extracellular matrix : A dynamic niche in cancer progression. *J. Cell Biol.* **196**, 395–406 (2012).

158. Hui, L. & Chen, Y. Tumor microenvironment : Sanctuary of the devil. *Cancer Lett.* **368**, 7–13 (2015).

159. Carmeliet, P. & Jain, R. Molecular mechanisms and clinical applications of angiogenesis. *Nature* **473**, 298–307 (2011).

160. Brychtova, S. *et al.* Stromal Microenvironment Alterations in Malignant Melanoma. (2011).

161. Villanueva, J. & Herlyn, M. Melanoma and the Tumor Microenvironment. *Curr. Oncol. Rep.* **10**, 439–446 (2017).

162. Brandner, J. & Haass, N. Melanoma ' s connections to the tumour microenvironment. *Pathology* **45**, 443–452 (2013).

163. Haass, N. K., Smalley, K. S. M. & Li, L. Adhesion , migration and communication in melanocytes and melanoma. *Pigment Cell Res.* **1**, (2005).

164. Li, G., Schaider, H., Satyamoorthy, K., Hanakawa, Y. & Hashimoto, K. Downregulation of E-cadherin and Desmoglein 1 by autocrine hepatocyte growth factor during melanoma development. *Oncogene* (2001).

165. Kalluri, R. & Zeisberg, M. Fibroblasts in cancer. *Nature* **6**, (2006).

166. Zhou, L., Yang, K., Andl, T., Wickett, R. R. & Zhang, Y. Perspective of Targeting Cancer-Associated Fibroblasts in Melanoma. *J. Cancer* **6**, (2015).

167. Nagasaki, T. *et al.* Interleukin-6 released by colon cancer-associated fibroblasts is critical for tumour angiogenesis : anti-interleukin-6 receptor antibody suppressed angiogenesis and inhibited tumour – stroma interaction. *Br. J. Cancer* **6**, 469–478 (2014).

168. Liu, R., Liu, L., Yu, J. & Ren, X. Fibroblast activation protein. *Cancer Biol. Ther.* **4047**, (2012).

169. Wäster, P., Rosdahl, I., Gilmore, B. F. & Seifert, O. Ultraviolet exposure of melanoma cells induces fibroblast activation protein-α in fibroblasts : Implications for melanoma invasion. *Int. J. Oncol.* 193–202 (2011) doi:10.3892/ijo.2011.1002.

170. Bhowmick, N. A., Neilson, E. G. & Moses, H. L. Stromal fibroblasts in cancer initiation and progression. *Nature* **432**, (2004).

171. Sahai, E. *et al.* A framework for advancing our understanding of cancer- associated fibroblasts. *Nat. Rev. Cancer* **20**, (2020).

172. Dimanche-Boitrel, M. *et al.* In vivo and in vitro invasiveness of a rat colon-cancer cell line maintaining E-cadherin expression: an enhancing role of tumor-associated myofibroblasts. *Int J Cancer* **56**, (1994).

173. Orimo, A. *et al.* Stromal Fibroblasts Present in Invasive Human Breast Carcinomas Promote Tumor Growth and Angiogenesis through Elevated SDF-1 / CXCL12 Secretion. *Cell* **121**, 335–348 (2005).

174. Erdogan, B. & Webb, D. J. Cancer-associated fibroblasts modulate growth factor signaling and extracellular matrix remodeling to regulate tumor metastasis. *Biochem Soc Trans.* **45**, 229–236 (2017).

175. Akhurst, R. J. TGF- β antagonists : Why suppress a tumor suppressor ? *J. Clin. Invest.* **109**, 1533–1536 (2002).

176. García-silva, S. & Peinado, H. Melanosomes foster a tumour niche by activating CAFs. *Nat. Cell Biol.* **18**, 911–913 (2016).

177. Quadri, M., Saltari, A. & Pincelli, C. Progress in melanoma modelling in vitro Alessandra Marconi. 578–586 (2018) doi:10.1111/exd.13670.

178. Raza, A. *et al.* Oxygen Mapping of Melanoma Spheroids using Small Molecule Platinum Probe and Phosphorescence Lifetime Imaging Microscopy. *Sci. Rep.* 1–9 (2017) doi:10.1038/s41598-017-11153-9.

179. Kunz-schughart, L. A. *et al.* Proliferative activity and tumorigenic conversion : impact on cellular metabolism in 3-D culture. *Am. Physiol. Soc.* (2000).

180. Quail, D. F., Maciel, T. J., Rogers, K. & Postovit, L. M. A Unique 3D In Vitro Cellular Invasion Assay. *J. Biomol. Screen.* (2012) doi:10.1177/1087057112449863.

181. Wever, O. D. E. *et al.* Modeling and quantification of cancer cell invasion through collagen type I matrices. *Int. J. Biol.* **896**, 887–896 (2010).

182. Friedrich, J., Seidel, C., Ebner, R. & Kunz-Schughart, L. Spheroid-based drug screen: considerations and practical approach. *Nat Protoc* **4**, (2009).

183. Lin, R. & Chang, H. Recent advances in three-dimensional multicellular spheroid culture for biomedical research. 1172–1184 (2008) doi:10.1002/biot.200700228.

184. Bull, J., Mech, F., Quaiser, T., Waters, S. & Byrne, H. Mathematical modelling reveals cellular dynamics within tumour spheroids. *PLOS Comput. Biol.* 1–25 (2020) doi:10.1371/journal.pcbi.1007961.

185. Lin, R.-Z. & Chou, L.-F. Dynamic analysis of hepatoma spheroid formation : roles of E-cadherin and β 1-integrin. *Cell Tissue Res.* **324**, 411–422 (2006).

186. Ryu, N., Lee, S. & Park, H. Spheroid Culture System Methods and Applications for Mesenchymal Stem Cells. 1–13 (2019).

187. Gryadunova, A. A. *et al.* Cytoskeleton systems contribute differently to the functional intrinsic properties of chondrospheres. *Acta Biomater.* **118**, 141–152 (2020).

188. Tsai, A., Liu, Y. & Yuan, X. Compaction, Fusion, and Functional Activation of Three-Dimensional Human Mesenchymal Stem Cell Aggregate. **21**, 1705–1719 (2015).

189. Saleh, N. *et al.* Three_dimensional multicellular cell culture for anti-melanoma drug screening: focus on tumor microenvironmentThree_dimensional multicellular cell culture for anti-melanoma drug screening: focus on tumor microenvironment. *Cytotechnology* **73**, (2021).

190. Flach, E. H., Rebecca, V. W., Herlyn, M., Smalley, K. S. M. & Anderson, A. R. A. Fibroblasts Contribute to Melanoma Tumor Growth and Drug Resistance. *Mol. Pharm.* (2011).

191. Klicks, J., Maßlo, C., Kluth, A., Rudolf, R. & Hafner, M. A novel spheroid-based co-culture model mimics loss of keratinocyte differentiation , melanoma cell invasion , and drug-induced selection of ABCB5-expressing cells. *BMC Cancer* 1–14 (2019).

192. Verjans, E.-T., Doijen, J., Luyten, W., Landuyt, B. & Schoofs, L. Three-dimensional cell culture models for anticancer drug screening: Worth the effort? *J Cell Physiol* **233**, (2018).

193. Meier, F. *et al.* Human Melanoma Progression in Skin Reconstructs. *Am. J. ofPathology* **156**, 193–200 (2000).

194. Nakazawa, K. *et al.* Pigmented human skin equivalent: new method of reconstitution by grafting an epithelial sheet onto a non-contractile dermal equivalent. *Pigment Cell Res.* **10**, (1997).

195. Mertsching, H., Weimer, M., Kersen, S. & Brunner, H. Human skin equivalent as an alternative to animal testing. **3**, 4–7 (2008).

196. Ponec, M. & Kempenaar, J. Use of human skin recombinants as an in vitro model for testing the irritation potential of cutaneous irritants. *Ski. Pharmacol Off J Ski. Pharmacol Soc* **8**, (1995).

197. Jansson, K., Kratz, G. & Haegerstrand, A. Characterization of a new in vitro model for studies of reepithelialization in human partial thickness wounds. *Vitr. Cell Dev Biol Anim* **32**, (1996).

198. Hill, D. S. *et al.* A Novel Fully Humanized 3D Skin Equivalent to Model Early Melanoma Invasion. *Mol. Cancer Ther.* 2665–2674 (2015) doi:10.1158/1535-7163.MCT-15-0394.

199. Vorsmann, H. *et al.* Development of a human three-dimensional organotypic skin-melanoma spheroid model for in vitro drug testing. *Cell Death Dis.* **4**, (2013).

200. Beaumont, K. A., Mohana-kumaran, N. & Haass, N. K. Modeling Melanoma In Vitro and In Vivo. 27–46 (2014) doi:10.3390/healthcare2010027.

201. Lee, J. PLX4032, a Potent Inhibitor of the B-Raf V600E Oncogene, Selectively Inhibits V600E-positive Melanomas. **23**, 820–827 (2013).

202. Bellas, E., Seiberg, M., Garlick, J. & Kaplan, D. In vitro 3D full thickness skin equivalent tissue model using silk and collagen biomaterials. **12**, 617–627 (2013).

203. Zalaudek, I. *et al.* Three Roots of Melanoma. *arch dermatol* **144**, 1375–1379 (2008).

204. Segura, S. *et al.* In Vivo Microscopic Features of Nodular Melanomas. *arch dermatol* **144**, 1311–1321 (2008).

205. Liu, X., Wu, J., Qin, H. & Xu, J. The Role of Autophagy in the Resistance to BRAF Inhibition in BRAF-Mutated Melanoma. *Target. Oncol.* **13**, 437–446 (2018).

206. Abrahamian, C. & Grimm, C. Endolysosomal Cation Channels and MITF in Melanocytes and Melanoma. *Biomolecules* (2021).

207. Marconi, A. *et al.* In Vivo Melanoma Cell Morphology Reflects Molecular Signature and Tumor Aggressiveness. *J. Invest. Dermatol.* (2021) doi:10.1016/j.jid.2021.12.024.

208. Shivakumar, M. *et al.* Identification of epigenetic interactions between miRNA and DNA methylation associated with gene expression as potential prognostic markers in bladder cancer. *BMC Med. Genomics* **10**, (2017).

209. Li, F., Ji, J., Xu, Y. & Liu, R. Identification a novel set of 6 differential expressed genes in prostate cancer that can potentially predict biochemical recurrence after curative surgery. *Clin. Transl. Oncol.* **21**, 1067–1075 (2019).

210. Huang, X., Godfrey, T. E., Gooding, W. E., Jr, K. S. M. & Gollin, S. M. Comprehensive Genome and Transcriptome Analysis of the 11q13 Amplicon in Human Oral Cancer and Synteny to the 7F5 Amplicon in Murine Oral Carcinoma. *Genes, Chromosom. cancers* **1069**, 1058–1069 (2006).

211. Stompor, M., Uram, Ł. & Podgórski, R. In vitro effect of 8-prenylnaringenin and naringenin on fibroblasts and glioblastoma cells-cellular accumulation and cytotoxicity. *Molecules* **22**, (2017).

212. Tundis, R. *et al.* In vitro cytotoxic activity of extracts and isolated constituents of salvia

leriifolia benth. Against a panel of human cancer cell lines. *Chem. Biodivers.* **8**, 1152–1162 (2011).

213. Iwashita, K., Kobori, M., Yamaki, K. & Tsushida, T. Flavonoids inhibit cell growth and induce apoptosis in B16 melanoma 4A5 cells. *Biosci. Biotechnol. Biochem* **64**, 1813–1820 (2000).

214. Nasr Bouzaiene, N., Chaabane, F., Sassi, A., Chekir-Ghedira, L. & Ghedira, K. Effect of apigenin-7-glucoside, genkwanin and naringenin on tyrosinase activity and melanin synthesis in B16F10 melanoma cells. *Life Sci.* **144**, 80–85 (2016).

215. Müller, M. Novel Chemical Tools to Target Two-Pore Channel 2 , P-Glycoprotein and Histone Deacetylase 6 in Cancer. (2020).

216. Gerndt, S. *et al.* Agonist-mediated switching of ion selectivity in TPC2 differentially promotes lysosomal function. *Elife* **9**, 1–63 (2020).

217. Kramer, R. *et al.* Laminin-binding integrin a7,1: functional characterization and expression in normal and malignant melanocytes Randall. *Cell Regul.* **2**, 805–817 (1991).

218. Syed, D. *et al.* Inhibition of human melanoma cell growth by dietary flavonoid fisetin is associated with disruption of Wnt/β-catenin signaling and decreased Mitf levels. *J Invest Dermatol* **131**, 1291–1299 (2011).

219. Ando, H., Yoshimoto, S., Yoshida, M., Shimoda, N. & Tadokoro, R. Dermal Fibroblasts Internalize Phosphatidylserine-Exposed Secretory Melanosome Clusters and Apoptotic Melanocytes. *Int. J. Mol. Sci.* 1–14 (2020).

220. Lian, G. Y. *et al.* Combination of Asiatic Acid and Naringenin Modulates NK Cell Anti-cancer Immunity by Rebalancing Smad3/Smad7 Signaling. *Mol. Ther.* **26**, 2255–2266 (2018).

221. Lentini, A., Forni, C., Provenzano, B. & Beninati, S. Enhancement of transglutaminase activity and polyamine depletion in B16-F10 melanoma cells by flavonoids naringenin and hesperitin correlate to reduction of the in vivo metastatic potential. *Amino Acids* **32**, 95–100 (2007).

222. Rebello, C. *et al.* Safety and Pharmacokinetics of Naringenin: A Randomized, Controlled, Single Ascending Dose, Clinical Trial. *Diabetes Obes Metab.* **22**, 91–98 (2021).

223. Skelding, K. A., Barry, D. L., Theron, D. Z. & Lincz, L. F. Targeting the two-pore channel 2 in cancer progression and metastasis. *Explor. Target. Anti-tumor Ther.* **3**, 62–89 (2022).

224. Ling, D. *et al.* Enhancing the anticancer effect of the histone deacetylase inhibitor by activating transglutaminase. *Eur. J. Cancer* **48**, 3278–3287 (2012).

225. Fernández, J. *et al.* Antiproliferative and palliative activity of flavonoids in colorectal cancer. *Biomed. Pharmacother.* **143**, (2021).

ACKNOWLEDGEMENTS

I thank Professor Alessandra Marconi for allowing me to do this project in her laboratory, thank you for all the time you have dedicated to me, for the patience, the encouragement and for guiding me in the realization of this project.

Thanks to all the “Dermo Lab”, to Professor Carlo Pincelli, for giving me the opportunity to join his research lab and to Marika for her teachings, her availability and infinite patience and her support. I would also like to thank Elisabetta and Roberta, with which I had the good fortune to share this experience, thank you for always helping me and for all your valuable advice. Thanks to Cristina, for your infinite availability, kindness and for having always listened and supported me.

A special thanks to my parents, for having always been close to me in these years, for having supported me and for having given me the opportunity to reach this goal.

Thanks to Giuni and Martina, because despite the distance and the years you have always been there. Finally, thanks to Emanuela, Sara, Giulia, Davide, Federico, Marcello, Jacopo and Francesca for made these years full of laughter and good times.